UNIVERSITÉ DU QUÉBEC À MONTRÉAL

ACCUMULATION AND SEQUESTRATION OF METALS IN DIFFERENT STRAINS OF *CHLAMYDOMONAS*

THESIS

PRESENTED

AS PARTIAL REQUIREMENT

OF DOCTORATE IN CHEMISTRY

BY

MAHSHID SAMADANI

AUGUST 2018

UNIVERSITÉ DU QUÉBEC À MONTRÉAL

L'ACCUMULATION ET LA SÉQUESTRATION DES MÉTAUX CHEZ DIFFÉRENTES SOUCHES DE *CHLAMYDOMONAS*

THÈSE

PRÉSENTÉE

COMME EXIGENCE PARTIELLE

DU DOCTORAT EN CHIMIE

PAR

MAHSHID SAMADANI

AOÛT 2018

ACKNOWLEDGMENTS

I would like to express the deepest appreciation to my supervisor, Professor David Dewez, who offered numerous helpful insights, suggestions, guidance, and corrections without which this dissertation would not have been possible to progress and finish. I have been very fortunate to work in his laboratory and to collaborate with his research group, and I am very grateful for all skills and knowledge which I have obtained working in his laboratory.

I would like to acknowledge gratefully the valuable explanations and many useful comments and suggestions from the jury members: Pr. Huu Van Tra, Pr. Abdelkrim Azzouz, Pr. Philippe Juneau, and Pr. William Zerges, who helped and encouraged me to continue and finalize this work.

I would like to thank deeply for the expert assistance of Professor François Perreault who taught me laboratory techniques and without his scientific helps, patience, and guidance the work would have been much harder for me.

I would like to appreciate greatly for the technical support of Denis Flipo at the confocal microscopy imaging facility of TOXEN (Department of Biological Sciences, UQAM).

I am very grateful for all supports and helps from my colleagues in laboratory, Dr. Laura Pirastru for her great knowledge of algal culture, who helped me to cultivate and to maintain microalgae in the laboratory, Dr. Abdallah Oukarroum for all his encouragement, Émillie for giving me lots of positive energy, Vahid and Jonathan for their collaboration to do some parts of practical experiments.

I have also special thanks to UQÀM's personnel those supported me kindly particularly my great appreciation to Dr. Gwenaël Chamoulaud and Mme Isabelle Rheault for technical services and helpful advices to accomplish my experimental tests with ICP-AES and FAAS.

I would also have a special gratitude for my best friend Dr. Pejman Nekoovaght for all his supports ever since I have arrived in Canada. He encouraged, gave me insights and enthusiasms to continue my graduate studies at UQÀM. He also graciously assisted in editing the present dissertation.

Finally, my special acknowledgment goes to my parents and my family for their great spiritual support and their encouragement.

TABLE OF CONTENT

LISTE OF FIGURES

LIST OF TABLES

LIST OF ABBREVIATIONS

AAS	Atomic Absorption Spectrometry
ADP	Adenosine Diphosphate
AEM	Analytical Electron Microscopy
AMP	Adenosine Monophosphate
APX	Ascorbate Peroxidase
ATP	Adenosine Triphosphate
CAT	Catalases
CCD	Charge-Coupled Device
Chl	Chlorophyll
Chl^*	Excited Chlorophyll
Cys	Cysteine
DAPI	4′,6-diamidino-2-phenylindole
EC_{50}	Half Maximal Effective Concentration
EDTA	Ethylene Diamine Tetra Acetic Acid
FAAS	Flame Atomic Absorption Spectrometry

Fd	Ferredoxin
FDA	Fluorescein Diacetate
FEG	Field-Emission Gun
FFP	Front-Focal Plane
F_M	Maximal Fluorescence Intensity
FNR	Ferredoxin–NADP Reductase
FSC	Forward-Angle Light Scatter
F_V	Variable Fluorescence Intensity
Glu	Glutamine
γ-Glu-Cys	Gamma Glutamylcysteine
γ-Glu-Cys synt	Gamma Glutamylcysteine Synthetase
Gly	Glycine
GSH	Glutathione
G synt	Glutathione Synthetase
H_2DFFDA	5-(and-6)-Carboxy-2′, 7′-Dihydrodifluorofluorescein Diacetate
HMW	High Molecular Weight
HSM	High Salt Medium
ICP	Inductively Coupled Plasma

LHCI	Light-Harvesting Complexes of Photosystems I
LHCII	Light-Harvesting Complexes of Photosystems II
LMW	Low Molecular Weight
LSCM	Laser Scanning Confocal Microscopy
M^{n+}	Metal Ions
MAM	Modified Acid Medium
MOPS	3-[N-Morpholino] Propanesulfonic Acid
NADP	Nicotinamide-Adenine Dinucleotide Phosphate
NMR	Nuclear Magnetic Resonance
OD_{600}	Optical Density at 600 nm
OES	Optical Emission Spectrometry
PAH	Polycyclic Aromatic Hydrocarbons
PC_s	Phytochelatins
PC	Plastocyanin
PCs	Phytochelatin Synthase
PC synt	Phytochelatin Synthetase
PEA	Plant Efficiency Analysis
Pheo	Pheophytin

Pi	Orthophosphate
PI	Performance Index of PSII Activity
Pit	Inorganic Phosphate Transport System
PMT	Photomultiplier Tube
^{31}P-NMR	Phosphorus-31 NMR
PolyP	Polyphosphate
PPi	Pyrophosphate
PPK	Polyphosphate Kinase
PPX	Exopolyphosphatase
PSI	Photosystem I
PSII	Photosystem II
PQ	Plastoquinone
PQH_2	Reduced Plastoquinone
RCDR	Relative Cell Division Rate
ROS	Reactive Oxygen Species
SOD	Superoxide Dismutase
SSC	Side-Angle Light Scatter
STEM	Scanning Transmission Electron Microscopy

TAP	Tris-Acetate-Phosphate Medium
TEM	Transmission Electron Microscopy
Q_A	Quinone A
Q_B	Quinone B
XEDS	X-ray Energy-Dispersive Spectrometry

LIST OF SYMBOLS AND UNITS

°C	Degree Celsius
d	Day
eV	Electron Volt
h	Hour
M	Mole per Liter
mM	Millimole per Liter
µM	Micromole per Liter
µg	Microgram
mg	Milligram
m^2	Meter Square
µm	Micrometer
nm	Nanometer
L	Liter
mL	Milliliter
min	Minute

%	Percentage
PPM	Parts per Million
rpm	Revolutions per Minute
S	Second

RÉSUMÉ

Le cadmium et le mercure sont des contaminants dangereux pour l'être humain et les écosystèmes aquatiques, et leur rejet d'origine anthropique dans les eaux et rivières continuent malheureusement. En particulier, du point de vue du milieu aquatique, la forme ionique du Cd peut être biodisponible pour les organismes aquatiques, et la transformation du Hg^{2+} sous sa forme organique toxique, le méthylmercure peut être bioaccumulé et sa dose bioamplifiée le long de la chaîne alimentaire aquatique. Dans ce projet de recherche, l'algue verte *Chlamydomonas* a été utilisée comme un organisme modèle pour investiguer l'accumulation et la séquestration du cadmium et du mercure dans les cellules algales, leurs toxicités cellulaires et moléculaires, et les mécanismes de protection impliqués dans les cellules. Par conséquent, ce projet de recherche est structuré en trois études en adressant chacune un objectif spécifique. Dans la première étude, la capacité d'accumulation du cadmium a été étudiée chez deux souches d'algues, la souche sauvage *Chlamydomonas reinhardtii* et la souche acido-tolérante *Chlamydomonas* CPCC 121 exposées durant 48 h aux différentes concentrations de Cd (100 à 600 µM) sous deux conditions de pH (4 et 7). La souche *C. reinhardtii* a montré une accumulation plus élevée de Cd par rapport à la souche CPCC 121 en induisant un impact toxique plus fort. En comparaison, *Chlamydomonas* CPCC 121 a montré une tolérance pour le Cd qui était corrélée avec la diminution de l'accumulation intracellulaire de Cd. Cependant, la capacité d'accumulation de cadmium était la plus faible chez CPCC 121 à pH 4, limitant son utilisation pour les applications de biorestauration. Dans la seconde étude, l'effet de $CdCl_2$ a été étudié sur le niveau de polyphosphate extracytoplasmique (polyP) en utilisant les souches CC-125 et CC-503 ayant une paroi cellulaire déficiente. Les souches de *C. reinhardtii* ont été exposées pendant 24-72 h aux différentes concentrations de Cd (200-600 µM). Les résultats ont montré la diminution de la synthèse ou la dégradation de polyP extracytoplasmique qui était corrélée avec l'accumulation de Cd, même chez la souche CC-503 avec un niveau inférieur de polyP. En plus, le niveau du polyP a été diminué en relation avec la diminution du ratio F_V/F_M pour les deux souches pendant 48 h. En comparaison avec CC-125, le niveau de polyP n'a pas été récupéré après 72 h chez CC-503. Cependant, les deux souches d'algues ont accumulé une quantité considérable de Cd dans leur biomasse et le polyP n'a pas participé à la séquestration de Cd. Par conséquent, cette étude a montré l'effet du Cd sur le niveau de polyP qui était dépendant de la concentration de Cd, tandis que le Cd a inhibé le taux de la croissance cellulaire indépendamment de la concentration de Cd. En utilisant *C. reinhardtii*, le niveau de polyP peut être utilisé comme un biomarqueur de la toxicité

des métaux, tels que le Cd. Dans la troisième étude, l'accumulation et l'effet de la toxicité du mercure a été déterminé chez deux souches de *C. reinhardtii*, CC-125 et CC-503 ayant une paroi cellulaire déficiente, pendant 24-72 h d'exposition à 1-7 μM de Hg. Le niveau de polyP extracytoplasmique a été déterminé afin de comprendre le rôle physiologique de polyP dans les cellules algales traitées au Hg. Lorsque les cellules d'algues ont été exposées à 1 et 3 μM de Hg, l'accumulation du Hg était corrélée avec la dégradation de polyP pour les deux souches. Ces résultats suggèrent que la dégradation de polyP a participé dans la séquestration de Hg, même chez CC-503 avec un niveau inférieur de polyP. Ce mécanisme pourrait expliquer à 72 h la récupération du niveau de polyP, la performance de la photochimie du PSII, la faible inhibition du taux de la croissance cellulaire, et la faible accumulation de Hg dans la biomasse. Nos résultats montrent que le changement du niveau de polyP est corrélé avec l'accumulation et l'effet du mercure sur les cellules d'algues, permettant son utilisation comme un biomarqueur de la toxicité du Hg.

Mots clés : Cadmium; Mercure; Accumulation; Toxicité; Tolérance; Polyphosphate; polyP extracytoplasmique; Algue verte; *Chlamydomonas reinhardtii*; *Chlamydomonas* CPCC 121.

ABSTRACT

Cadmium and mercury represent dangerous contaminants for both aquatic ecosystems and human health, and their release in waters and rivers continue unfortunately from anthropogenic activities. Particularly, from the point of view of aquatic environment, the ionic form of Cd can be bioavailable to aquatic organisms, and the transformation of Hg^{2+} into high toxic organic form, methylmercury, can be bioaccumulated and its dose bioamplified through the aquatic food chain. In this research project, the use of green alga *Chlamydomonas* was used as a model organism to investigate the accumulation and the sequestration of Cd and Hg in algal cells, their toxicity effects at cellular and molecular levels, and the protection mechanisms involved in algal cells. Therefore, this research project is divided into three studies addressing each a specific objective. In the first study, the capacity of cadmium accumulation was investigated for two algal strains, *Chlamydomonas reinhardtii* and the acid-tolerant strain CPCC 121, during 48 h under 100-600 µM of Cd and two pH conditions (4 and 7). *C. reinhardtii* demonstrated a higher accumulation of Cd compared to the strain CPCC 121, inducing a stronger cellular toxic impact. In comparison, *Chlamydomonas* CPCC 121 demonstrated a tolerance for Cd, which was correlated with the decrease of intracellular Cd accumulation. However, the capacity of cadmium accumulation was lower in CPCC 121 at pH 4 than pH 7, limiting its use for bioremediation applications. In the second study, the effect of $CdCl_2$ on the level of extracytoplasmic polyphosphate (polyP) was investigated using CC-125 and the cell wall-deficient CC-503. Two strains of *C. reinhardtii* were exposed under neutral pH during 24-72 h to different concentrations of Cd (200-600 µM). The results demonstrated the decrease in synthesis and/or the degradation of extracytoplasmic polyP, which was correlated with the accumulation of Cd, even in CC-503 having a lower level of polyP. Furthermore, the level of polyP decreased in relation to the decrease of F_V/F_M value for both strains during 48 h. In comparison with CC-125, the level of polyP could not be recovered at 72 h for CC-503. Nevertheless, both algal strains were able to accumulate significant amount of Cd in their biomass, and the polyP did not participate in the sequestration of Cd. Therefore, this study demonstrated the effect of Cd on the polyP level, which was dependent on the concentration of Cd, whereas Cd inhibited the growth rate regardless of Cd concentration. By using *C. reinhardtii*, the polyP level can be used as a biomarker of Cd toxicity. In the third study, the accumulation and toxicity effect of mercury was determined on two strains of *C. reinhardtii*, CC-125 and CC-503 as a cell wall-deficient strain, during 24-72 h of exposure to 1-7 µM of Hg. The level of extracytoplasmic polyP was determined to understand the polyP physiological role in

Hg-treated cells. When the algal cells were exposed to 1 and 3 μM of Hg, the accumulation of Hg was correlated with the degradation of polyP for both strains. These results suggested that the degradation of polyP participated in the sequestration of Hg even in CC-503 with a lower level of polyP. This mechanism might explain at 72 h the recovery of the polyP level, the efficiency of maximum PSII quantum yield, the low inhibition of growth rate, and the low accumulated Hg in algal biomass. Our results demonstrated that the change of polyP level was correlated with the accumulation and effect of Hg on algal cells, which can be used as a biomarker of Hg toxicity.

Keywords: Cadmium; Mercury; Accumulation; Toxicity; Tolerance; Polyphosphate; Extracytoplasmic polyP; Green algae; *Chlamydomonas reinhardtii*; *Chlamydomonas* CPCC 121.

INTRODUCTION

Having access to safe drinking water is one of the most important needs for humans society, considering that more than a third of the people in the world have been affected by unsafe drinking water (Schwarzenbach *et al.*, 2010). Aquatic environments have been subjected to the contamination by organic and inorganic chemicals since the beginning and the development of the industrial age (Adriano *et al.*, 2005). From the environmental point of view, inorganic pollutants (for example: Cr, Ni, Cu, Zn, Cd, Pb, Hg) and metalloids (e.g., Se, As), are not degraded like organic pollutants, and their transport and bioavailability can be influenced by oxidation/reduction, complexation, adsorption, and precipitation/dissolution reactions (Schwarzenbach *et al.*, 2010). Among the metals mentioned above, some are considered as essential micronutrients, such as copper and zinc, while others including mercury, cadmium, and lead are not essential for biological activities to regulate physiological processes in plants (Clemens, 2001).

In addition, humans can be exposed to pollutants including toxic metals via contaminated water and the food chain by the consumption of vegetables high in Cd and seafood high in Hg (Adriano *et al.*, 2005; Schwarzenbach *et al.*, 2010). Serious health disorders have been reported following public exposure to different metals. For example, mercury is considered as a neurotoxic material that can damage DNA and the kidneys (Tchounwou *et al.*, 2003). Cadmium can also cause kidney and bone damage, and the increase of cancer risks has been reported even at low level of environmentally exposed populations (Jarup et Akesson, 2009).

Industrial and municipal wastewaters can contain many toxic metals that must be removed before discharge or reuse. Physicochemical methods, such as ion exchange, electrolysis, chemical precipitation, membrane filtration and adsorption have been typically used to decontaminate wastewaters (Fu et Wang, 2011). However, these methods can be ineffective or expensive for treating large volumes of water, since they consume high amount of chemicals and energy, making these conventional approaches less practical for low metal concentrations. Recently, the use of microalgae in wastewater bioremediation started to be a promising low-cost alternative to conventional methods. Indeed, it is well known that microalgae have a high capacity for metal uptake *via* channel-mediated transport due to their unicellular morphology that provide a large contact surface area to aquatic pollutants (Monteiro *et al.*, 2012). Moreover, microalgae are able to use inorganic nitrogen and phosphorus for growth, and the produced biomass can be used for various applications including the production of biogas such as methane from anaerobic digestion (Munoz *et al.*, 2005).

Since one must consider that algal strains differ in their capacity to uptake metals, in-depth studies of metal uptake and sequestration on different algal strains are necessary for providing the knowledge in the development of wastewater bioremediation strategies. Furthermore, the selection of algal strains must consider the capacity of cells to tolerate intracellular metals, since deleterious effects may limit cellular accumulation and sequestration capacity. For the study of cellular functions related to metal accumulation and tolerance, strains of *Chlamydomonas* represent appropriate unicellular model organisms due to rapid life cycle and their widespread use in cellular physiological studies (Hanikenne, 2003; Mendez-Alvarez *et al.*, 1999). Previously, the toxicity of Cd has been reported on *Chlamydomonas* strains, and deleterious effects were indicated by the inhibition of growth (Jamers *et al.*, 2009; Prasad *et al.*, 1998), ultrastructural cellular changes such as cytoplasmic vacuolization, starch accumulation and cytoplasmic electron-dense granules

(Aguilera et Amils, 2005; Nishikawa *et al.*, 2003), the development of membranous organelles (Visviki et Rachlin, 1994), the increase of the relative cell size (Jamers *et al.*, 2009; Visviki et Rachlin, 1994), and the inhibition of the photosynthetic activity (Faller *et al.*, 2005; Perreault *et al.*, 2011; Vega *et al.*, 2006).

Since microalgae are primary producers in aquatic ecosystems, they are widely used in laboratory bioassays for analyzing metal toxicity mechanisms and effects. It was found by Juneau *et al.* (2001) that *Microcystis aeruginosa* was the most sensitive species among six algal species to mercury since they observed a fast inhibitory effect of 37 nM Hg ($HgCl_2$) on the photosynthetic (PSII-PSI) activity only after 5 h (Juneau *et al.*, 2001). In another study, the maximum quantum efficiency of PSII photochemistry (F_V/F_M) and PSII operating efficiency ($\Delta F/Fm'$) were decreased in *Chlamydomonas reinhardtii* under treatment with MeHg at concentrations above 1 µM. However, this inhibitory effect was not observed under treatment with 5 µM $HgCl_2$ for 5 h on both ratios (Kukarskikh *et al.*, 2003). Moreover, previous studies on metal toxicity in microalgae showed the accumulation of metals (Cd^{2+}, Cu^{2+} and Zn^{2+}) in the cell wall (Macfie *et al.*, 1994), the alteration of cellular ultrastructures (Jamers *et al.*, 2009; Visviki et Rachlin, 1994), and the increase in number and volume of vacuoles containing metallic electron-dense deposits (Aguilera et Amils, 2005; Nishikawa *et al.*, 2003). Others investigations emphasized on understanding metal tolerance mechanisms in microalgae. A previous study found that intracellular Hg^{2+} was able to activate antioxidant enzymes (superoxide dismutase, catalase, and ascorbate peroxidase) for the elimination of generated reactive oxygen species (Elbaz *et al.*, 2010). Others studies demonstrated that the uptake of metals (Cu^{2+}, Hg^{2+}, Ag^{2+}, and Cd^{2+}) in microalgae increased significantly the synthesis of chelating compounds such as cysteine, glutathione, and phytochelatins permitting to regulate the intracellular concentrations of metals (Howe et Merchant, 1992; Lavoie *et al.*, 2009; Perales-Vela *et al.*, 2006; Stoiber *et al.*, 2010). Another tolerance mechanism was suggested to be involved in microalgae under cadmium stress effect. In fact, the effect

of Cd (20 μM) on the metabolism of polyphosphate (polyP) was investigated on *Chlamydomonas acidophila* (KT-1) by *in vivo* ^{31}P-nuclear magnetic resonance and by energy-dispersive X-ray analysis (Nishikawa *et al.*, 2003). Under Cd treatment for 3 days, the authors showed a complete degradation of polyP which was related to a strong increase of phosphate and the accumulation of Cd in vacuoles. They suggested that the vacuolar compartmentalization of Cd was as a cellular detoxification mechanism. In another study on *C. acidophila* KT-1, the same research group presented a decrease of 43 % in accumulated Cd, when Cd-treated algal cells were transferred into a Cd-free medium (Nishikawa *et al.*, 2009). Therefore, they proposed that the polyP metabolism in *C. acidophila* KT-1 contributed to the cellular tolerance for Cd, by chelating Cd in the vacuole as a Cd-phosphate complex and releasing it out of the cell.

The main objective of this research project was to investigate the accumulation and the sequestration of cadmium and mercury in different algal strains of *Chlamydomonas*. Therefore, this research project is presented in this thesis as three specific studies:

In the first study, the specific objective was to investigate the effect of Cd accumulation on green algae *Chlamydomonas reinhardtii* and *Chlamydomonas* CPCC 121. Both algal strains were exposed during 48 h to different concentrations of Cd (100-600 μM). Since acidic waters contain higher amounts of dissolved metals, the capacity of Cd accumulation and cellular tolerance of CPCC 121 was determined under two different pH conditions (4 and 7). Indeed, the tolerance ability for metals of CPCC 121 has been poorly studied. Under these experimental conditions, changes in cellular and biochemical parameters indicating the growth rate, cellular morphology, activity level of esterases, and PSII activity performance were used as indicators of Cd toxicity. The accumulation of Cd was confirmed by TEM images and energy-dispersive X-ray spectroscopy (EDX). Therefore, advantages and

limitations of both *Chlamydomonas* strains were discussed in the perspective of Cd bioremediation. The results are presented and discussed in Chapter IV.

In the second study, the specific objective was to determine the accumulation and toxicity effect of $CdCl_2$ on the level of extracytoplasmic polyphosphate (polyP). Two strains of *Chlamydomonas reinhardtii*, CC-125 and CC-503 that has an impaired cell wall, were exposed under neutral pH during 24-72 h to different concentrations of Cd (200-600 μM). Under these conditions, the level of extracytoplasmic polyP was investigated in relation to the presence or the deficiency of the cell wall barrier. In addition, the monitoring of polyP level as a biomarker of Cd toxicity using alga *C. reinhardtii* was discussed. Therefore, our results contributed to understand the involvement of extracytoplasmic polyP on algal cells of *C. reinhardtii* under Cd stress effect at neutral pH. The results are presented and discussed in Chapter V.

In the third study, the specific objective was to investigate the accumulation and toxicity effect of $HgCl_2$ on two strains of *Chlamydomonas reinhardtii*, CC-125 and CC-503 as a cell wall-deficient mutant, to evaluate the importance of the cell wall as a protective barrier. In this perspective, the level of polyphosphate (polyP) in the cell wall (extracytoplasmic) was determined to understand the physiological involvement of polyP under Hg stress effect. Therefore, we discussed the role of polyP in the cellular tolerance for Hg and the use of polyP level as a toxicity biomarker of Hg in algal cells. The results are presented and discussed in chapter VI.

CHAPTER I

ENVIRONMENTAL IMPACT OF METALS AND GREEN ALGAE

1.1 Environmental impact of mercury and cadmium

From the point of view of ecotoxicology and depending on the source of contaminants, environmental contaminants can be divided initially into two major categories: organic (from living organisms) or inorganic (from mineral sources). However this distinction is not precise since for example carbon dioxide is classified as an inorganic gas, but it is produced by living organisms. It should be noted that, some important environmental organic contaminants were obtained from both natural and anthropogenic sources, and as a good example polycyclic aromatic hydrocarbons (PAH) can be indicated. In the term of inorganic contaminants, metallic elements are considered as a major class of these contaminants. Metals are natural elements in crustal rocks and soils, as well it can be released into the water, air, and terrestrial environment by human activities from industrial manufacturing, mining, combustion products, and agricultural pesticides (Newman et Unger, 2002).

Mercury (Hg) is one the most hazardous metals that is known as a global aquatic contaminants, and its distribution continues through the global cycle of mercury and anthropogenic sources in waters and rivers. In the global cycle of mercury, 99 % of mercury is in the form of mercury vapor, which is considerable. Mercury vapor is a

chemically stable monatomic gas, so its residence time in the atmosphere is estimated to be of a year or more. Therefore, it is obvious that the global cycle of mercury begins with its evaporation from land and water surfaces (sea and rivers). However, its oxidation via the action of ozone leads to its conversion into water-soluble ionic mercury (Hg^{2+}) that can be returned on the surface of earth as rain water. Human can be exposed to mercury via the methylation of divalent inorganic mercury (Hg^{2+}) by organisms (bacteria and phytoplankton) and its accumulation in the aquatic food chain (from plankton and algae to fish and then to human). On the other hand, the atmosphere contains less than 1 % of methylmercury compounds that their origin is not yet known and these compounds can be taken by the aquatic biota. The reduction of Hg^{2+} by aquatic microorganisms leads to the formation of Hg^0 in surface waters (Clarkson, 1998).

The methylation of inorganic mercury (Hg^{2+} as the main species) occurs in waters and sediments, which needs the presence of a suitable methyl donor molecule such as biotic or abiotic materials (Ullrich *et al.*, 2001). However, many studies suggested a high potential of microbial methylation in sediment sites under anaerobic conditions and sulfate-reducing bacteria as the principal methylators (Compeau et Bartha, 1985). In aquatic environment, the biotic methylation of inorganic mercury happens in microorganisms (aerobes and anaerobes) after the uptake of the soluble mercury (Ullrich *et al.*, 2001). Abiotic methylation is possible in the presence of chemical methylating agents such as methylcobalamin and methyltin compounds, and humic matter released to the environment by biotic processes. Although the origin of these compounds comes from biotic processes, the abiotic term refers to any non-enzymatic methylation (Weber, 1993).

Methylmercury is the most abundant organomercury compound that exists in freshwaters (lakes and rivers) and can be generated from Hg^{2+} by different mechanisms (Ullrich *et al.*, 2001). Although the hydrolysis reaction of

methylmercury is thermodynamically feasible, kinetically it is not realizable, so it can be stable in an aqueous solution. It should be noted that, however, methylmercury can be degraded photochemically by microbial action. The Hg^0 and dimethylmercury could not be simply accumulated by the aquatic biota because they are not reactive with cellular components, while the Hg^{2+} and methylmercury are able to be accumulated in the aquatic food chain. However, the bioaccumulation of methylmercury is more possible than inorganic mercury in the aquatic biota. One reason that can explain the difference between the bioaccumulation of inorganic ($HgCl_2$) and organic mercury (CH_3HgCl) is the lipid solubility of CH_3HgCl that permits to maintain it in the fatty tissues of animals (Morel *et al.*, 1998). In fish, however, the study of Boudou and Ribeyre (1997) showed that methylmercury liposolubility could not be the only reason for more bioaccumulation of methylmercury in fish muscle. In fact, the high absorption of MeHg by the intestine wall was more important since inorganic mercury was adsorbed at the microvilli interface (Boudou et Ribeyre, 1997).

Besides natural sources of mercury, human activities such as combustion of fossil fuels (coal) and municipal waste incineration, metal smelting, mining and industrial waste discharges of mercury led to add the large quantities of mercury to the environment. Organic forms of mercury including methyl, ethyl, and phenyl types have been used as biocides, pesticides, and household antiseptics which can explain their presence into the industrial environment. Therefore, the wide mercury distribution in waters and rivers is clear (Tchounwou *et al.*, 2003). From the point of view of human exposure to mercury, two forms of mercury are more important, dental amalgam fillings and methylmercury compounds (Clarkson, 1998). Indeed, the use of mercury amalgam tooth fillings is very common since nineteenth century. Therefore, mercury vapor can be inhaled during chewing (Clarkson, 2002), while there is no serious restriction against using these compounds. Methylmercury compounds can be accumulated in fish tissues and its dose can be bioamplified

through the aquatic food chain (Boudou et Ribeyre, 1997; Ullrich *et al.*, 2001). Indeed, these compounds are considered toxic towards public health, causing brain, kidneys and immune system damages (Bernard, 2011; Tchounwou *et al.*, 2003).

Today, toxic effects of cadmium towards human, plants, and animals are well-known. Cadmium can be released in atmospheric, aquatic and terrestrial environment from natural and anthropogenic sources. Volcanoes, forest fires, and airborne soil particles are the major natural sources of cadmium which can be transferred in atmosphere by aerosol, and deposited in soils, aquatic systems, and sediments. Moreover, cadmium exists naturally in many minerals, rocks and soils in low concentrations. Water soluble cadmium compounds can be mobile and bioavailable for living cells in water and soils depending on their chemistry. The major anthropic sources of Cd released to aquatic environment are non-ferrous metal smelting and refining, manufacturing of chemicals and metals, mining, waste incineration, and domestic wastewater. Nickel-cadmium batteries were considered as a major source of cadmium disposed with municipal wastes (UNEP, 2010).

Non-smoking human populations are exposed to cadmium by multiple sources predominately from food (90 %). In general, all foods contain cadmium with different concentrations depending on the level of contaminated areas and the type of food. Cadmium can be found more in vegetables than other types of food including meat, egg, and milk (Jarup et Akesson, 2009; UNEP, 2010). Kidneys are the first target organs in chronic cadmium poisoning (Bernard, 2011). Kidney tubular damage, renal dysfunction, bone damage, and cancer have been shown as the result of environmentally exposed populations to low-level concentrations of Cd (Jarup et Akesson, 2009; Satarug *et al.*, 2010).

Therefore, appropriate strategies and efficient and economic methods should be applied to remove metals from freshwater aquatic reservoirs and to reduce their impact on aquatic environment and human health. We noticed this importance and it

was our interest to develop the knowledge of phycoremediation of contaminated water by metals using different strains of *Chlamydomonas*. Furthermore, it is important to notice that microalgae are the primary producers in aquatic environment which occupy the first place in the food chain with a high capacity for metal uptake.

1.2 Using green algae for the phycoremediation of metals

Metal removal from aquatic environment has become an important challenge in wastewaters remediation, since population growth and industrialization. Even though various conventional methods including chemical precipitation, ion exchange, adsorption, ultrafiltration, reverse osmosis, electrodialysis, coagulation-flocculation, flotation and electrochemical methods have been used to remove metals from wastewaters, some disadvantages have limited their use in metal removal. For example, chemical precipitation is less practical for low metal concentrations and creates large amount of sludge. As well, ion exchange can be expensive for large volumes of water since it needs the regeneration of resins by chemical reagents, and electrochemical methods consume high amount of electrical energy (Fu et Wang, 2011).

Bioremediation technologies became a promising low-cost and efficient alternative in an eco-friendly manner for contaminant removal from aqueous system. Phycoremediation as a new approach of biological remediation technologies represents the use of algae for the removal or biotransformation of contaminants including metals from polluted environmental matrices (Kumar *et al.*, 2015). Unicellular morphology of microalgae provides a large contact surface area to aquatic pollutants therefore a high capacity for metal uptake (Monteiro *et al.*, 2012). On the other hand, microalgae have shown efficient defense mechanisms to detoxify metal and to survive in metal-containing media (It will be discussed in Section 1.3). Both of these capacities, the uptake and detoxifying process, make them appropriate candidates for biological remediation systems to remove metals. The advantages of

using microalgae in the removal of metals from aquatic environment are a high and rapid capacity to accumulate metals, no toxic sludge generation, the elimination of azote and phosphorous preventing eutrophication, the inexpensive and easy growth using solar light and CO_2, saving time and energy, the rapid growth rate compared to higher plants, the potential for CO_2 capture and biofuel production (Kumar *et al.*, 2015; Monteiro *et al.*, 2012; Sivakumar *et al.*, 2012).

Some species of *Chlamydomonas* are able to grow under both conditions: the phototrophic growth by using CO_2 as a sole carbon source and light energy involving photosynthesis process, and the heterotrophic growth in darkness with acetate as a carbon source. This heterotrophic property permits the isolation of viable mutants which are light-sensitive and unable to perform photosynthesis (Dent *et al.*, 2001; Harris, 2009). The cell structure of *C. reinhardtii* (wild-type) includes the central nucleus with a prominent nucleolus, a single basal chloroplast surrounding the nucleus, pyrenoid within the chloroplast, and contractile vacuoles. The cell wall is located close to the plasma membrane and depending on the genus can vary in thickness (Harris, 2009). As Figure 1.1 shows most of the cellular volume is occupied by the chloroplast.

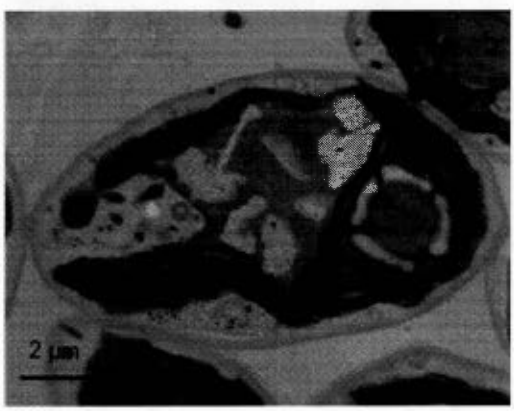

Figure 1.1 TEM image of algal cell ultrastructure for *Chlamydomonas reinhardtii* wild-type (CC-125) cultivated in High Salt Medium (HSM).

Green alga *Chlamydomonas* is a unicellular eukaryote organism having a rapid growth rate with a doubling time less than 10 h (Dent *et al.*, 2001). Therefore, its manipulation can be performed easily for the study of detoxification mechanisms associated with metallic stress. *Chlamydomonas* is an excellent genetic model (Dent *et al.*, 2001), so numerous genetically modified strains are available (Joint Genome Institute, JGI, vers 4.0). *Chlamydomonas reinhardtii* is an organism with capability of growth in the laboratory either in liquid culture or on agar in simple media (Harris, 2009). Cell population in the liquid cultures of *Chlamydomonas* are almost homogenous (Dent *et al.*, 2001). Therefore, it would be possible to analyse cellular and biochemical changes induced by metal toxicity. *Chlamydomonas* species represent an appropriate unicellular model organism for physiological and toxicological studies (Dent *et al.*, 2001; Hanikenne, 2003; Mendez-Alvarez *et al.*, 1999). In addition, acid tolerant *Chlamydomonas* species were isolated from different acid environment in Japan, Germany, Canada, and the United States of America. These species were able to maintain the internal pH to neutral (Harris, 2009). An acid resistant *Chlamydomonas* species, *C. acidophila*, showed high tolerance to the exposure of several metals in acidic conditions (Nishikawa et Tominaga, 2001; Perreault *et al.*, 2010; Spijkerman *et al.*, 2007).

1.3 Using green algae as a model of cellular toxicity

1.3.1 Cellular defense mechanisms against metal toxicity

In response to metal toxicity, different resistance mechanisms have been developed by microalgae to allow their survival in media when toxic metals are present. In this subsection, the tolerance mechanisms by microalgae for metals are explained by the binding of metal ions to the cell wall, the chelation with phytochelatins (PC_s), the sequestration and compartmentalization in the vacuole, the cell ultrastructural changes, the polyphosphate sequestration and metabolism, and the metal excretion.

The role of the cell wall to protect microalgal cells against toxic metal ions was studied by Macfie and co-workers by using two strains of *C. reinhardtii*. The cell density of the wild-type strain of *C. reinhardtii* was significantly higher than the strain having an impaired cell wall when exposed to Cd^{2+}, Cu^{2+}, Co^{2+}, Ni^{2+}, and more clearly to Co^{2+} and Cu^{2+} at pH conditions 5 and 6.8. Therefore, they suggested the presence of sensitive sites inside or at the surface of the cell wall that can prevent metal uptake into the cellular cytoplasm through its binding (Macfie *et al.*, 1994). However, in another study of this research group, the wild-type strain of *C. reinhardtii* showed more capability of Cd accumulation per unit weight than the wall-less cells, while both strains showed a comparable amount of Cu uptake with more sensitivity of the wall-less cells. Thus, they concluded both detoxification mechanisms, external and internal, of metal ions in *C. reinhardtii* (Macfie et Welbourn, 2000). As a consequence, although the microalgal cell wall acts as the first barrier to metal ions uptake inside the cells, the cell wall capacity of microalgae for high metal-binding can be accounted for metal removal from the aquatic environment.

Chelation of metals with phytochelatins (PC_s) is considered as an important cellular mechanism for metal detoxification. Phytochelatins consist of three amino acids, glutamine (Glu), cysteine (Cys), and glycine (Gly), which are characterized by the repetition of the dipeptide units (γ-Glu-Cys) followed by a terminal Gly (Pal et Rai, 2010). Indeed, monomer is provided by tripeptide glutathione (GSH; γ-GluCysGly). The enzyme, phytochelatin synthase (PCs), is a γ-glutamylcysteine dipeptidyl transpeptidase, which catalyzes the transpeptidation of γ- Glu-Cys moiety from glutathione to a second glutathione molecule. This process leads to produce $(\gamma\text{-Glu-Cys})_2$-Gly or an n + 1 oligomer, $(\gamma\text{-Glu-Cys})_n$-Gly which is the general formula of phytochelatins (Grill *et al.*, 1989) (Figure 1.2). In $(\gamma\text{-Glu-Cys})_n$-Gly, "n" generally ranges from 2 to 5, but can be as high as 11 (Cobbett, 2000). Phytochelatin synthase

(PCs) is constitutively present in various plant species, and the Cd^{2+} has demonstrated to be a strong activator of this enzyme (Grill *et al.*, 1989).

The mechanism of metal detoxification by phytochelatins in microalgae is summarized in Figure 1.3. At first, in the presence of metal ions such as Cd^{2+}, the activity of PCs is increased (Perales-Vela *et al.*, 2006). Equally important, the enzymes involved in glutathione synthesis, γ-glutamylcysteine synthetase and glutathione synthetase, play an essential role in the regulation of phytochelatin biosynthetic pathway since glutathione is the primary peptide involved in binding metal ions (Howe et Merchant, 1992). The second step is the chelation of metal ions

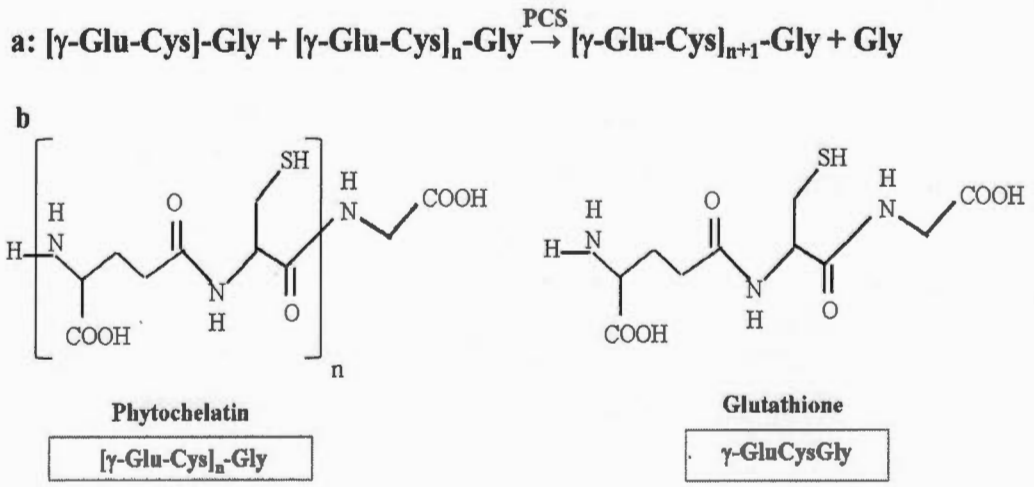

Figure 1.2 a) General mechanism involved in PC_s synthesis b) Chemical structures of phytochelatin and glutathione.

and the formation of metal-PC_s complex by the synthetized phytochelatins. This process prevents the circulation of free metal ions in cytoplasm, so toxic reactions are reduced between metal ions and essential macromolecules such as enzymes, nucleic acids, and lipids. Finally, the metal-PC_s complexes will be transported to the vacuoles by vacuolar transporter (HMT1) and are stored as a final form (HMW). Indeed, metal-PC_s complexes are divided into two categories: low molecular weight (LMW) and high molecular weight (HMW) forms. The metal-PC_s complexes with a high

molecular weight are formed by the incorporation of sulfide inorganic ions (S^{2-}) that improve the stabilization of metal-PC_s complexes (Perales-Vela *et al.*, 2006).

Sequestration and compartmentalization of metal ions in the vacuole is also suggested as a detoxification mechanism in algae. Spherical vacuolar inclusions in marine diatom *Skeletonema costatum*, which contained either sulfur and cadmium or sulfur and copper, were detected when exposure to Cd (1 mg L^{-1}) or copper (0.05 mg L^{-1}), respectively with a sulfur/metal ratio of 1.5 (Nassiri *et al.*, 1997). The appearance of electron-dense granules was observed in the vacuoles of *C. acidophila* and *Chlamydomonas* sp. exposed to Cd, which contributed in detoxification mechanisms (Aguilera et Amils, 2005; Nishikawa *et al.*, 2003).

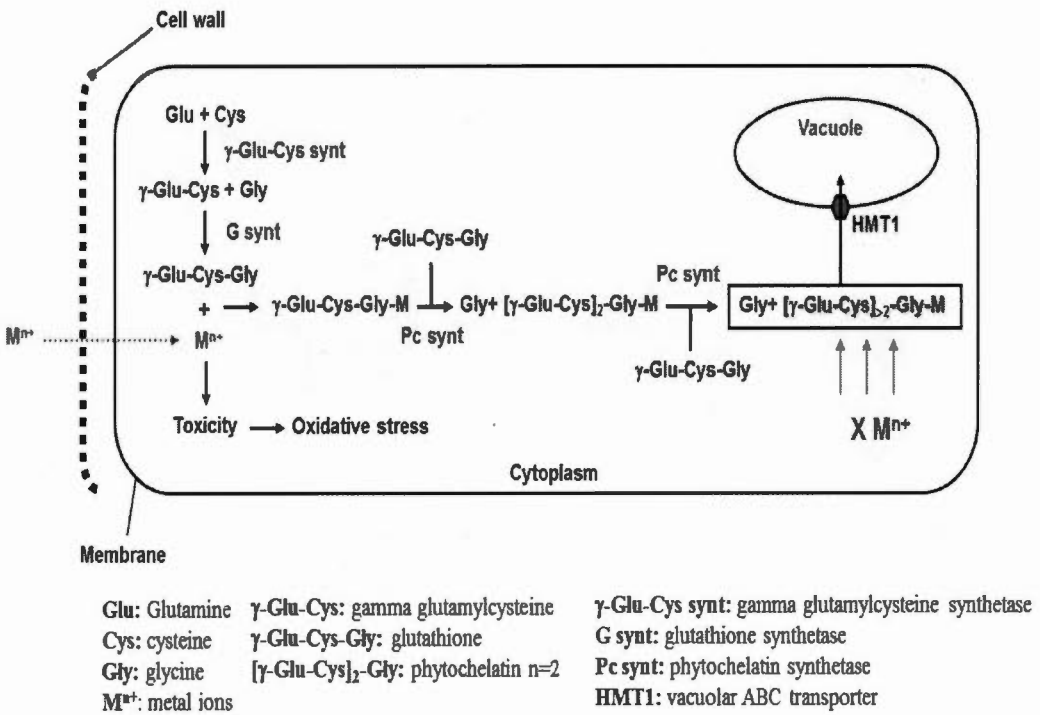

Figure 1.3 General schema of metal detoxification mechanism by phytochelatins in microalgae (made from Howe and Merchant., 1992, Perales-Vela *et al.*, 2006).

The accumulation of lipid was observed in alga *Dunaliella salina* after a long term exposure to Cu^{2+} (4.9 x 10^{-4} µM) and Cd^{2+} (4.5 x 10^{-6} µM), which was suggested as a response to nutrient limitation induced by copper and cadmium (Visviki et Rachlin, 1994). The appearance of membranous organelles was detected in 45.5 % and 60.6% of *C. bullosa* cells exposed to Cd^{2+} (0.025 µM) and Cu^{2+} (0.78 µM), respectively at 96 h. The authors suggested the development of these organelles as a detoxification mechanism, since their great surface area can bind metal ions to sulfhydryl groups (Visviki et Rachlin, 1994). The accumulation of starch granules was detected in *C. acidophila* when the cells were exposed to Cd (20 µM) for three days to compensate the deterioration of mitochondria (Nishikawa *et al.*, 2003).

Metal excretion is another mechanism that algal cells used to protect against the toxicity of metals in the environment. For example, the excretion of Cd from *C. acidophila* KT-1 cells was reported by the study of Nishikawa *et al.* (2009). Finally, the role of polyphosphate bodies in metal detoxification in algae will be discussed in Chapter II.

1.3.2 Wild-type and cell wall-deficient mutants of *Chlamydomonas*

As mentioned before (Section 1.2), *Chlamydomonas* represents an appropriate unicellular model organism for physiological and toxicological studies. The cell wall is considered as a barrier between the physical environment and the cytoplasm, which is able to bind metals (Kumar *et al.*, 2015).

The cell wall of *Chlamydomonas* consists mainly of hydroxyproline-rich glycoproteins with galactose and arabinose as the predominant sugars in *C. reinhardtii* (Harris, 2009). Robert *et al.* (1972) defined seven wall layers in electron micrographs of C. *reinhardtii*, and Goodenough and Heuser (1985) described the structure of each layer (Goodenough et Heuser, 1985; Roberts *et al.*, 1972). The deepest layer, W1, varies in thickness from 30 to 200 nm. The second layer, W2, is composed of a fibrous glycoprotein network, and with layers W4 (a granular layer)

and W6 all together make the "central triplet". These layers are very constant in appearance and size, while the outer layer, W7, may be absent under some growth conditions. Layers W3 and W5 were electron-transparent regions, so Goodenough and Heuser (1985) could not describe their structures. *Chlamydomonas* wall-deficient mutants were isolated and classified into three morphological groups. The cw92 mutant, used in our studies, is classified in class C in which the cell walls are absent or produced in a quantity less than wild-type cells (Harris, 2009).

1.3.3 Toxicity impact of metals at the cellular level

Toxicity impact of metals on algal cells can be related to the displacement of essential metal ions in biomolecules with toxic metals as well to the increase of the cellular concentration of reactive oxygen species (ROS). As it was shown by different studies, toxicity impact of metals can cause the alteration of physiological and biochemical processes such as cell growth and photosynthesis and the change of cellular morphology (Aguilera et Amils, 2005; Elbaz *et al.*, 2010; Jamers *et al.*, 2009; Macfie *et al.*, 1994; Nassiri *et al.*, 1997; Nishikawa et Tominaga, 2001; Nishikawa *et al.*, 2003; Perreault *et al.*, 2011; Pinto *et al.*, 2003; Szivak *et al.*, 2009; Tripathi *et al.*, 2006; Visviki et Rachlin, 1994; Walsh et Hunter, 1992).

Cell growth as a toxicity indicator of metals to microalgae was used in many eco toxicological studies. However, growth inhibition in microalgae is dependent on the concentration and the chemical nature of metal ions as well as algal strains. For example, a low concentration of Hg (1 µM) did not show growth inhibition in *C. reinhardtii* during 96 h, while high mercury concentrations inhibited strongly its growth (Elbaz *et al.*, 2010). In another study, effective metal concentrations limiting the growth by 50% (EC_{50}) in *C. acidophila* varied among used metals (14.4 µM Cd^{2+}, 81.3 µM Co^{2+}, 141 µM Cu^{2+}, 1.16 µM mM Zn^{2+}) during 72 h (Nishikawa et Tominaga, 2001). As mentioned before (Subsection 1.3.1), the wild-type and wall-

less mutants of *C. reinhardtii* manifested different cell density against toxicity effects of four metals (Macfie *et al.*, 1994).

Oxygenic photosynthesis is a biological oxidation-reduction process by which all oxygen-evolving organisms including algae absorb light energy to produce carbohydrates from carbon dioxide and water. Oxygenic photosynthesis depends on two reaction center complexes, Photosystem I (PSI) and Photosystem II (PSII). Each reaction center contains its own reaction center chlorophyll pair: P680 in PSII and P700 in PSI. PSII and PSI are connected by the cytochrome *bf* complex and a series of mobile electron carriers including plastoquinone and plastocyanin. PSII and PSI participate in the noncyclic transport of electrons from water to $NADP^+$, and the PSII and PSI antenna systems capture light to provide the energy for this process. Accompanying this electron transport, a proton gradient is created across the membrane, and the energy stored in this electrochemical proton gradient is used for the synthesis of ATP by ATP synthase. NADPH and ATP, the products of the light-driven electron and proton transport reactions, provide the necessary energy to reduce carbon dioxide to carbohydrate (Figure 1.4) (Govindjee *et al.*, 2010; Malkin et Niyogi, 2000; Whitmarsh et Govindjee., 1999). Both Photosystems I and II activities can be altered by toxic metals. For example, chl *a* fluorescence intensity was decreased gradually for all PSII reduction steps (shown by the O-J, J-I, and I-P transients) when cells of C. *reinhardtii* were exposed to different concentrations of Cd^{2+} from 0.15 to 4.62 µM during 24 h, indicating a decrease of electron transport from the water-splitting system to PSI. Such gradual inhibition was also observed for PSI activity. In fact, a reduced maximal (delta I)/ $I_{O\ 820nm}$ showed the decrease in the number of photoactive PSI reaction centers that was of 50 % for cells treated with 4.62 µM of Cd^{2+} compared to control (Perreault *et al.*, 2011).

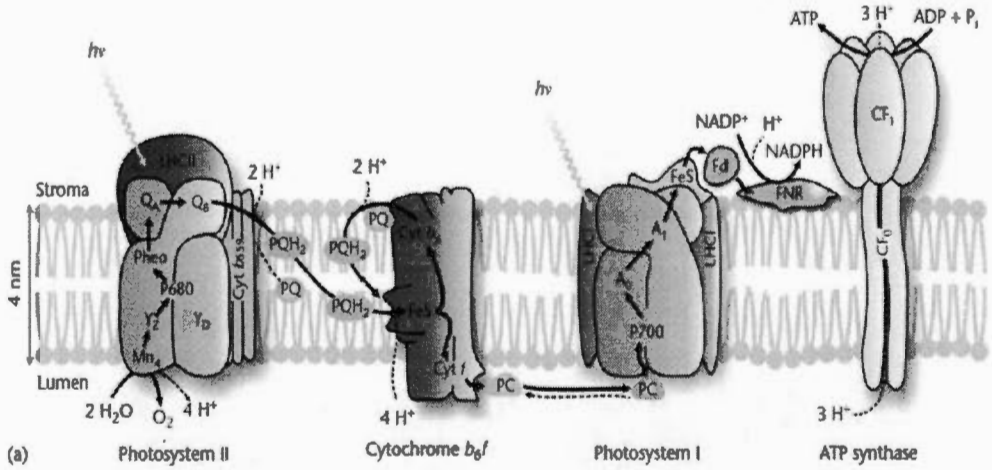

Figure 1.4 Protein complexes and cofactors involved in the linear transport of electrons and protons of photosynthesis in higher plants. Abbreviations: (Mn_4) Mn_4O_xCa where $x \geq 4$, (Y_z) tyrosine-161, (Pheo) pheophytin, (Q_A) and (Q_B) two plastoquinone molecules, (PQ) plastoquinone molecules, (FeS) iron–sulfur protein, (PC) plastocyanin, (A_0) a special chlorophyll *a* molecule, (A_1) vitamin K, (Fd) ferredoxin, (FNR) ferredoxin–NADP reductase, (LHCI and LHCII) light-harvesting complexes of photosystems I and II, (NADP reductase and $NADP^+$), nicotinamide–adenine dinucleotide phosphate (Whitmarsh et Govindjee., 1999).

The generation of ROS including the superoxide anion ($O_2 \cdot^-$), hydrogen peroxide (H_2O_2), hydroxyl radical ($\cdot OH$), singlet oxygen ($^1O_2$), and many others is another reason which explains the toxic effect of metals to aquatic organisms including algae affecting different cell compartments. Indeed, the oxidative stress induced in living organisms can be the result of the increase of cellular concentration of ROS (Pinto *et al.*, 2003). Catalases (CAT), peroxidases like glutathione peroxidase (GSH), ascorbate peroxidase (APX), and superoxide dismutase (SOD) were known as the enzymatic defense in *C. reinhardtii* against these toxic oxygen species (Mendez-Alvarez *et al.*, 1999). As well, the enzymatic activity of SOD was increased with an increase in the concentrations of Cu^{2+} (from 2.5 to 10 µM) and Zn^{2+} (from 5 to 25 µM), when green alga *Scenedesmus* sp. was exposed for both short (6 h) and long-term (7 d) experiments. In parallel, the activity of both enzymes, APX and CAT, was

significantly increased under 2.5 μM Cu^{2+} for both short- and long-term experiments, and under a long-term exposure to 25 μM Zn^{2+}. However, 10 μM Cu^{2+} inhibited the activity of APX and CAT during the long-term experiment (Tripathi *et al.*, 2006). They suggested that the antioxidant enzymes played a protective role against the toxic effect of Cu^{2+} and Zn^{2+}, when the oxidative stress was moderate at low concentrations. In another study, both redox [Fe (III), Cu (II), Ag (I), Cr (III), Cr (VI)] and non-redox [Pb (II), Cd (II), Zn (II)] active metals induced slightly the increase of intracellular ROS levels in *C. reinhardtii*. Flow cytometry analysis of algal cells treated with different metals and stained with H_2DFFDA (5-(and-6)-carboxy-2′, 7′-dihydrodifluorofluorescein diacetate) revealed that both redox and non-redox active metals at environmental levels were capable of inducing oxidative stress for a short-term exposure (2.5 h). They reported that the effective free metal ion concentrations from 10^{-6} to 10^{-9} M, except for Fe (III), were effective at 10^{-18} M. Moreover, the intracellular localization of ROS production in H_2DFFDA-stained cells by fluorescence microscopy showed that the detoxification mechanisms were localized in the mitochondria (Szivak *et al.*, 2009).

Finally, the toxicity impact of metals on algal cells can lead to the change of the cellular morphology including the cytoplasmic vacuolization, the accumulation of lipid and starch granules, the appearance of membranous organelles, the change of periplasmalemmal space, the increase of cell size, the appearance of electron-dense granules in vacuoles, and the increase or decrease in the number of polyphosphate bodies. Some of these changes were discussed in previous section (Subsection 1.3.1), and some others will be discussed in Chapter II.

CHAPTER II

ROLE OF INORGANIC POLYPHOSPHATE IN LIVING CELLS

2.1 Chemical structure of inorganic polyphosphate

Inorganic polyphosphate (polyP) is a linear polymer of many orthophosphate (Pi) residues linked by high-energy phosphoanhydride bonds (Figure 2.1). The presence of polyP has been known for a long time in many organisms such as fungi, bacteria, and yeast. Otherwise, insufficient attention toward this polymer has been given due to the lack of simple, sensitive, and definitive methods and techniques to evaluate its concentration in biological sources (Kornberg, 1995; Kornberg *et al.*, 1999; Kulaev *et al.*, 2004). Indeed, the most information about physiological functions of polyP was obtained from the microbial studies by Kornberg and co-workers even though some studies showed the importance of polyphosphate in algae. For example, as more recently polyphosphate contribution for metal tolerance was found in green alga *Chlamydomonas* (Nishikawa *et al.*, 2009).

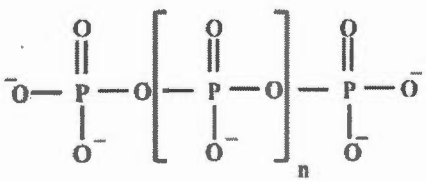

Figure 2.1 Inorganic polyphosphate structure.

2.2 Polyphosphate in living organisms and its localization

Inorganic polyphosphate was detected in many living organisms including bacteria, fungi, protozoa, yeast, algae, plants and animals (Kornberg, 1995; Kulaev *et al.*, 2004). Using light and electron microscopy and nuclear magnetic resonance (NMR), polyP has been identified in different cellular compartments. The electron-dense polyphosphate bodies were found in the prokaryotic alga *plectonema boryanum*, and STEM micrograph showed generally one large body detected in each cell. Elemental analysis by energy dispersive X-ray spectrometer showed the presence of Mg, P, K, and sometimes Ca in polyphosphate bodies of control cells in *P. boryanum* (Jensen *et al.*, 1982a).

The study of Sianoudis *et al.* (1986) demonstrated that one part of polyP in *Chlorella fusca* cells was located outside of the cytoplasmic membrane as complexes with Mg^{2+}. ^{31}P-NMR spectra of cell suspensions of *C. fusca* at physiological pH (pH 7.1) detected the signal of polyP (PP_4) at -22.5 ppm. However, the PP_4 signal had its origin from polyP located outside of the cytoplasmic membrane. The evidence for this localization of polyP was obtained either under alkalization after adjustment of pH to 12.9 or EDTA addition to the cell suspensions. Indeed, under these environmental changes the PP_4 signal was shifted to -20.9 ppm, and its intensity was decreased indicating that polyP was accessible to environmental changes. Since the PP_4 signal of polyphosphates in *Chlorella* was not related to H^+ concentration (between pH 4.3-12.8) in the presence of Mg^{2+}, they concluded that the chemical shift of the PP_4 signal was due to the loss of Mg^{2+} ions (Sianoudis *et al.*, 1986).

Polyphosphate bodies were also detected in the vacuoles of alga *C. fusca*, and the analysis by electron microscopy (STEM) demonstrated that they were non-membranous without a defined shape (Wong *et al.*, 1994). Cytoplasmic vacuoles in the cell wall-deficient *Chlamydomonas reinhardtii* contained dense granules, and ^{31}P-NMR demonstrated the presence of pyrophosphate (PPi) and polyphosphates in the

purified granules. Moreover, phosphorous as the major inorganic element was detected by EDX in these granules (Komine *et al.*, 2000). Electron dense vacuoles were also seen, when the whole cells of *Chlamydomonas* were visualized by transmission electron microscopy without fixation and staining. A large number of dense vacuoles of 30-40 vacuoles was reported in each *Chlamydomonas* cell with varying sizes and an average diameter of 200 nm. The localization of polyphosphate was also performed by staining, and *C. reinhardtii* cells incubated in solution of DAPI (0.2 mg/mL) were examined by confocal fluorescence microscopy. DAPI fluorescence was observed in numerous intracellular and small vacuoles, which in some cells it was fused into the large vacuoles. The presence of high concentrations of PPi and of short and long chain of polyphosphates were reported in purified electron-dense vacuoles by chemical analysis (using iodixanol density gradients). In fact, these organelles demonstrated vacuolar proton ATPase ($V\text{-}H^+$ ATPase) and proton pyrophosphatase (H^+-PPase) activities (Ruiz *et al.*, 2001).

The study of Nishikawa *et al.* (2006) demonstrated the presence of extracellular polyP in *Chlamydomonas acidophila* KT-1 combined with cations, since two major and sharp polyP signals, inorganic phosphate and polyphosphate, were detected upon addition of EDTA to the suspension of control cells in *C. acidophila* KT. They suggested that EDTA was not permeable to cell membrane and was bound to outer cellular cations, preventing the formation of the wide polyP peaks in NMR by these cations (Nishikawa *et al.*, 2006). The cell wall bound polyphosphate was also found in *C. reinhardtii* by staining with specific polyP binding proteins (EcPPXc). The wild-type (mt^+ 137c) cells were stained at various times during mitosis and confocal microscopy analysis revealed the strongest cell wall bound polyphosphate signal after 3 h in darkness. In other word, its abundance reached a highest point at the end of cytokinesis during the cell cycle. At 2.25 h, only few cells demonstrated intensive cell wall bound polyphosphate signal and no fluorescence from the cell wall was

visualized after 0.5 h, indicating a fluctuation of polyP during the cell growth (Werner *et al.*, 2007).

2.3 Polyphosphate metabolism

Two types of enzyme are responsible for the regulation of intracellular polyphosphate in most microorganisms. The reversible polymerization of polyphosphate ($polyP_n$) can be catalyzed by PPK or polyphosphate kinase. In fact, this enzyme transports the terminal phosphate from ATP to the polyphosphate chain that was purified from *Escherichia coli* (Ahn et Kornberg, 1990). As well, ADP (Bonting *et al.*, 1991) and glucose-6-phosphate (Pepin et Wood, 1986) were also found as the high-energy phosphate donors to polyphosphate. In addition to the polyP synthesis from ATP, polyP can be used as a donor or substrate in the presence of PPK, which provides its conversion to ATP with ADP in excess (Kornberg *et al.*, 1999). Exopolyphosphatase or PPX is also considered as one of the most important enzymes associated with polyP metabolism (Kulaev *et al.*, 2004). PPX is responsible for the removal of the terminal phosphate from polyphosphate according to this reaction:

$$PolyP_n + ATP \xleftrightarrow{PPK} PolyP_{n+1} \xrightarrow{PPX} Pi$$

In other word, PPX hydrolyzes irreversibly polyphosphate to orthophosphate (Pi) and this enzyme was purified from *E. coli* (Akiyam *et al.*, 1993; Keasling *et al.*, 1993). Although polyphosphate kinase was found in many bacteria (Kulaev *et al.*, 2004), the biochemistry of polyphosphate synthesis was not known in microalgae. Indeed, the mold *Dictyostelium discoideum* was known as the only eukaryote to have a PPK similar to the bacterial PPK. It was reported that *D. discoideum* had similar vacuoles (acidocalcisomes) to electron-dense vacuoles in *C. reinhardtii* which

accumulated the large amounts of polyP and Ca^{2+}, which were responsible for Ca^{2+} flux in cells (Gomez-Garcia et Kornberg, 2004; Ruiz *et al.*, 2001).

2.4 Physiologic functions of polyphosphate

The first and main function of polyP is the phosphate storage. An excess of phosphate (Pi), when its utilization by cells is limited, can be accumulated in the form of polyP. A constant level of phosphate in cells is very important, since the phosphate controls powerfully biochemical processes. On the other hand, any excess of phosphate especially in cells, which are not able to synthesize polyP in large amounts, can be caused by the change of osmotic pressure and pH (Kulaev *et al.*, 1999; Kulaev *et al.*, 2004). Indeed, inorganic polyphosphate is considered as a multifunctional molecule. PolyP has been implicated as an ATP substitute and phosphate storage, a regulator of genetic and enzymatic activities in the metabolism of nucleic acids and others acid biopolymers. Moreover, polyP is a strong chelator of metals ions, and its role against environmental stresses including nutrition deficiency, metallic, osmotic, and alkalization stress is explained in the following. Briefly, polyP has numerous biological functions that vary depending on the organism and the compartment where it is located (Kornberg *et al.*, 1999; Kulaev *et al.*, 1999).

2.4.1 Reservoir of phosphate (Pi) energy

PolyP under the combination of different enzymatic activities can be used as a substitute for ATP. To illustrate, AMP phosphotransferase catalyzes an attack by AMP at the end of the polyP chain that generates ADP (Equation 1 of Figure 2.2). Then, ADP can be converted to ATP by the action of PPK (Equations 2 of Figure 2.2). As well, ATP can be formed from two molecules of ADP by coupling with adenylate kinase (Equation 3 of Figure 2.2). Indeed, adenylate kinase equilibrates AMP, ADP, and ATP (Kornberg, 1995; Kornberg *et al.*, 1999). AMP phosphotransferase was purified from *Acinetobacter* strain 210A (Bonting *et al.*, 1991), and they concluded that polyphosphate can act directly as a reservoir for

energy in this strain by a combined action of AMP phosphotransferase and adenylate kinase. Glucokinase activities can be involved in phosphorylation of glucose either using ATP or polyP as donors (Equations 4 and 5 of Figure 2.2) (Hsieh *et al.*, 1993).

As it was shown by previous studies, multiple exopolyphosphatases did regulate a stable level of intracellular phosphates for metabolism and growth in *E.coli* (Akiyam *et al.*, 1993; Keasling *et al.*, 1993). The major storage form of phosphate in *Chlamydomonas* was polyphosphate according to the study of Siderius *et al.* 1996 (Siderius *et al.*, 1996). It was also found that polyphosphate bodies of *C. reinhardtii* (Ruiz *et al.*, 2001) and acidocalcisomes organelles in protozoa (Docampo et Moreno, 2001), having pyrophosphate (PPi) and polyP, were used as phosphate storage in eukaryotic microorganisms. Probably, the function of polyphosphate as phosphate storage was associated with the activity of different forms of exopolyphosphatase (Kulaev *et al.*, 2004).

2.4.2 Cation sequestration and storage

As mentioned before (section 2.2), the electron microscopy was capable of the visualization of polyP in electron-dense regions. When this technique was combined with X-ray energy dispersive analysis, the presence of the phosphorous probably as polyP and different metal cations were revealed in these granules. Following the response to how metals may be sequestrated in polyphosphate bodies, Jensen *et al.* (1982a) concluded that lipids, proteins and polyphosphates are the composition of these bodies. Indeed, the polyphosphate compound is a polyanion having a strong affinity with cations, and it can interact with metal ions in a typical Lewis acid-base reaction. Moreover, vacuolar granules in *C. reinhardtii* revealed the presence of polyphosphate and a major protein with a mass of about 70 KDa as the major components of these granules. Protein characterization was done in order to better understand the functions of these granules. It was found that probably the vacuoles

could perform both functions: the degradation within the cell and the secretion of specific proteins when it was necessary for living cells (Komine *et al.*, 2000).

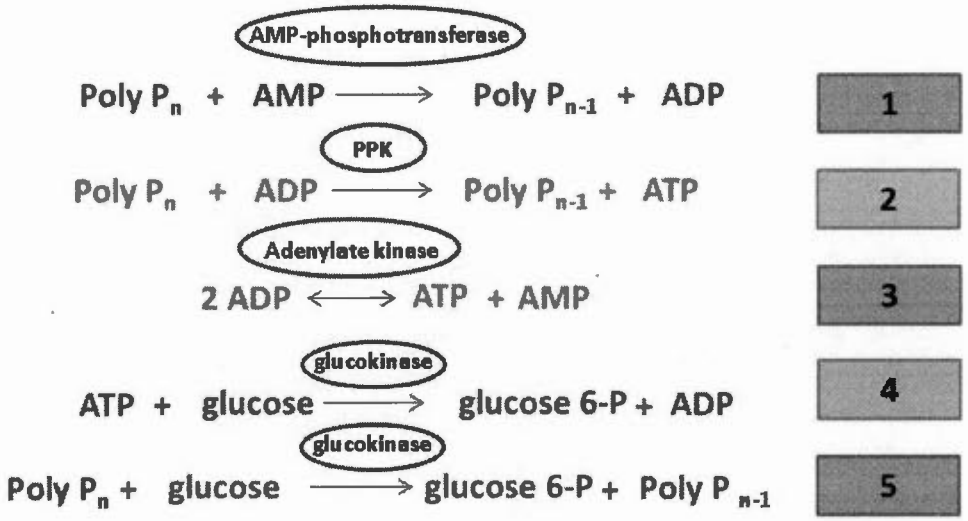

Figure 2.2 Polyphosphate as a substitute for ATP, made from (Hsieh *et al.*, 1993; Kornberg, 1995; Kornberg *et al.*, 1999).

The elements Mg, P, K and Ca were detected in polyphosphate bodies of three planktonic eukaryotic alga *Chlorella saccharophila*, *Navicula incerta*, and *Nitzschia closteriu* (Jensen *et al.*, 1982b). The accumulation of polyphosphate bodies was detected in the vacuoles of *Chlorella fusca* consisted of the high levels of P and several elements such as Mg, S, Cl, K, and Ca (Wong *et al.*, 1994). The study of Siderius *et al.* (1996) indicated that 40 % of cellular phosphate and 100 % of the intracellular calcium were stored in polyphosphate bodies of *C. eugametos* (Siderius *et al.*, 1996). The predominant cations Ca and Mg were detected in polyphosphate bodies of the cell wall-deficient strain of *C. reinhardtii* (Komine *et al.*, 2000). Electron-dense vacuoles or polyphosphate bodies of the wild-type strain of *C. reinhardtii* were composed of large amounts of phosphorous, magnesium, calcium, and zinc (Ruiz *et al.*, 2001).

All these studies confirm that polyphosphate bodies are the major source for phosphate, and a storage site for essential metals in living cells including algae. Since phosphorous is an important element, which living organisms are unable to live without, the importance of polyphosphate in living cells can be clear.

2.4.3 Protective role against environmental stresses

2.4.3.1 Nutrition deficiency

The enzyme polyphosphate .kinase (PPK) responsible for making inorganic polyphosphate demonstrated an important role in the survival of *E. coli* under starvation during the stationary phase of growth. To illustrate, *E. coli* mutants (CA10), which were not able to synthesize polyphosphate kinase (PPK), were subjected to the long term survival assay in the stationary phase of growth and compared to the wild-type cells. After 10 days of incubation in the stationary phase limited in glucose (0.1 %) at 37°C, about 20 % of the wild-type cells survived, while the viable cells of CA10 mutants (both small- and big-colony phenotypes) were only of 3 %. Indeed, a supportive role was demonstrated by polyphosphate to survive *E. coli* cells in the stationary phase that is considered as the stressful and deprived state in most bacteria (Rao et Kornberg, 1996).

In another study, different bacteria subjected to nutritional limitation demonstrated the accumulation of polyP depending on the strains. Cells grown in MOPS medium containing 2 mM Pi and 4 mg mL^{-1} of glucose were reinoculated into the same medium with limited phosphate (0.1 mM) and amino acids (2 µg mL^{-1}). A rapid and large transient accumulation of polyP was detected in *Acinetobacter johnsonii* and *Pseudomonas aeruginosa*, which was greater than *E.coli*. However, no polyP accumulation (<200 pmol polyP $mg^{-1}$of protein) was observed for the mutant *PPK PPX*, which failed to produce polyP. As well, the stopping growth of *E.coli* cells grown under nitrogen limitation (2 mM) was correlated with a rapid accumulation of polyP (Ault-Riché *et al.*, 1998). Therefore, the accumulation of polyP under

nutritional limitation was suggested as a defense mechanism to dominate the undesirable growth conditions in bacteria.

Fluorescence microscopy with DAPI-staining detected the polyP granules inside of the control cells in *C. acidophila* KT-1. In cells incubated in Pi- deficient medium (1.25 mM of Pi, 1/50 compared to standard condition) during 6 days, polyP granules disappeared. The recovered cells by transferring into modified SG medium (Sager Granick medium) rich in phosphate for one and three days demonstrated the appearance of polyP. In fact, many small granules were detected after one day of recovery, and with a large occupation of cell volume following three days. In the recovery cells, polyP was rapidly synthesized around the cell surface (Nishikawa *et al.*, 2006). Indeed, algal cells such as bacteria can accumulate excess Pi in the form of polyP during their growth, and the disappearance of polyP after starvation can indicate its utilization under stressful conditions to provide cellular needs.

2.4.3.2 Metallic stress

Different studies on algae, cyanobacteria and bacteria revealed the appearance and the accumulation of electron-dense bodies or polyphosphate bodies, which were capable of toxic metals incorporation into their structure as cellular detoxification centers. The study of Jensen *et al.* (1982a) showed the sequestration of Cd, Co, Cu, Hg, Ni, Pb, and Zn by electron-dense polyphosphate bodies of cyanobacterium *Plectonema boryanum* as a detoxification mechanism (Jensen *et al.*, 1982a). As well, Pb and Zn were compartmentalized in polyphosphate bodies of three planktonic eukaryotic algae, *C. saccharophila*, *N. incerta*, and *N. closterium*. For example, in *C. saccharophila*, Zn was observed in polyphosphate bodies starting at 1.0 ppm Zn, and significant peaks in polyP were detected by increasing the concentrations of Zn (Jensen *et al.*, 1982b).

Moreover, the detoxification of low concentrations of Zn^{2+} by polyphosphates was found in *C. variabilis* (Bate *et al.*, 1985). The rapid accumulation of aluminum (190

μM) into polyphosphate granules was a reason to detoxify the Al of the cyanobacterium *Anabaena cylindrical* (Pettersson *et al.*, 1985). The reduction of intracellular copper toxicity in a sensitive strain of alga *Scenedesmus acutus* was due to the polyP involvement for copper detoxification (Twiss et Nalewajko, 1992).

Furthermore, the TEM images of the strain RT1 of *Clamydomonas* sp. manifested the accumulation of spherical electron-dense bodies or polyphosphate bodies within periplasmalemma space, when exposed to 0.1 mM Cd. These small bodies with diameters of 200 nm were located in vesicles, and were found in higher numbers for cells treated to 0.2 mM Cd (Aguilera et Amils, 2005). The Al deposition in electron-dense granules and the increase in the number of polyphosphate bodies in Pb-treated cells of marine alga *Dunaliella tertiolecta* suggested that polyP contributed to detoxify these toxic metals (Sacan *et al.*, 2007).

In addition, the degradation of polyphosphate occurred when the phosphate availability was limited for living cells. For example, a reduction in the number of polyphosphate bodies was found for *C. bullosa* treated with copper. For *Anabaena flos-aquae* a reduction was detected in both the number and relative volume of polyphosphate bodies under the exposure to cadmium (Rai *et al.*, 1990; Visviki et Rachlin, 1994). The degradation of polyphosphates by the activation of both enzymes exopolyphosphatase and endopolyphosphatase was related to the detoxification of copper in the green alga *Stichococcus bacillaris* (Zhang et Majidi, 1994). A membrane model was proposed by Keasling (1997) that explains the importance of polyphosphate hydrolysis to detoxify the Cd in *E.coli*. Based on this model, in the presence of metallic cations, the activity of exopolyphosphatase or PPX was stimulated which led to phosphate (Pi) liberation from polyphosphate. Then, the transport of liberated inorganic phosphate was accomplished out of the cell via the inorganic phosphate transport (Pit) system that was accompanied by toxic metals such as Cd (Keasling, 1997).

As well, the role of vacuoles and polyphosphate degradation was studied by Nishikawa *et al.* (2003). Vacuolization was observed in *C. acidophila* KT-1 exposed to 20 µM Cd for three days. Following that, electron-dense deposits without defined shape were detected in vacuoles contained Cd and phosphate, which occupied the whole vacuole. Finally, analysis by ^{31}P-NMR demonstrated the degradation of polyphosphate to orthophosphates combined with Cd in vacuoles. Therefore, vacuolar polyphosphate metabolism induced by Cd^{2+} was suggested as a mechanism to detoxify Cd in *C. acidophila* KT-1 (Nishikawa *et al.*, 2003).

Acidithiobacillus ferrooxidans was able to synthesize and to accumulate electron-dense granules containing phosphates. Under low concentrations (1 to 2 µM) of copper, a great increase of PPX activity in *A. ferrooxidans* was observed and a part of liberated Pi was found out of the cells. The stimulation of PPX activity in the treated-cells with copper was related in time to the decrease in polyP levels. Therefore, the polyphosphate hydrolysis and following by the transport of copper-phosphate complexes out of the cells was suggested as a copper tolerance mechanism in this acidophilic bacterium (Alvarez et Jerez, 2004). Polyphosphate/phosphate involved in the sequestration and the excretion of Cd from *C. acidophila* KT-1 was suggested as a two-step mechanism for Cd tolerance in this alga (Nishikawa *et al.*, 2009). Finally, a direct chelation between polyphosphate and Hg^{2+} in the recombinant strain of *Escherichia coli* was a reason for more resistance of this strain to Hg^{2+} (Pan-Hou *et al.*, 2002).

2.4.3.3 Osmotic and alkalization stress

The involvement of polyphosphate in survival of bacteria and algae under osmotic and alkalization stress was shown by some studies. For example, *E. coli* mutants that were characterized as polyP-deficient cells (CA10) were more sensitive to osmotic stress. In the stationary phase after 3 h of starvation for glucose, only about 1% of mutant cells (CA10) survived after 21.5 h of exposure to 2.5 M NaCl, while this

number was of 10% for wild-type cells under osmotic condition (Rao et Kornberg, 1996). In another study, *E. coli* cultures grown to mid-log phase (OD_{600} of 0.9) that were subjected to the exposure with different concentrations of NaCl demonstrated significant differences in polyP accumulation, while the change in osmolarity was only of 27% (1.17 versus 0.85). Therefore, the accumulation of polyP was induced as a response to osmotic stress (Ault-Riché *et al.*, 1998). Ammonium induced internal alkalinization in the cytoplasm and inside the vacuole in *Dunaliella salina.* Following the accumulation of amines within vacuoles, a massive hydrolysis of polyphosphates to tripolyphosphate ($polyP_3$) occurred, and the produced protons led to protonate and to trap a large quantity of amines. Therefore, *D. salina* cells were able to protect their cytoplasmic pH against alkaline stress (Pick *et al.*, 1990; Pick et Weiss, 1991).

CHAPTER III

METHODOLOGICAL APPROACHES: PRINCIPLES OF METHODS

3.1 Cultivation and maintenance of *Chlamydomonas* strains in the laboratory

Chlamydomonas reinhardtii wild-type (CC-125) was obtained from the Chlamydomonas Resource Center (University of Minnesota, MN, UAS) and *Chlamydomonas* CPCC 121 (formerly UTCC 121), was provided by the Canadian Phycological Culture Centre (University of Waterloo, Waterloo, ON, Canada). Both *Chlamydomonas* strains were maintained on agar plates containing Tris-acetate-phosphate (TAP Medium). For experimental treatment, *C. reinhardtii* was cultivated in 1-L batch culture of High Salt Medium (HSM, chemical composition according to Harris, 1989) at pH 7 (Harris, 1989), and *Chlamydomonas* CPCC 121 was cultivated either in 1-L batch culture of Modified Acid Medium (MAM) at pH 4 (Olaveson et Stokes, 1989) or in 1-L batch culture of HSM at pH 7 for testing under two different pH conditions (4 and 7). Liquid cultures were permanently aerated to maintain constant CO_2 concentration in the growing medium. To illustrate, physiological analysis indicated that CPCC 121 was an acid-tolerant able to grow in pH condition between 2.5 and 7, by maintaining a neutral intracellular pH and its ability to accumulate inorganic carbon through the diffusive uptake of CO_2 (Balkos et Colman, 2007). For other experiments, two strains of *Chlamydomonas*, CC-125 (wild-type)

and CC-503 (cw92 mt^+) that has an impaired cell wall, were provided by the Chlamydomonas Resource Center (University of Minnesota, MN, UAS), and maintained on agar plates containing High Salt Medium (HSM) with a composition according to Sueoka *et al.* (1967) (Sueoka *et al.*, 1967). Algal cultures were grown in 25 mL liquid culture of HSM (pH 6.8). All liquid cultures were placed on orbital agitator platforms and were shaken at a constant speed. As well, liquid cultures were grown under constant conditions as shown at Figure 3.1. Continuous illumination was provided by white fluorescent lamps (Sylvania Grolux F36W). All glassware were acid-washed in 10 % HNO_3 for 12 h before use to avoid any metal contamination. Glassware and liquid culture medium were sterilized by standard autoclave procedures and stand overnight before use.

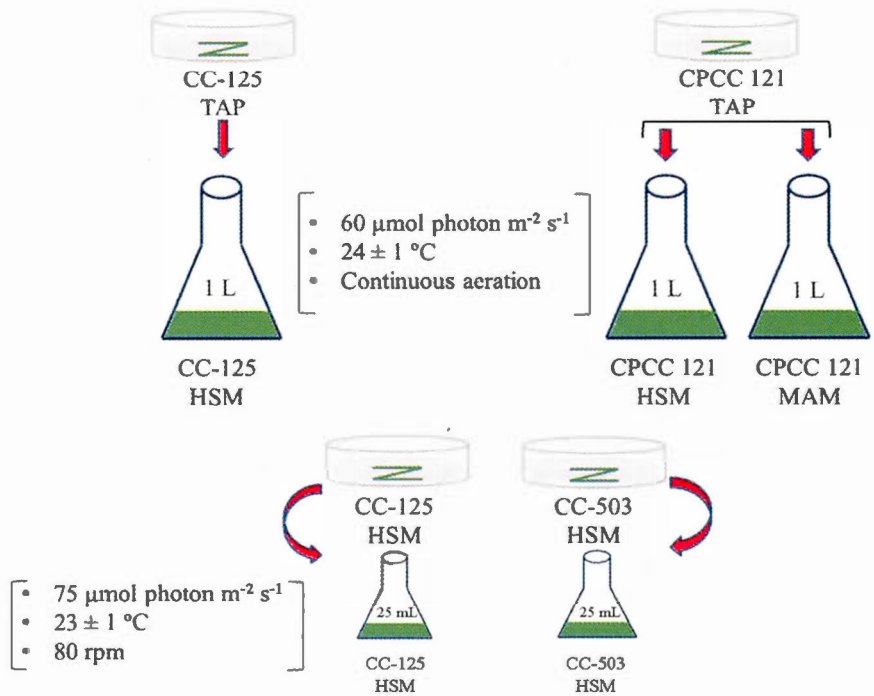

Figure 3.1 Cultivation and maintenance of *Chlamydomonas* strains.

Standard and growth curves were obtained for each alga grown in liquid cultures with a cell counter (Multisizer Z3, Beckman Coulter Inc, Fullerton, CA) and a UV-Vis spectrophotometer (Lambda 40, Perkin-Elmer, Woodbridge, Canada) (Figure 3.2). Standard curves represent the change of cell density versus the absorbance of alga at 750 nm, which were started from 0, when there was no cells in medium, to a maximum in the exponential growth phase. Linear equations were obtained from the standard curves (Table 3.1). We used linear equations to determine the cell density of alga before experimental treatments with UV-Vis spectrophotometer in which Y and X represent the cell density and the absorbance at 750 nm, respectively. Growth curves represent the change of cell density versus the day up to the exponential growth phase. The initial cell density for all algal strain grown in each culture medium was obtained from the growth curves.

Table 3.1 Linear equations for each culture grown in used medium, where Y and X represent the cell density and the absorbance (750 nm) of cultures, respectively. Linear regression was started at Y = 0 and X = 0 when there was no cells in medium.

Green alga	Linear equation	Culture medium
CC-125	$Y = 3 \times 10^6 X - 15965$	HSM
CPCC 121	$Y = 3 \times 10^6 X - 40384$	HSM
CPCC 121	$Y = 4 \times 10^6 X - 31833$	MAM

Green alga	Linear equation	Culture medium
CC-125	$Y = 1 \times 10^7 X - 46289$	HSM
CC-503	$Y = 1 \times 10^7 X + 66969$	HSM

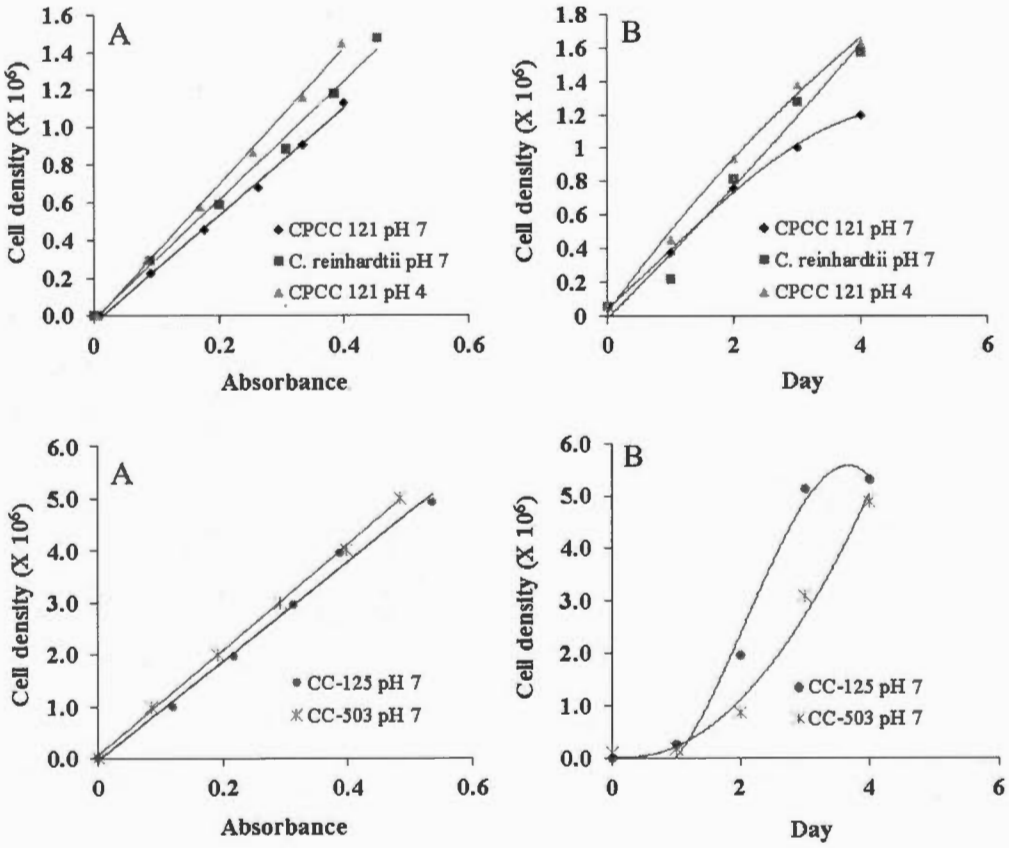

Figure 3.2 Standard (A) and growth (B) curves related to *Chlamydomonas* strains.

3.2 Experimental treatment of algal cells (general aspects)

Stock solutions of 600 mM of $CdCl_2$ and of 7 mM of $HgCl_2$ were prepared in Nanopure-purified water (Thermo Scientific Barnstead Nanopure ultrapure water purification system). To prepare the experimental cultures, algal samples were taken from the stock culture at the exponential growth phase. Therefore, cultures having an initial cell density of 5×10^5 cells mL^{-1} were exposed to either $CdCl_2$ (100-600 μM) in a final volume of 20 mL of HSM or MAM during 48 h or $CdCl_2$ (200-600 μM) or $HgCl_2$ (1-7 μM) in a final volume of 25 mL of HSM during 72 h for the second and third experiment, respectively. All experimental cultures were shaken during the

entire exposure time under the same illumination and temperature conditions used for stock cultures. Samples with no addition of $CdCl_2$ or $HgCl_2$ were considered as the control (Figure 3.3). Since CPCC 121 was subjected to determination of its capacity for Cd accumulation under two different pH conditions (4 and 7), Cd speciation was estimated based on the chemical equilibrium calculation by using Visual MINTEQ 2.61 software in both growth media (HSM and MAM). The results are presented in Chapter IV.

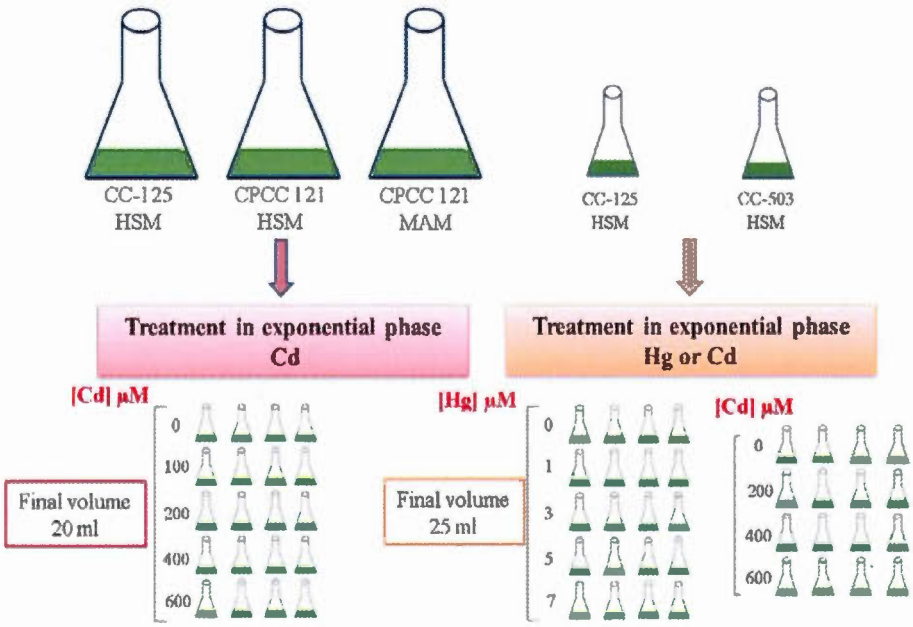

Figure 3.3 Experimental treatment of algal cells with Cd or Hg (II).

Indeed, in the medium, chemical speciation of metal ions can influence the toxicity of metals due to speciation. Metal ions can form the various types of complexes such as hydroxo-complexes, organic and inorganic complexes, and some complexes with humic substances in solution. It should be noted that, free metal ions do not exist completely as free chemical species in an aqueous solution. Indeed, water as an important ligand forms a hydration sphere around cations influencing their

bioavailability (Campbell et Couillard, 2004). It is well-known that free metal ions are more bioavailable to be uptaken by aquatic organisms including algae causing more toxicity of metals towards aquatic organisms (Campbell et Couillard, 2004). However, bioavailability of metal ions can be affected by different factors such as complexation by the presence of inorganic or organic ligands, competitive effects between metals to bind with uptake sites, and pH (Campbell et Couillard, 2004; Lavoie *et al.*, 2012; Worms *et al.*, 2006).

3.3 UV-Vis spectrophotometer for the monitoring of cell density

Photosynthetic organisms contain different pigment molecules; mainly chlorophyll *a* and *b* and carotenoids, which can absorb visible light (400 to 700 nm) (Malkin et Niyogi, 2000). The most applications of ultraviolet and visible absorption spectroscopy to organic compounds are based on transitions for "n" or "π" electrons to the π^* excited state. Indeed, the energy needed for both transitions; $n \rightarrow \pi *$ and $\pi \rightarrow \pi *$ provides the absorption bands into the ultraviolet-visible region (200 to 700 nm). The presence of an unsaturated functional group to provide the π orbitals is necessary to accomplish both mentioned transitions (Skoog *et al.*, 2007). In terms of the absorption of light by pigments, the electrons responsible for the interaction with visible light are π electrons, which are organized in the conjugated π-electron system of Chl *a* (Farineau et Morot-Gaudry, 2006).

The quantity of light which is absorbed by an analytical sample can be measured by a UV-Vis spectrophotometer. All spectrophotometric methods that measure absorption are based on the Beer-Lambert law as expressed mathematically with the equation $A = -\log T = \log P\,0/P = \varepsilon bc$, where symbols are defined by the following: (A) absorbance, (T) transmittance, (P_0) incident radiant power, (P) transmitted radiant power, (ε, $Lmol^{-1}cm^{-1}$) molar absorptivity, (b, cm) path length of sample, and (c, mol L^{-1}) concentration of absorber (Skoog *et al.*, 2007).

For the first experiment of our study, the change in growth rate was determined by the change in cell density (cells mL^{-1}) during 48 h. The cell count was measured with a Multisizer Z3 (Beckman Coulter Inc, Fullerton, CA), and the growth rate of cultures was calculated as $\mu = (\ln N_t - \ln N_0) / t_n$, where N_t is the final cell density at 48 h, t represents the period of exposure (day), and N_0 is the initial cell density. The change in growth rate was displayed as a percentage of the control. The coefficient of variation (CV %) was used to express the data dispersion based on four experimental replicates. Significant differences between the control and Cd-treated cultures were determined using a One-way ANOVA followed by a Dunnett test, and *p* values less than 0.05 were considered as significant ($p<0.05$). The results are presented in Chapter IV.

For the second and third experiment of our study, the cell density (cells mL^{-1}) was measured by using a cell counter Multisizer Z3 (Beckman Coulter Inc, Fullerton, CA), when algal cells were exposed during 72 h to different concentrations of Cd or Hg. The growth rate of cultures during 72 h was evaluated according to this formula: $\mu = (\ln N_t - \ln N_0) / t_n$; N_t as the final cell density at 72 h, t as the entire time period of exposure (day), and N_0 as the initial cell density. Analytical results showing the mean and the standard deviations were based on four experimental replicates. Statistical analysis was performed with OriginPro software (Sr2.b9.3.2.303 Research Lab, 2016). Significant differences between the control and Cd- or Hg-treated cultures were determined using a One-way ANOVA followed by a Tukey test, and *p* values less than 0.05 were considered as significant ($p<0.05$). The results are presented in Chapter V and VI.

3.4 Flow cytometer for the determination of the relative cell size, cellular granularity, and cell viability of algal cells

Flow cytometry is a rapid technique for the quantitative measurement of individual cells in a fluid stream, when they pass through the light source (lamp or laser) (Adan

et al., 2017; Macey, 2007; Stauber *et al.*, 2002). Although it is widely used in medical, flow cytometry as a useful tool has recently been used in ecotoxicological studies using microalgae (Franklin *et al.*, 2001; Jamers *et al.*, 2009; Stauber *et al.*, 2002). The principle of flow cytometry is related to light-scattering and fluorescence emission as light passes from a moving fluid (Adan *et al.*, 2017). Two types of light-scatter detectors provide data related to structure and morphology of the cell. The forward-angle light scatter (<15°) detector provides information on the cell size (FSC signal) and the side-angle light scatter (90°) detector provides data related to cell granularity (SSC signal) (Adan *et al.*, 2017; Franklin *et al.*, 2001).

Flow cytometry can also provide information about physiological status of cells and can assess the toxic action of toxicants by measuring fluorescence emission obtained from a fluorescence probe (Adan *et al.*, 2017; Stauber *et al.*, 2002). For example, fluorescein diacetate (FDA) was used as a probe of esterases enzymatic activity in algal cells. FDA is a nonfluorescent and lipophilic molecule which can penetrate inside the cell, e.g. algal cells, through non damaged membranes. Inside viable cells, FDA can be hydrolyzed by esterases to produce fluorescent fluorescein, which can be detected as green fluorescence emission (530-560 nm) (Franklin *et al.*, 2001).

In our study, we used a FacScan flow cytometer (Becton Dickinson instrument, USA) to measure the relative cell size and granularity based on forward and side light scattering properties. The relative cell size was determined by the forward light scatter signal (FSC), and the cell granularity was estimated by the side light scatter signal (SSC). As well, we used Fluorescein diacetate (FDA, Invitrogen Molecular Probe, Eugene, OR) as a probe of esterases enzymatic activity in cells (Breuwer *et al.*, 1995). Measurement of esterases activity was based on green fluorescence emission of fluorescein as a product of FDA hydrolysis by esterases. A Stock solution of FDA was prepared by dissolving 4.16 mg in 1 mL of 100 % acetone. Before

analysis, 10 µL of prepared FDA was added to 500 µL of algal sample with a final concentration of 0.2 mM and incubated for 10 min at room temperature. Fluorescence measurement was expressed in logarithmic scale. The time required for building each fluorescence histogram was 90 s, recording a total of 100 000 events per sample at a flow rate of 12 µL min^{-1}. Finally, data were collected using the list mode, analyzed by WinMDI 2.8 software, and results were expressed as a percentage of the control. Analytical results showing the mean and the coefficient of variation (CV %) were based on eight experimental replicates. Significant differences between the control and Cd-treated cultures were determined using a One-way ANOVA followed by a Dunnett test, and p values less than 0.05 were considered as significant ($p<0.05$). The results are presented in Chapter IV.

3.5 Atomic absorption (FAAS) and ICP-OES for the determination of the accumulation of metals in algal biomass

Bioaccumulation is the net accumulation of a contaminant in an organism from all sources in the environment including water (Newman et Unger, 2002). To determine the elements present in a sample, atomic spectrometric techniques, absorption and emission, are used as well as atomic mass spectrometry and X-ray spectrometry. In atomic spectrometric techniques, the constituents of a sample must be converted to gaseous atoms by atomization process, which is an important step influencing the accuracy and precision of atomic methods. Flame and inductively coupled argon plasma (ICP) are two common types of atomizers, and in a steady manner sample is introduced into plasma or flame. Briefly, in atomic absorption spectrometry (AAS) a selected wavelength is sent through the atomic vapor of an interested element, which can be absorbed by the atoms of this element. The amount of light that is absorbed by these atoms indicates the concentration of the selected element in sample (Skoog *et al.*, 2007). In optical emission spectrometry (OES) sample is subjected to high temperature for excitation of its atoms. More recently, plasmas have been used as atomization/excitation sources for OES. Plasma is a gaseous mixture containing a

significant concentration of electrons and cations, which can conduct electricity and can be affected by a magnetic field. There are three types of high-temperature plasmas among those the inductively coupled plasma (ICP) is widely used as a sensitive elemental analysis in OES (Boss et Fredeen, 1997; Skoog *et al.*, 2007).

In our experiment, to measure Cd or Hg accumulation in algal biomass, the control and Cd- or Hg-treated cultures were filtered on cellulose nitrate filter papers (Millipore 0.45 µm) using vacuum filtration. Adsorbed Cd or Hg on the cell surface was removed by washing with 1 mM EDTA, and the dry biomass was obtained by keeping filter papers in an oven at 60 °C during 15 h. Dried algal biomass were digested during 12 h at 120 °C by adding 1 mL of concentrated HNO_3 and 125 µL of 30 % hydrogen peroxide (Caledon laboratory chemicals). Digested samples and standard solutions of Cd or Hg were diluted to 10 % HNO_3. For the first experiment, the quantity of Cd was determined by Flame Atomic Absorption Spectrometry (FAAS, Varian spectrAA 220 FS). For the second and third experiment, the quantity of Cd or Hg was determined by inductively coupled plasma atomic emission spectrometry (Inductively Coupled Plasma/Optimal emission spectrometry, ICP-OES, Agilent Technologie 5100). The values were then normalized per mass unit as µg of Cd / mg of dry mass or µg of Hg / mg of dry mass). Analytical results showing the mean and the standard deviations were based on four experimental replicates. Significant differences between the control and Cd- or Hg-treated cultures were determined using a One-way ANOVA followed by either a Dunnett test for the first experiment or a Tukey test for the second and third experiment, and p values less than 0.05 were considered as significant ($p<0.05$). The results are presented in Chapter IV, V, and VI.

3.6 Chlorophyll *a* fluorescence measurement for the determination of the performance of photosynthetic activity in algae

Chlorophyll *a* fluorescence is a highly sensitive and reliable tool for measuring photosynthetic efficiency (Stirbet et Govindjee, 2011). The first step of photosynthesis is the absorption of photons by a light harvesting antenna system containing light-absorbing molecules, chlorophyll and other accessory pigments, which leads to the formation of excited chlorophylls (Chl^*) (Govindjee *et al.*, 2010). Excitation energy can return to the ground state via three processes: it can be transferred to reaction centers and used to drive photochemistry in which an electron is transferred from the reaction center chlorophyll, P680, to the primary acceptor of PSII, Q_A, or it can be dissipated as heat or re-emitted as chlorophyll fluorescence. Therefore, these three processes occur in competition for excitation energy (Baker, 2008).

The main phenomenon which occurs in the fluorometric methods is called fluorescence induction, fluorescence transient, or Kautsky effect which can be observed when photosynthetic sample is transferred from the dark (kept in darkness for 10 min) into the light (Stirbet et Govindjee, 2011). Indeed, the yield of chlorophyll fluorescence increases rapidly during a short time exposure to a saturating light flash of 1 second. It is first labeled as OJIP transients by Strasser *et al.* (1995) by presenting the rapid fluorescence induction on a logarithmic time scale. The yield of chlorophyll *a* fluorescence was known to be related to the PSII electron transport activity. Therefore, the rapid fluorescence transients have the potential to describe the PSII electron transport activity. The photochemical phase, O-J transient, corresponds to Q_A reduction showing the PSII shift from an open (when photosynthetic sample kept in the dark) to close state (after transferring from darkness into light). The fluorescence at the level of I transition shows the first reduction of Q_B, a secondary electron transport acceptor in PSII ($Q_A^- Q_B^-$). Finally, the I-P transition is the result of $Q_A^- Q_B^{2-}$ accumulation, and the maximum

fluorescence yield can obtain by the complete reduction of the PQ pools (Figure 3.4) (Strasser *et al.*, 1995).

The acquisition of the rapid chlorophyll *a* fluorescence induction provides the various JIP parameters indicating the performance of photosynthetic activity of PSII. Minimum fluorescence, F_0, is defined when the PSII reaction center is open and is represented on the fluorescence transient curve as O ($F_{20\mu sec\ or\ 50\mu sec}$). J and I transients are appeared at 2 (F_{2msec}) and 30 msec (F_{30msec}) respectively, and in less than 1 s Chl *a* fluorescence reaches its maximum P (F_M). The difference between F_M and F_0 is called the variable fluorescence, F_V, and the ratio F_V/F_M represents the maximum quantum yield of PSII photochemistry (Stirbet et Govindjee, 2011; Strasser *et al.*, 2004).

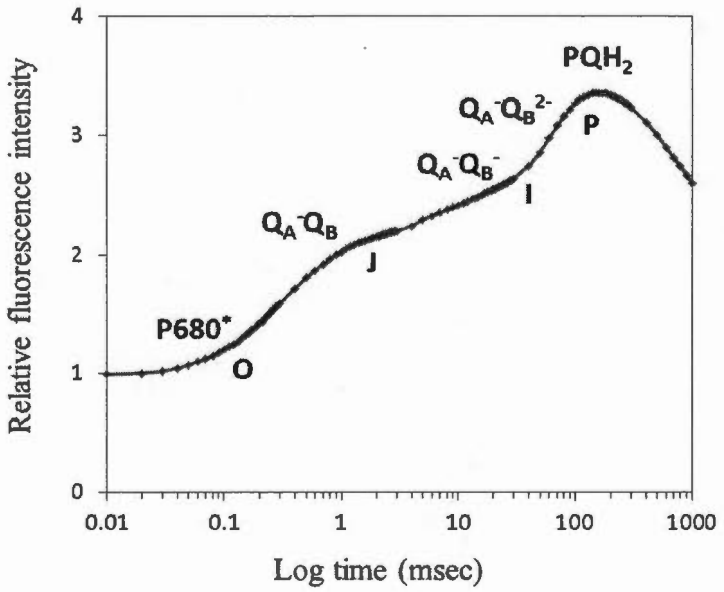

Figure 3.4 Rapid chlorophyll *a* fluorescence induction on logarithmic time scale showing the transient O-J-I-P; (Q_A) and (Q_B) represent the primary and secondary acceptors of PSII respectively , (P680*), excited electronic state of P680, (POH_2), reduced plastoquinone (measured in the laboratory with Handy-PEA, Hansatech Ltd, Norfolk, UK, *C. reinhardtii* in HSM medium.

In our work, prior to fluorescence measurements, control and treated algal samples were dark-adapted for 20 min with manual stirring to keep oxygenation. Samples of

algal cells corresponding to 10 µg of total chlorophylls were uniformly placed on glass fiber filter (Millipore No. AP2001300) using a manual low pressure filtration. Rapid Chl *a* fluorescence induction from 10 µs to 1 s was recorded with a Plant Efficiency Analyzer fluorometer (Handy-PEA, Hansatech Ltd, Norfolk, UK) by triggering a saturating flash of 3500 µmol photons m^{-2} s^{-1}. Fluorescence intensity at 20 µs was considered to be the O transient noted as $F_{20\mu s}$. Variable fluorescence intensities at J and I transients were determined at 2 ms (F_{2ms}), and 30 ms (F_{30ms}) respectively. The maximum fluorescence yield (F_M) reached a maximal value of fluorescence intensity under saturating illumination. Fluorescence parameters related to Photosystem II (PSII) activity were determined according to Stirbet and Govindjee (2011) and Strasser *et al.* (2004) (Stirbet et Govindjee, 2011; Strasser *et al.*, 2004). However, the usefulness of the fluorescence parameters can be different depending on the pollutants among the algal species. For example, the maximal PSII quantum yield was shown as a sensitive indicator for the effect of mercury in different algal species (Juneau *et al.*, 2001). Therefore, for the first experiment of our study, the performance index of PSII activity was evaluated as $PI(abs) = [(1-(F_{20\mu s}/F_M))]/(M_0/V_J)]\times((F_M-F_{20\mu s})/F_{20\mu s})\times((1-V_J)/V_J)$. Representing the net rate of reduced PSII by electron transport, M_0 parameter was determined as $M_0 = [4\times(F_{300\mu s}-F_{20\mu s})/(F_M-F_{20\mu s})]$, where $F_{300\mu s}$ represents the fluorescence intensity at 300 µs; As the proportion of reduced Q_A relative to the plastoquinone pool, V_J parameter was evaluated as $V_J = [(F_{2ms}-F_{20\mu s})/(F_M-F_{20\mu s})]$. For the second and third experiment, the maximal PSII quantum yield was evaluated by the ratio between the variable (F_V) and the maximal (F_M) fluorescence intensities, as $F_V/F_M = (F_M - F_{20\mu s})/F_M$. The F_M was acquired under saturating illumination, and the fluorescence intensity at 20 µs was considered as the basal fluorescence level, $F_{20\mu s}$. Analytical results showing the mean, the standard deviations or the coefficient of variation (CV %) were based on four experimental replicates. Significant differences between control and Cd- or Hg-treated cultures were determined using a One-way ANOVA followed by either a Dunnett test for the first experiment or a Tukey test for the second and third

experiment, and p values less than 0.05 were considered as significant ($p<0.05$). The results are presented in Chapter IV, V, and VI.

3.7 TEM and EDX analysis for the cellular localization of metals in algal biomass

Electrons are one type of ionizing radiation which can be used to produce a wide range of secondary signals from the sample when a high-energy beam of electrons interacts with a thin specimen. These signals such as secondary electrons (SE), characteristic X-rays, backscattered electrons (BSE), auger electrons, and many others can be detected in different types of TEM. As well, these secondary signals are used in analytical electron microscopy (AEM) providing chemical information and lots of other details about the interested sample (Williams et Carter, 2009). X-ray spectrometry converts the TEM to more powerful instrument called an analytical electron microscope (AEM). X-ray energy-dispersive spectrometer (XEDS) is the only commercial spectrometer, which is used on the TEM (Williams et Carter, 2009).

In our study, for the acquisition of TEM micrographs, samples of 20 mL from control and Cd-treated cultures (600 µM) at 24 h were centrifuged, and the supernatant was discarded. Cells were fixed with 2.5 % glutaraldehyde in 0.1 M of sodium cacodylate buffer overnight at 4 °C. Without disturbing the pellet, cells were washed three times during 1 h with 0.1 M of sodium cacodylate washing buffer. The post-fix was done with 1 % aqueous OsO_4 (Mecalab) adding 1.5 % aqueous potassium ferrocyanide during 2 h. Then, samples were washed with washing buffer (3 × 15 min), and dehydrated with increasing concentrations of acetone (30 %, 50 %, 70 %, 80 %, 90 %, and 3 × 100 % each for 10 min). Dehydrated samples were infiltrated with Epon (Mecalab) with increasing concentrations of Epon in acetone, as 1:1 (overnight), 2:1 (all day), and 3:1 (overnight). The pellet was placed in pure Epon the next day during 4 h, and then polymerized during 48 h at 60 °C. Hardened pellets were cut at 90-100 nm thick sections with UltraCut E ultramicrotome (Reichert-Jung), and put onto a 200 mesh copper grid. Sections were stained with Uranyl

acetate for 8 min, then Reynold's lead for 5 min. Samples were visualized with a FEI Tecnai 12 120 kV transmission electron microscope (TEM) equipped with an AMT XR80C 8 megapixel CCD camera. At least three images were taken for each experimental condition. General techniques were done for modified morphometric analysis. The results are presented in Chapter IV.

The elemental analysis of intracellular Cd was determined by energy-dispersive X-ray spectroscopy (EDX). Analysis was done on the same section thickness placed onto a carbon-coated grid using Philips CM200 200 kV TEM, equipped with a Gatan Ultrascan 1000 2k × 2k CCD Camera System Model 895 and EDAX Genesis EDS. The results are presented in Chapter IV.

3.8 Confocal microscope for the measurement of fluorescence emission from extracytoplasmic polyphosphate

The laser scanning confocal microscope (LSCM) is a useful tool for imaging either fixed or living tissues that have been stained by fluorescent probes. In a conventional light microscope, the whole sample is illuminated in light from a mercury or xenon source and the image can be directly captured by eye. While, in a confocal microscope, the illumination is performed by scanning one or more focused beams from a laser rather than a lamp across the sample (Paddock, 2000).

In this study, we developed a methodology to evaluate the level of polyP bound to the cell wall of algal cells by using confocal laser scanning microscopy (CLSM, Nikon A1 Confocal). Prior to measurement, samples were stained with 4′,6-diamidino-2-phenylindole (DAPI, Sigma-Aldrich, stock solution of 10 mg mL^{-1}) to a final concentration of 50 μg mL^{-1} according to Streichan *et al.* (1990) (Streichan *et al.*, 1990). Then, the fluorescence intensity of polyP related to the cell wall (extracytoplasmic) was measured through a PLAN Apo 60×/1.4 NA Oil objective. Indeed, DAPI is a blue fluorescence dye (having a maximum emission at 460 nm), and this compound is usually used for the detection of DNA in dead cells by

interacting with the nucleus. However, polyphosphates can shift its maximum fluorescence emission (at 488 nm) to a higher wavelength (525 nm), which is not produced by pyrophosphate or others anions (Allan et Miller, 1980; Nishikawa *et al.*, 2006; Ruiz *et al.*, 2001). In this study, we developed a method to stain the polyP in the cell wall (extracytoplasmic) of viable cells, by introducing 20 µL of algal sample stained with 50 µg mL^{-1} of DAPI into an adapted microplate (ibidi, µ-Slide Angiogenesis). Since the cell membrane of viable cells is impermeable to DAPI compound, this used concentration of DAPI was appropriate to visualize the extracytoplasmic polyP by avoiding the penetration of DAPI inside the cell. Then, the microplate containing stained algal cells was analyzed by confocal microscopy up to 2 min from the addition of DAPI. The intensity of green fluorescence emission (maximum at 525 nm) was measured by using an excitation light at 404 nm. With this timing, we were able to acquire images of viable cells on microplates, and the data was analyzed using Image J (U.S. National Institutes of Health, Bethesda Maryland). Therefore, this methodology permitted to determine the polyP fluorescence emission from the cell wall of viable cells, which was distinguished from dead cells by using the emission of red fluorescence from chlorophylls (650 nm). At least three independent experiments were performed to determine the reproducibility of the method. For each experimental condition, the results of the polyP fluorescence intensity are presented as the average (and the coefficient of variation) of ten cells, which were expressed as a percentage of the control. Significant differences between the control and treated cultures were determined using a One-way ANOVA followed by a Tukey test, and p values less than 0.05 were considered as significant ($p < 0.05$). The results are presented in Chapter V and VI.

3.9 Zeta potential measurement

The zeta potential shows the charge at the cell surface and plays an important role in the uptake of metal cations (Gimmler *et al.*, 1991). In the first study of our experiment, we measured the charge at the cell surface for CPCC 121 under two

different pH conditions (4 and 7) in the exponential growth phase at 25 °C with Zeta potential analyzer (Brookhaven, ZetaPlus / Bl-PALS). The results are presented in Chapter IV.

CHAPTER IV

EFFECT OF CADMIUM ACCUMULATION ON GREEN ALGAE *CHLAMYDOMONAS REINHARDTII* AND ACID-TOLERANT *CHLAMYDOMONAS* CPCC 121

4.1 Results and discussion

4.1.1 Speciation and bioavailability of Cd

The speciation of Cd was estimated for both testing media based on the chemical equilibrium calculation (Visual MINTEQ 2.61), and all Cd species was presented as % in Table 4.1. This methodological approach based on the biotic ligand model was previously used to determine the concentration of free Cd^{2+} in laboratory testing media, indicating the bioavailability of Cd to be uptake by algal cells (Lavoie *et al.*, 2012; Paquet *et al.*, 2015). Here, our estimation showed that the proportion of free Cd^{2+} was dependent on the tested pH and nominal concentrations of Cd. At pH 7 in HSM, the proportion of free Cd^{2+} was 12-13 % of tested nominal concentrations of Cd. Under this pH condition, concentrations of 12, 25, 50 and 76 µM of free Cd^{2+} were estimated for tested 100, 200, 400 and 600 µM of Cd, respectively. At pH 4 in MAM, the proportion of free Cd^{2+} was respectively for these nominal concentrations 51 % (51 µM), 59 % (119 µM), 63 % (253 µM) and 64 % (385 µM) of free Cd^{2+}. Under the experimental conditions of this study, the proportion of free Cd^{2+} represented the soluble fraction and bioavailable chemical form of Cd, which can interact with algal cells in the media. Our results showed that the soluble fraction of

Cd at pH 4 was higher by 4-5 times than at pH 7, indicating that Cd was more bioavailable to interact with algal cells of *Chlamydomonas* CPCC 121 under this condition.

Table 4.1 Proportion of Cd species (%) in culture medium at pH 7 and 4 determined by the chemical equilibrium calculation (Visual MINTEQ 2.61).

pH 7	[Cd] μM			
Species	100	200	400	600
Cd^{2+}	12	12	13	13
$CdCl^{+}$	6	6	6	6
$CdHPO_4$	81	81	81	81
$CdCl_2$ $CdSO_4$ $CdEDTA^{2-}$ $CdNH_3^{2+}$	1	1	0	0
pH 4	**[Cd] μM**			
Species	100	200	400	600
Cd^{2+}	51	59	63	64
$CdCl^{+}$	2	3	5	6
$CdSO_4$	19	23	24	23
$Cd(SO_4)_2^{2-}$	1	2	2	2
$CdEDTA^{2-}$	21	10	5	4
$CdHEDTA^{-}$	6	3	1	1
$CdHPO_4$ CdH_2EDTA $CdCl_2$	0	0	0	0

4.1.2 Inhibition of growth rate

When both *Chlamydomonas reinhardtii* and CPCC 121 were exposed to different nominal concentrations of Cd, the change in growth rate was determined for a period of 48 h, providing a global indication of the cellular toxicity impact induced by Cd (Figure 4.1). The growth rate of *C. reinhardtii* at pH 7 was already significantly ($p < 0.05$) inhibited by 25 ± 5 % under the lowest tested Cd concentration (100 μM), and

this effect was dependent on the nominal concentrations of Cd. Under 400 and 600 µM of Cd, the growth rate decreased by 38 ± 9 % and 41 ± 1 % relative to control ($p < 0.05$), respectively. However, the effect of Cd was different on the growth rate of CPCC 121. At pH 7, the inhibition of growth rate remained constant, decreasing significantly by 30 ± 3 % relative to control ($p < 0.05$) under Cd treatments (100-600 µM). At pH 4, the growth rate decreased by 20 ± 4 % and 31 ± 5 % compared to control ($p < 0.05$) only under 400 and 600 µM of Cd. Therefore, CPCC 121 was more resistant at pH 4 to the effect of Cd compared to pH 7 condition, although the proportion of free Cd^{2+} was higher in the medium at pH 4. Indeed, it was previously suggested that the resistance to metal under acidic condition (pH 4-6) of green algae *Chlamydomonas reinhardtii* and *Chlorella pyrenoidosa* was attributed primarily to a competition between H^+ and metal ions for binding sites at the cell surface (Fortin *et al.*, 2007; Parent et Campbell, 1994). Therefore, this mechanism can explain the tolerance of *Chlamydomonas* CPCC 121 for the exposure of Cd under low pH condition. In fact, our results clearly showed that this algal strain of *Chlamydomonas* was more resistant than *C. reinhardtii* under Cd stress effect during 48 h of exposure.

4.1.3 Cd accumulation in algal biomass

The accumulation of Cd was determined in algal biomass to better understand the inhibitory effect of Cd on the growth rate. Since each algal species may have different ability to accumulate Cd, both *C. reinhardtii* and CPCC 121 were investigated and compared at 24 and 48 h of exposure (Figure 4.2). Under 100 µM of Cd, the quantity of accumulated Cd in both algal strains was already significantly higher ($p < 0.05$) compared to control. At pH 7, results showed that the accumulation of Cd strongly increased ($p < 0.05$) for both algal strains under 400 and 600 µM of Cd. In particular,

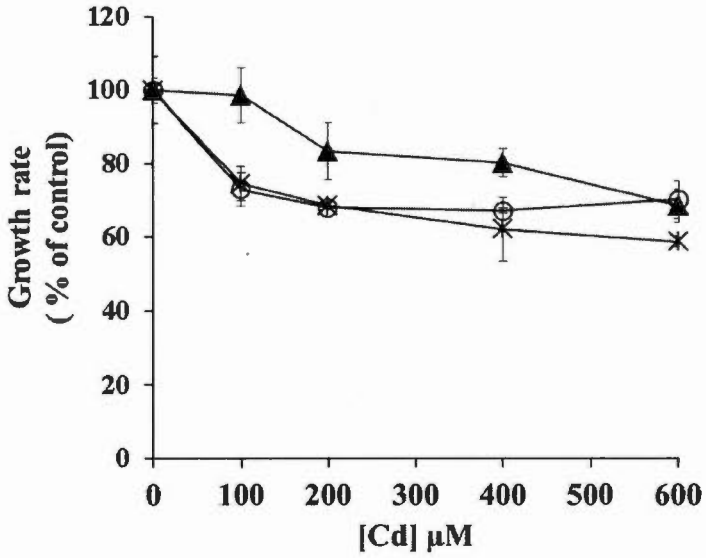

Figure 4.1 Change in the growth rate (% of control) under different concentrations of Cd (µM) and pH condition for a period of 48 h. Legend: ×, *C. reinhardtii* at pH 7; ○, CPCC 121 at pH 7; ▲, CPCC 121 at pH 4. At pH 7, both control *C. reinhardtii* and CPCC 121 had a growth rate of 0.7 cell per day, and at pH 4, CPCC 121 had a growth rate of 0.6 cell per day. Each data indicated the average and coefficient of variation (CV %) of 4 replicates. Differences between treated-samples and control were all significant at the level of 0.05 ($p < 0.05$) with the exception of CPCC 121 at pH 4 under 100 µM of Cd versus control.

C. reinhardtii and CPCC 121 accumulated respectively 2.37 ± 0.23 and 1.33 ± 0.55 µg Cd / mg of dry mass under 400 µM of Cd (50 µM of free Cd^{2+}). Under 600 µM of Cd (76 µM of free Cd^{2+}), *C. reinhardtii* and CPCC 121 accumulated 2.76 ± 0.22 and 2.08 ± 0.36 µg Cd / mg of dry mass, respectively (Figure 4.2A, B). Therefore, these results clearly indicated that CPCC 121 was able to limit the accumulation of Cd at pH 7 in comparison to *C. reinhardtii*. As a possible protection mechanism, Macfie *et al.* (1994) suggested that sensitive sites inside or at the surface of cell wall have the capacity to bind metal ions, preventing their uptake into the cellular cytoplasm (Macfie *et al.*, 1994). This hypothesis based on the saturation of metal binding in the cell wall may also explain the higher Cd accumulation in *C. reinhardtii* under treatment of 400 and 600 µM.

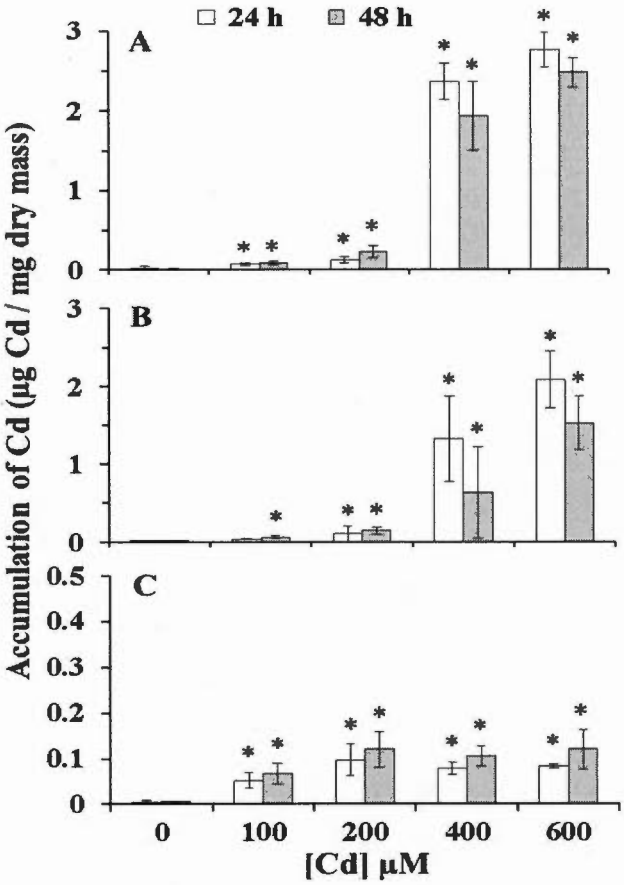

Figure 4.2 Accumulation of Cd in *Chlamydomonas reinhardtii* and CPCC 121 exposed during 48 h to different concentrations of Cd (µM) and two pH conditions. Legend: A, *C. reinhardtii* at pH 7; B, CPCC 121 at pH 7; C, CPCC 121 at pH 4. Each data indicated the average and standard deviation of 4 replicates. Significant differences relative to the control at the level of 0.05 ($p < 0.05$) were indicated by asterisk (*).

At pH 7, the accumulation of Cd in algal biomass reached its maximum capacity for both strains already at 24 h under the exposure to 600 µM of Cd.

Moreover, results of Figure 4.2C showed that *Chlamydomonas* CPCC 121 accumulated very low amount of Cd at pH 4 (< 0.1 µg Cd / mg of dry mass) when

algal cells were exposed during 24 h and 48 h to 100-600 µM of Cd. These results indicated that CPCC 121 did possess a mechanism to limit the accumulation of Cd, especially at pH 4. It was also suggested that positive membrane potential under low pH, due to protonation at surface sites, reduced the uptake of metal cations (Gimmler *et al.*, 2001). In our study, the charge at the cell surface (zeta potential) was -41 and -4 mV for CPCC 121 cells at pH 7 and 4, respectively. Since our results showed less accumulation of Cd at pH 4 in algal biomass of CPCC 121 compared to pH 7 condition, we may suggest that the high protonation at the cell surface reduced the electrostatic interactions between the cell wall and metal cations.

4.1.4 Alteration of cellular characteristics

In previous environmental toxicology studies, the flow cytometry method has been successfully applied for the investigation of metal toxicity in algal cells, by allowing the analysis of structural characteristics as the cell size and granularity (Franklin *et al.*, 2001; Franqueira *et al.*, 2000; Jamers *et al.*, 2009). In our study, the cellular analysis of *C. reinhardtii* showed an increase in the relative cell size significantly higher than the control, especially for cells exposed during 48 h to 400 and 600 µM of Cd (Figure 4.3A). When *C. reinhardtii* was exposed during 24 h to 600 µM of Cd, the relative cell size showed an increase of 84 ± 13 % ($p < 0.05$) in comparison to control. Furthermore, the relative cell size increased by 75 ± 26 % and 119 ± 11 % ($p < 0.05$) compared to control in *C. reinhardtii* exposed during 48 h to 400 and 600 µM of Cd, respectively. For the strain CPCC 121 exposed at pH 7 during 24 h to 400 and 600 µM of Cd (Figure 4.3B), this cellular parameter increased by 26 ± 8 % and 45 ± 6 % compared to control ($p < 0.05$), respectively. However, no significant changes in the relative cell size was found for CPCC 121 exposed to Cd at pH 4 during 48 h.

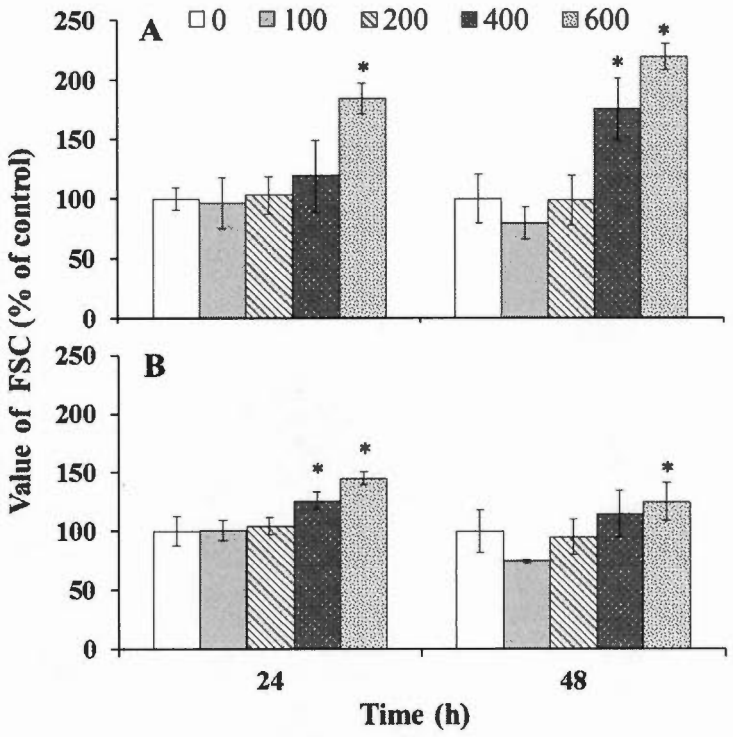

Figure 4.3 Change in the relative cell size (% of control) evaluated by the forward light scattered (FSC) of *C. reinhardtii* (A) and CPCC 121 (B) exposed at pH 7 during 48 h to different concentrations of Cd (μM). Each data indicated the average and coefficient of variation (CV %) of 8 replicates. Significant differences relative to the control at the level of 0.05 ($p < 0.05$) were indicated by asterisk (*).

In a previous study, Visviki and Rachlin (1994) found a significant increase in total cell volume of *Chlamydomonas bullosa* after 96 h of treatment with 0.025 μM of Cd (Visviki et Rachlin, 1994). Later, it was also showed that copper (1 mg L^{-1}) induced an increase of 49 % on the relative cell size (FSC signal) of the marine microalga *Phaeodactylum tricornutum* after 96 h of exposure (Franqueira *et al.*, 2000). These authors suggested that the increase in cell volume might have been triggered by an increase in the permeability of the cell membrane to Na^+ due to the effect of copper. In another study, 18 and 30 μg L^{-1} of Cu induced respectively an increase in the cell size of *Chlorella sp.* and *Selenastrum capricornutum*, which was

accompanied by a decrease in the cell division rate, suggesting that cells could not be divided completely and instead get larger (Franklin *et al.*, 2001). Similarly, it was recently found that *C. reinhardtii* cells exposed during 72 h to 5 µM of Cd were significantly larger than control cells (Jamers *et al.*, 2009). Therefore, our results showed an increase in the relative cell size of *C. reinhardtii* exposed during 48 h to 400 and 600 µM of Cd that may be due to an alteration in the algal cell division cycle. Indeed, our results on the accumulation of Cd in algal biomass and the inhibition of growth rate support this hypothesis.

In addition, our results showed that cellular granularity (SSC signal) increased significantly by 57 ± 13 % in comparison to control ($p < 0.05$) when *C. reinhardtii* was exposed at pH 7 during 24 h to 600 µM of Cd (Figure 4.4A). Under the same pH condition, the granularity of CPCC 121 cells exposed to Cd showed no significant change compared to control ($p < 0.05$). However at pH 4, this cellular indicator increased significantly by 9.5 and 10 fold compared to control ($p < 0.05$) for CPCC 121 cells exposed during 48 h to 400 and 600 µM of Cd (Figure 4.4B). Indeed, Franklin et al. (2001) introduced the SSC signal as a useful indicator related to cellular complexity and granularity. In their study, authors found a maximum increase of this indicator in *Chlorella sp* exposed during 48 h to 18 µg L^{-1} of Cu (Franklin *et al.*, 2001). Furthermore, the work of Jamers et al. (2009) demonstrated an increase of algal cell granularity, which was related to the increasing tested nominal Cd concentrations after both 48 and 72 h of exposure (Jamers *et al.*, 2009). It was then suggested that the increase of algal cell granularity was due to ultrastructural alterations inside the cell. Indeed, ultrastructural changes induced by the stress effect of metals have been reported in different algal species by microscopic methods. For example, vacuolization was observed in the majority (95 %) of cytoplasm and chloroplasts when the marine diatom *Skeletonema costatum* was exposed to 0.2, 0.5 and 1 mg L^{-1} of Cd (Nassiri *et al.*, 1997). They reported that Cd was sequestrated in spherical vacuolar inclusions enriched in sulfur and nitrogen, suggesting that Cd was

probably bounded to organic molecules through S-Cd bonds in order to reduce the cytosolic concentration of Cd.

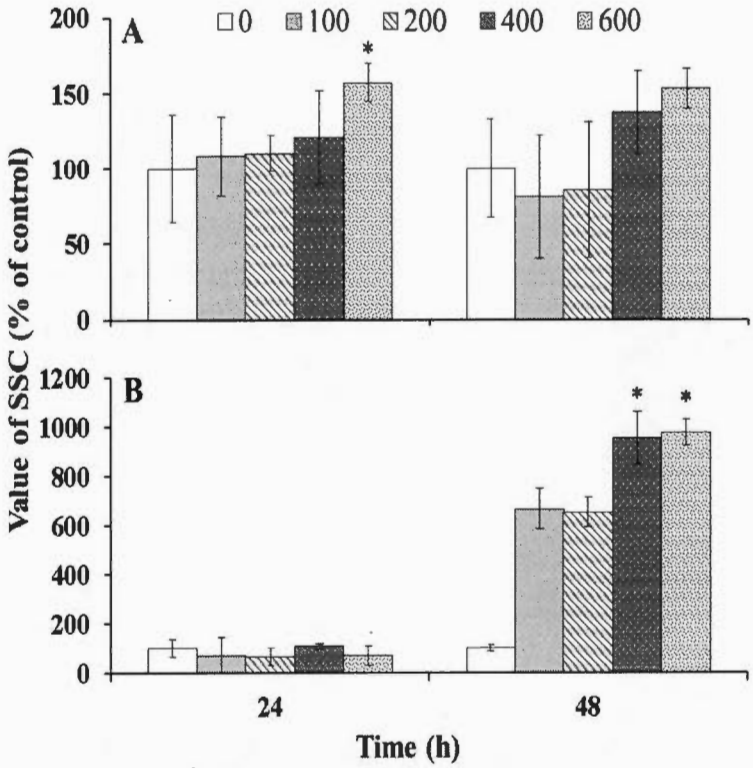

Figure 4.4 Change in the cell granularity (% of control) evaluated by the side light scattered (SSC) of *C. reinhardtii* at pH 7 (A), and CPCC 121 at pH 4 (B) exposed during 48 h to different concentrations of Cd (μM). Each data indicated the average and coefficient of variation (CV %) of 8 replicates. Significant differences relative to the control at the level of 0.05 ($p < 0.05$) were indicated by asterisk (*).

Furthermore, the work of Nishikawa *et al.* (2003) showed the increase of starch granules and vacuoles, including electron-dense deposits in *Chlamydomonas acidophila* exposed to 20 μM Cd during 72 h (Nishikawa *et al.*, 2003). Supporting this explanation, it was also found in *Chlamydomonas* sp exposed to 0.2 mM of Cd at pH 2 that the number and volume of cytoplasmic vacuoles increased, causing a larger periplasmalemmal space (Aguilera et Amils, 2005). Authors showed in this study that

0.1 and 0.2 mM of Cd induced the accumulation of electron-dense granules containing Cd and P, and a significant number of voluminous starch granules. Therefore, we suggested that ultrastructural changes such as cytoplasmic vacuolization, appearance of electron-dense granules, accumulation of starch granules and cellular debris induced by intracellular Cd may explain the increase in cellular granularity of *C. reinhardtii*. However, our results demonstrated no cellular alterations related to the increase in cell granularity for *Chlamydomonas* CPCC 121 exposed at pH 7. At pH 4, we assumed that the abundance of Cd ions out of the cytosol (controlled by the cell wall, the periplasmalemmal space and the plasma membrane) induced an alteration of the cell wall and membrane as indicated by the change of the cell granularity after 48 h of treatment under the highest tested concentrations of Cd.

Moreover, the cell viability marker FDA, related to the enzymatic activity of esterases, did not changed significantly compared to control in either species exposed at pH 7 to different nominal concentrations of Cd during 48 h, and for CPCC 121 cells exposed at pH 4 (Figure 4.5). Previously, Jamers et al. (2009) suggested that an increase in the activity of esterases was indicative of their involvement in cellular detoxification processes, when *C. reinhardtii* was exposed to 100 µM of Cd during 48 and 72 h (Jamers *et al.*, 2009). Consequently, we proposed that the activity level of esterases remained high for both strains of *Chlamydomonas* exposed to Cd due to their participation in intracellular detoxification processes.

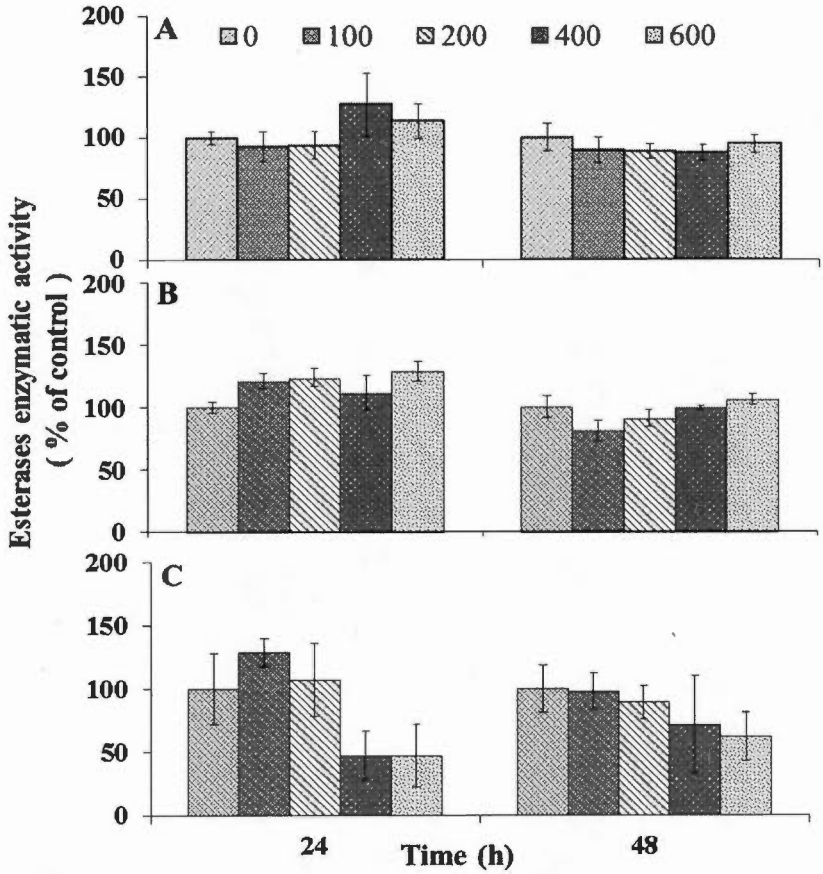

Figure 4.5 Change in esterases enzymatic activity (% of control) of *C. reinhardtii* and CPCC 121 at pH 7 (A, B) and CPCC 121 at pH 4 (C) exposed during 48 h to different concentrations of Cd (μM). Each data indicated the average and coefficient of variation (CV %) of 8 replicates. Data showed no significant differences at the level of 0.05 ($p < 0.05$) between treated-samples and control.

4.1.5 Alteration of PSII activity

The effect of Cd on primary photochemistry and electron transport activity of PSII was investigated by monitoring the change of the performance index of PSII activity (PI), when the highest Cd accumulation in algal biomass was reached at 24 h (Figure 4.7). The photosynthetic-fluorescence parameter PI was determined from the chlorophyll fluorescence kinetic (Figure 4.6), which previously demonstrated to be

indicative of the efficiency of PSII photochemical reactions of photosynthesis (Strasser *et al.*, 2004). When algal cells of *C. reinhardtii* were exposed to 200 µM of Cd, a significant decrease of PI value by 60 ± 4 % relative to the control ($p < 0.05$) was already noticed. In comparison, algal cells of CPCC 121 exposed at pH 7 and pH 4 showed respectively a decrease of PI value by 26 ± 1 % and 16 ± 5 % compared to the control ($p < 0.05$). Based on these results, it was evident that the toxicity impact of Cd was stronger on PSII activity of *C. reinhardtii*, which might be due to a higher intracellular accumulation of Cd. In addition, the low accumulation of Cd in CPCC 121 was correlated with a lower effect on PSII activity performance.

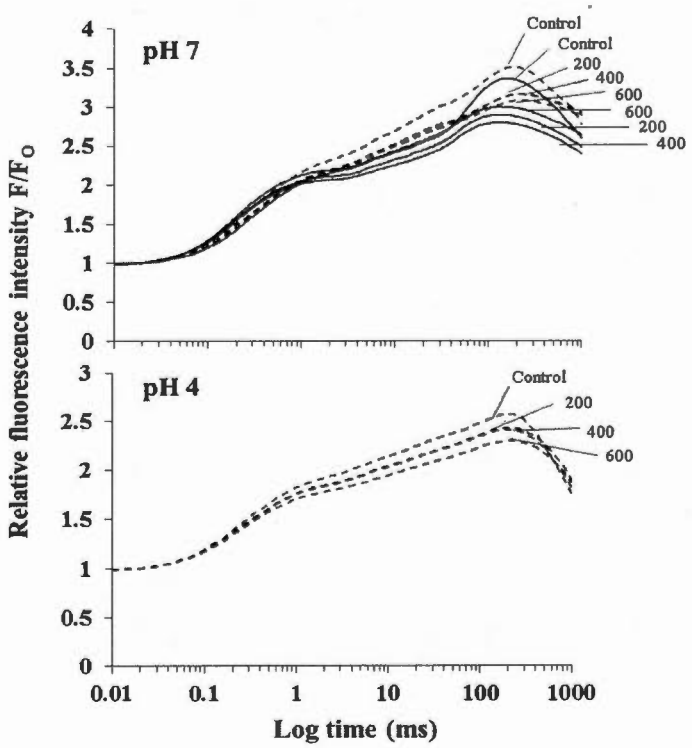

Figure 4.6 Chl *a* fluorescence kinetics of *Chlamydomonas* strains exposed at pH 7 and 4 during 24 h to different concentrations of Cd in µM. Data represents the average of 4 replicates. Solid and dashed lines represent respectively the fluorescence intensity of *C. reinhardtii* at pH 7 and CPCC 121 at pH 7 and 4.

Therefore, our results on the change of PI value suggested that Cd induced the inactivation of PSII reaction centers, causing a decrease of PSII electron transport toward PSI. This interpretation is in agreement with previous works concerning the toxicity of Cd on the photosynthetic activity of green algae. For instance, the alteration of energy transfer from antenna complexes to PSII reaction centers was reported in *Scenedesmus obliquus* under Cd stress effect (Mallick et Mohn, 2003). In fact, this alteration was even observed after 1 h of exposure under all nominal concentrations of Cd, from 10 to 500 µM. These authors showed that the primary targeted inhibitory site of Cd was the water splitting system of PSII complex, causing a reduction of the photosynthetic electron transport. Furthermore, it was reported on algal cells of *C. reinhardtii* that low concentrations of Cd^{2+} (at µM) inhibited the last step in the assembly of PSII complex before becoming photochemical active (Faller *et al.*, 2005). The authors suggested that Cd^{2+} did competitively bound to Ca^{2+} sites in the PSII system during the photoactivation, causing the inhibition of the water splitting system. In another study, 300 µM of Cd inhibited the photosynthetic activity of algal cells of *C. reinhardtii* while the respiration activity remained highly functional even after 24 h of exposure (Vega *et al.*, 2006). More recently, when algal cells of *C. reinhardtii* were exposed during 24 h to different concentrations of Cd^{2+} from 0.15 to 4.62 µM, the fluorescence yield of O-J-I-P transients decreased in a concentration-dependent manner (Perreault *et al.*, 2011). These results were a clear indication of the inhibition of the PSII electron transport from water-splitting system to PSI activity. In our study, we demonstrated that the inhibitory effect of Cd on PSII activity was correlated with the accumulation of Cd in algal biomass of studied *Chlamydomonas* strains.

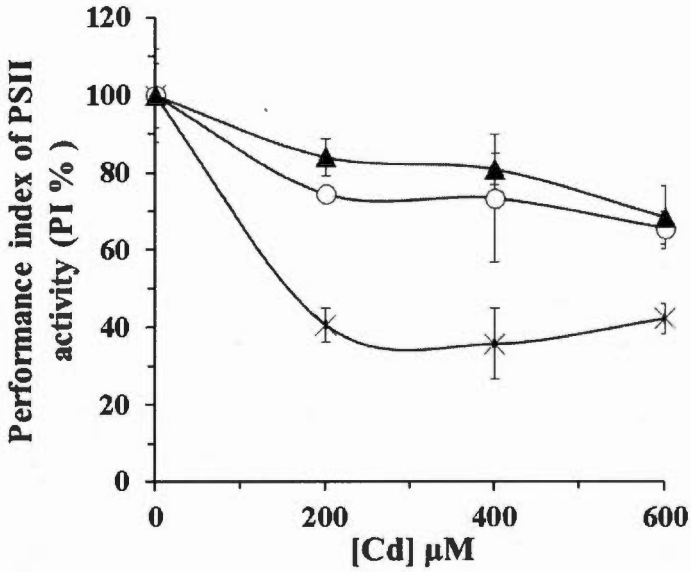

Figure 4.7 Change in the performance index of Photosystem II activity (PI, % of control) for algal cells exposed during 24 h to different concentrations of Cd (µM) and pH condition. Legend: ×, *C. reinhardtii* at pH 7; ○, CPCC 121 at pH 7; ▲, CPCC 121 at pH 4. Each data indicated the average and coefficient of variation (CV %) of 4 replicates. Statistical analysis indicated that all treated samples (200-600 µM of Cd) were significantly different to their respective control at the level of 0.05 ($p < 0.05$).

4.1.6 Cellular localization of Cd

A TEM cross-section analysis was performed on algal cells exposed to 600 µM of Cd during 24 h, and results clearly indicated the accumulation of Cd in algal cells of both *Chlamydomonas* species at pH 7, and in algal cells of CPCC 121 at pH 4. TEM micrographs showed the ultrastructure of algal cells in which the chloroplast occupied most of the cellular volume (Figure 4.8a, b). However, no alterations in cellular ultrastructure of treated samples (600 µM of Cd) were noticed in comparison to the control. In Cd-treated cells, the accumulation of intracellular Cd was observed as several black deposits. Particularly, in *Chlamydomonas* CPCC 121 exposed at pH 7, a significant distribution of black deposits was observed in the cell wall (Figure 4.8b).

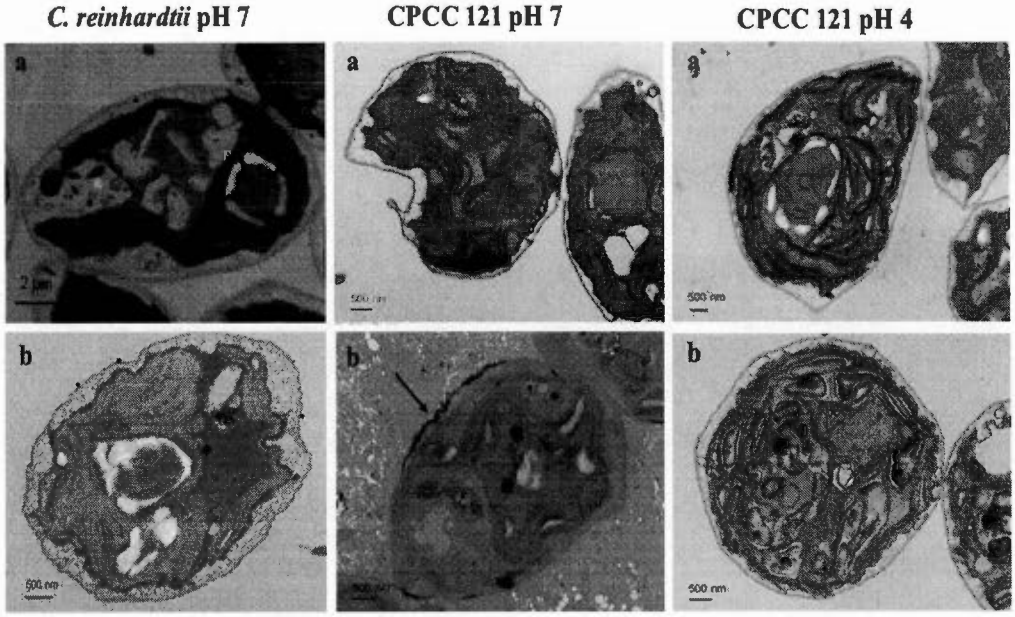

Figure 4.8 TEM images of algal cell ultrastructure for *Chlamydomonas reinhardtii* and CPCC 121. Control samples (a), and 24 h Cd-treated (600 μM) samples (b).

Furthermore, energy-dispersive X-ray analysis (EDX) was performed to evaluate the local elemental distribution in algal cells that confirmed the presence of Cd at selected areas (B, C and A) within the cell (Figure 4.9), and at a selected area (A) on the cell wall of CPCC 121 exposed at pH 7 (Figure 4.10). The presence of X-ray peaks representing C, P, N, Cl and Ca was attributed to biological components of the cell, O peaks to the post-fix step, and the Fe to the TEM column. Indeed, previous studies showed by EDX analysis that P and Cd signals were in electron-dense deposits within cells of *C. acidophila* treated to 20 μM Cd during 3 days, and *Chlamydomonas sp.* treated to 200 μM Cd during 12 days (Aguilera et Amils, 2005; Nishikawa *et al.*, 2003). Based on our results, there was no peak related to the presence of Cd on the high-energy region of the EDX spectrum (Figure 4.9c) confirming the low Cd accumulation of CPCC 121 cells at pH 4, which was indicated by the accumulation of Cd in algal biomass by quantitative analysis (see Figure 4.2).

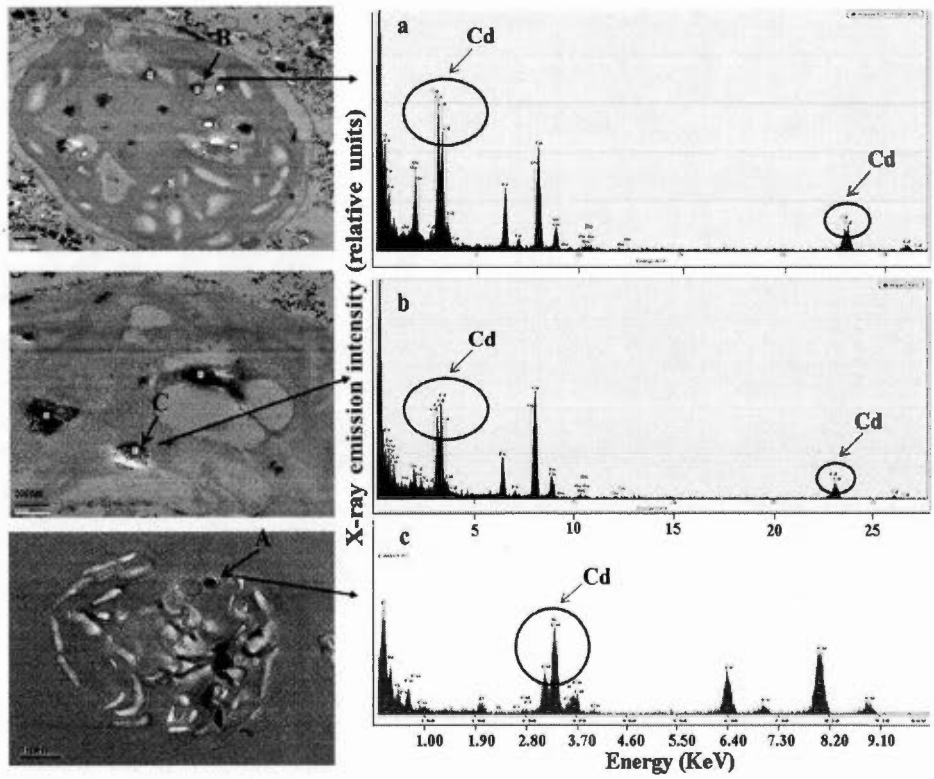

Figure 4.9 Energy dispersive X-ray spectroscopy of localized intracellular Cd in the cytoplasm for 24 h Cd-treated (600 μM) *C. reinhardtii* at pH 7 (a), 24 h Cd-treated (600 μM) CPCC 121 at pH 7 (b), and 24 h Cd-treated (600 μM) CPCC 121 at pH 4 (c). The EDX spectrum was obtained by collecting X-ray signals from the selected area of the sample, when it was radiated by the focused e-beam. Legend: B, selected area in algal cell of *C. reinhardtii* at pH 7; C, selected area in algal cell of CPCC 121 at pH 7; and A, selected area in algal cell of CPCC 121 at pH 4.

Moreover, the distribution of Cd within the cell wall of CPCC 121 exposed to 600 μM of Cd at pH 7 was determined by EDX analysis (Figure 4.10). Our results showed that Cd within the cell wall was not found in cells of *C. reinhardtii* at pH 7 or cells of CPCC 121 at pH 4. In comparison, only a low quantity of Cd was accumulated in CPCC 121 cells exposed at pH 4. Under this condition, Cd was not distributed within the cell wall of algal cells, which can be explained by the high protonation of the cell surface of CPCC 121 and the competition of H^+ against Cd^{2+}

for binding sites at the cell wall. Indeed, it was previously showed that positive zeta potential at the cell wall surface was an effective protection against the toxic effect of metals for *Dunaliella acidophila* grown in acidic medium (Gimmler *et al.*, 1991).

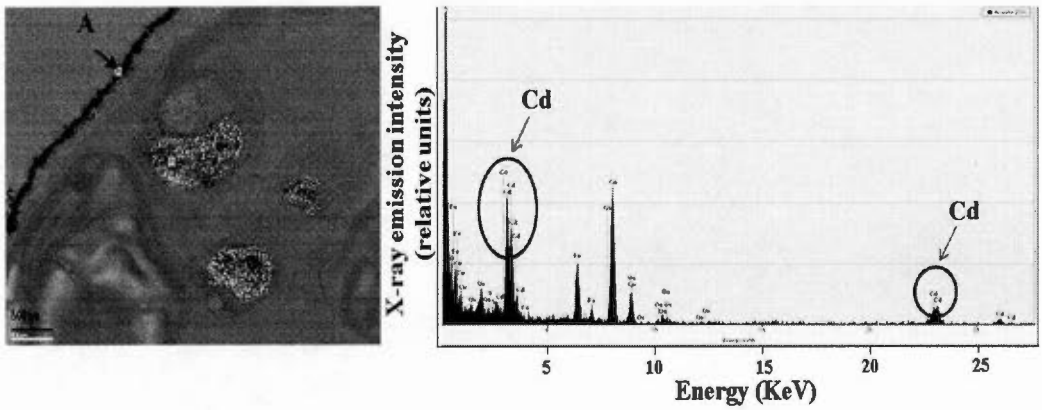

Figure 4.10 EDX spectrum of Cd distribution within the cell wall of CPCC 121. The electron probe was focused on (A) representing a selected area on the cell wall of CPCC 121 treated during 24 h to 600 µM of Cd at pH 7.

4.2 Summary: algal tolerance for accumulated Cd effect

In this study, cellular toxic effects of Cd were investigated on *C. reinhardtii* and CPCC 121, by analyzing the accumulation of Cd in algal biomass, the cellular growth rate, the relative size and granularity of cells, and the PSII activity. Our results estimated the capacity of algal cells to accumulate and tolerate Cd during 48 h under two pH condition. The maximum capacity of Cd accumulation in algal biomass was reached at 24 h of exposure under 600 µM of Cd for both algal strains (Figure 4.11). Under this condition, *C. reinhardtii* showed significantly higher accumulation of Cd compared to CPCC 121, although it was more sensitive to Cd toxic effects as indicated by a lower performance index of PSII activity and cellular growth rate. In fact, the low accumulation and effect of Cd^{2+} on CPCC 121 indicated that this algal strain was more tolerant for Cd^{2+} than *C. reinhardtii*. Even when the concentration of

Cd^{2+} was the highest in the medium at pH 4, the accumulation of Cd was extremely low in algal biomass of CPCC 121 due to the high protonation at the cell surface. Therefore, *Chlamydomonas* CPCC 121 was the most tolerant strain at pH 4 for Cd^{2+} accumulation and toxicity.

4.3 Conclusion: significance for bioremediation

The concept of phycoremediation represents the use of algae to remediate polluted environmental matrices, and this new approach of bioremediation needs more research and development studies in order to be applied for water decontamination of metals. Therefore, fundamental studies concerning the accumulation capacity of metals over time on different algal species are necessary in order to select the most appropriate strain according to environmental conditions. In this perspective, we demonstrated in our study the potential use of both green algal strains *C. reinhardtii* and CPCC 121 for the removal of Cd in aqueous solution, which was dependent on the environmental condition. Our results suggested that the use of both strains of *Chlamydomonas* for bioremediation applications under acidic condition was not recommended. At neutral pH, *C. reinhardtii* showed the highest ability to accumulate Cd compared to CPCC 121 although having a lower tolerance for Cd toxic effects. Therefore, the efficiency of *C. reinhardtii* for the removal of Cd was dependent on the concentration of Cd and the time of exposure. However, our results concerning the accumulation of Cd by CPCC 121 indicated that this algal strain was not enough efficient to be considered for the phycoremediation of Cd.

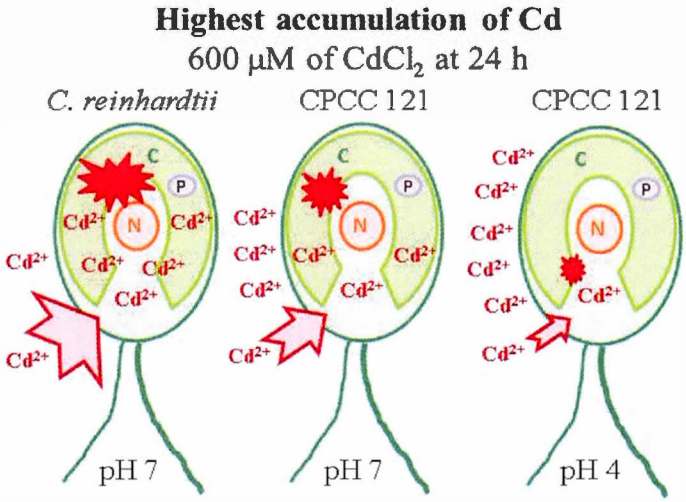

Figure 4.11 Scheme representing algal cells of *Chlamydomonas reinhardtii* and CPCC 121 at 24 h of exposure to 600 μM of Cd under two pH conditions. C, chloroplast; N, nucleus; P, pyrenoid. The stars illustrate the toxicity impact of Cd^{2+} in algal cells. As indicated by the results (see subsection 4.1.3), the toxicity impact is related to the accumulation of Cd^{2+} in the cells.

CHAPTER V

CADMIUM ACCUMULATION AND TOXICITY AFFECT THE EXTRACYTOPLASMIC POLYPHOSPHATE LEVEL IN *CHLAMYDOMONAS REINHARDTII*

5.1 Results and discussion

In previous studies, the change of the algal growth rate demonstrated to be a global indicator of Cd toxicity on *Chlamydomonas* strains (Jamers *et al.*, 2009; Perreault *et al.*, 2010). Here, as a toxicity indicator, we determined the inhibitory effect of Cd on the cell density of both *Chlamydomonas* strains, when exposed during 24-72 h to different concentrations of Cd (Figure 5.1). When compared to the control, the results showed that all Cd-treated conditions induced a strong and continuous inhibitory effect (significant for $p < 0.05$) during 72 h on the growth of the cell density of *Chlamydomonas* strains. However, no significant difference between Cd-treated conditions were noticed at 24-48 h, indicating that 200-600 µM of Cd did induce a similar toxicity effect. At 72 h, the inhibitory effect of Cd was stronger than at 24-48 h, in a concentration dependent manner. Furthermore, the growth rate (cell d^{-1}) was determined based on the change of the cell density during 72 h of exposure (Table 5.1). When algal cells were exposed during 72 h to 200-600 µM of Cd, the growth rate decreased by 42-51 % for the strain CC-125 and by 52-60 % for CC-503 compared to control ($p < 0.05$). However, the inhibitory effect of Cd on the growth rate was not significantly different between the strains CC-125 and CC-503.

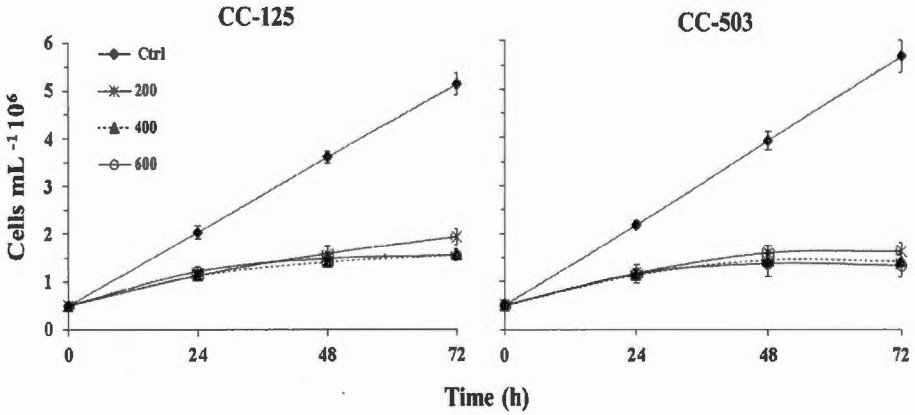

Figure 5.1 Change in the cell density for both strains of *Chlamydomonas* exposed during 24-72 h to 200-600 µM of Cd. Differences between the control and all treated-samples were significant for $p < 0.05$ during 24-72 h.

Table 5.1 Change in the growth rate (in cell d^{-1}) for both *Chlamydomonas* strains exposed during 72 h to different concentrations of Cd.

Growth rate (cell d^{-1})		
[Cd] µM	CC-125	CC-503
0	0.78 ± 0.02	0.81 ± 0.02
200	0.45 ± 0.03	0.39 ± 0.04
400	0.38 ± 0.02	0.35 ± 0.03
600	0.38 ± 0.03	0.32 ± 0.06

The physiological stress induced by Cd was further investigated by measuring the level of extracytoplasmic polyP, which was determined on viable cells by confocal microscopy (see Chapter III). Acquired microscopy images of both strains (control sample) showed specific fluorescence peaks of polyP-DAPI related to the cell wall (Figure 5.2, A and B). In comparison to CC-125, the fluorescence intensity of polyP-

DAPI was significantly lower by half for the strain CC-503, probably because of the deficiency in the cell-wall structure of this mutant strain.

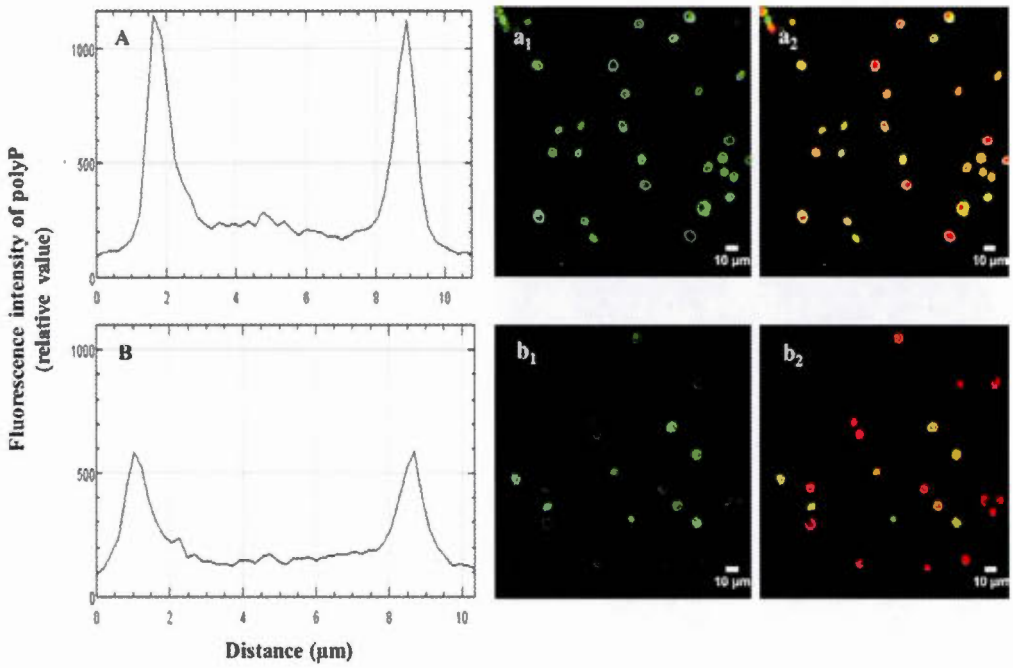

Figure 5.2 Fluorescence emission of extracytoplasmic polyP-DAPI from cells of CC-125 (A) and CC-503 (B), determined by confocal microscopy imaging. Green and red fluorescence from cells represent respectively polyP and chlorophylls in confocal microscopic images (scale bar of 10 µm) for CC-125 (a_1 and a_2) and CC-503 (b_1 and b_2).

When algal cells were exposed during 72 h to different Cd concentrations, the level of extracytoplasmic polyP was monitored to determine the effect of Cd on the metabolism of polyP. The results showed that the level of polyP was significantly affected by Cd toxicity for both strains, CC-125 and CC-503 (Figure 5.3).

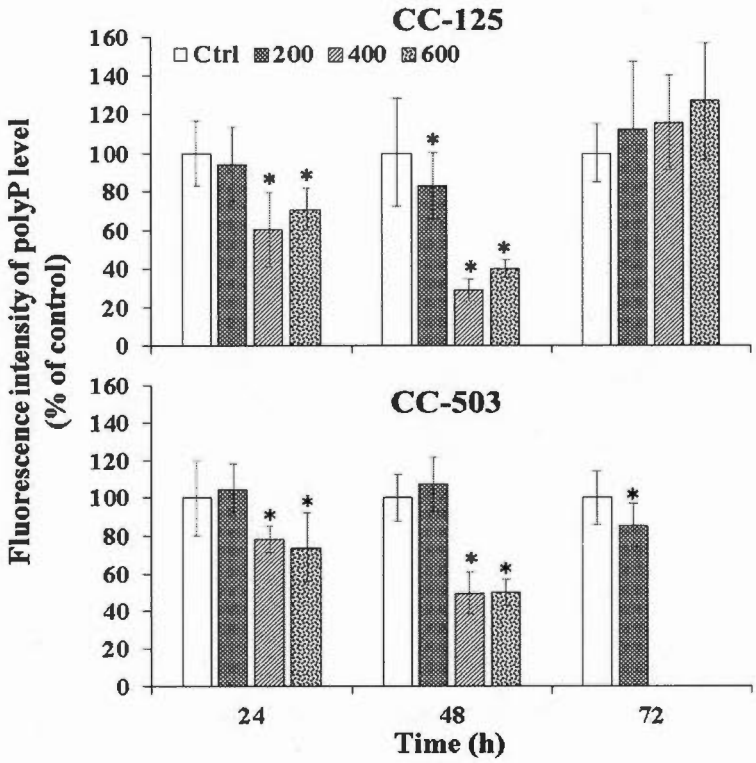

Figure 5.3 Fluorescence intensity of the extracytoplasmic polyP level (% of control) for both *Chlamydomonas* strains exposed during 24-72 h to 200-600 µM of Cd. Data represents the average of 10 cells captured for each microscopic image, and the bars indicate the coefficient of variation (CV %). The asterisk (*) indicates significant differences between treatments and the control condition ($p < 0.05$).

At 24 h, the polyP level decreased significantly compared to control ($p < 0.05$) under 400 and 600 µM of Cd, and this decrease was stronger by half at 48 h. However, the polyP level was different when comparing both strains at 72 h: The polyP level of Cd-treated cells recovered to the control level for CC-125, while the level decreased completely for CC-503 cells exposed to 400-600 µM of Cd (Figure 5.3). In a previous study, Nishikawa *et al.* (2003) showed a significant decrease in the polyP level of *Chlamydomonas acidophila* KT-1, when exposed during 72 h to 20 µM of Cd in acidic condition. They suggested that Cd toxicity induced the

degradation of vacuolar polyP into Pi (Nishikawa *et al.*, 2003). Later, this research group demonstrated that Cd toxicity induced the degradation of both high and low molecular weight of polyP, while orthophosphate was still detected (Nishikawa *et al.*, 2009). Already at 24-48 h, our results indicated that high concentrations of Cd (400-600 µM) might induce a decrease in synthesis and/or a degradation of extracytoplasmic polyP in cells of *C. reinhardtii* at neutral pH. Based on these results (Figure 5.1 and 5.3, Table 5.1), the decrease of polyP level and of growth rate were both related to the toxic effect of Cd, only for the strain CC-503 exposed during 72 h to 400-600 µM of Cd. Under the others treatment conditions, the toxicity of Cd affected independently the metabolism of polyP (synthesis and/or degradation of polyP) and the process of growth rate for both algal strains.

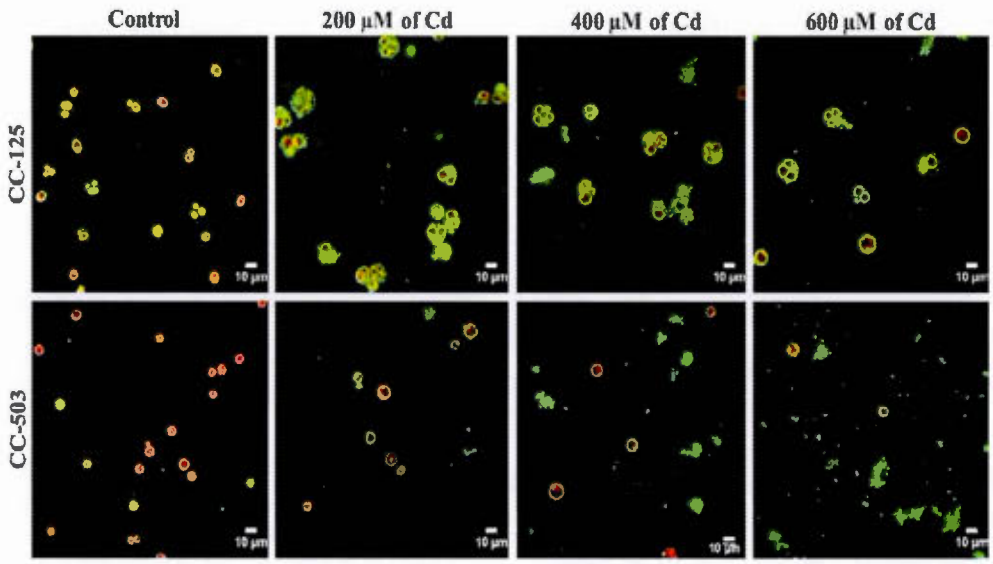

Figure 5.4 Confocal microscopic images of *Chlamydomonas* cells (scale bar of 10 µm) exposed during 72 h to 200-600 µM of Cd. These images show the green fluorescence of extracytoplasmic polyP-DAPI and the red fluorescence of chlorophylls (from the chloroplast).

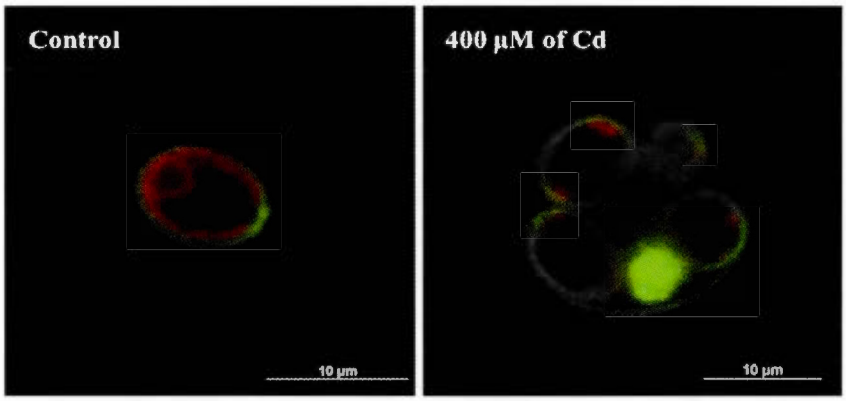

Figure 5.5 Image magnification of CC-125 cells from confocal microscopy (scale bar of 10 µm). At the left, an individual control cell. At the right, palmelloid colonies of 4 cells, under 400 µM of Cd during 72 h. The green fluorescence is emitted from the extracytoplasmic polyP-DAPI, and the red fluorescence by the Chlorophylls.

From confocal microscopy images, we analyzed the morphology of algal cells to compare the effect of Cd between both strains during 72 h (Figure 5.4, and the magnification of algal cells in Figure 5.5). The Cd-treated cells of CC-503 clearly showed necrosis, which increased in relation to the concentration of Cd from 200 to 600 µM. Nevertheless, we did not observe a similar effect for CC-125 under Cd treatments at 72 h. In fact, algal cells formed palmelloid colonies of 2-4 cells with a common cell wall, probably to protect themselves against the bioavailability of Cd in the medium. It was previously suggested that *C. reinhardtii* cells can form palmelloid colonies under stress condition. Indeed, light micrographs analysis showed the aggregation of 4-8 non-motile cells within a common mother cell wall, which was probably caused by an alteration of mitosis (Harris, 2009). At 24 h, we observed palmelloid colonies only under the exposure of 200 µM of Cd, and at 48 h under the exposure of 200-400 µM of Cd (Figure 5.6 and 5.7). Nevertheless, only few individual cells were observed under these Cd treatments, and their cell sizes appeared to be larger than the control. In a previous study, flow cytometry analysis showed an increase by 84-119 % in the relative cell size of *C. reinhardtii* cells

exposed during 24-48 h to 600 µM of Cd (Samadani *et al.*, 2018). The authors suggested that such increase in the cell size was correlated with the inhibitory effect of Cd during the cell division cycle.

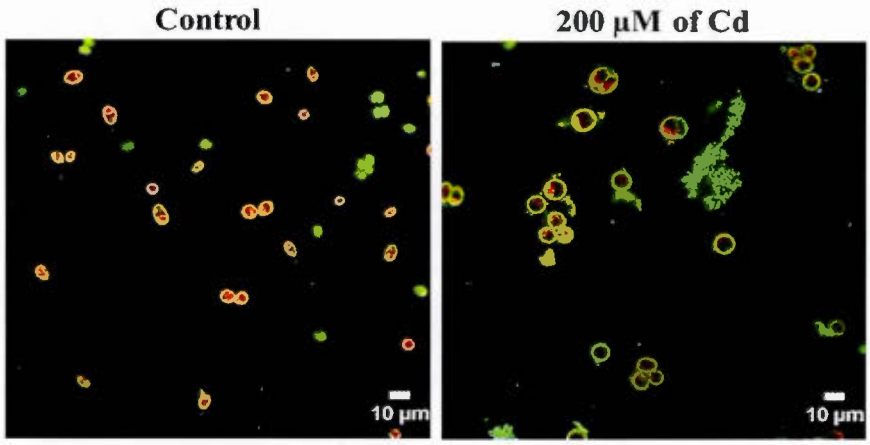

Figure 5.6 Confocal microscopic images of CC-125 cells (scale bar of 10 µm) treated during 24 h to 0 and 200 µM of Cd. The formation of palmelloid colonies was noticed for Cd-treated algal cells. The green fluorescence: Extracytoplasmic polyP-DAPI; and the red fluorescence: Chlorophylls (from the chloroplast).

Therefore, our results showed that the formation of palmelloid colonies was dependent on the concentration of Cd and the time of exposure. This phenomenon explained why the Cd-treated cells of CC-125 were able to have a high level of extracytoplasmic polyP at 72 h, although the inhibition of growth rate was similar between CC-125 and CC-503. Since the strain CC-503 had an impaired cell wall, cells were not able to form palmelloid colonies. Consequently, the level of extracytoplasmic polyP did collapse at 72 h under 400-600 µM of Cd, which was probably caused by a high level of cellular necrosis.

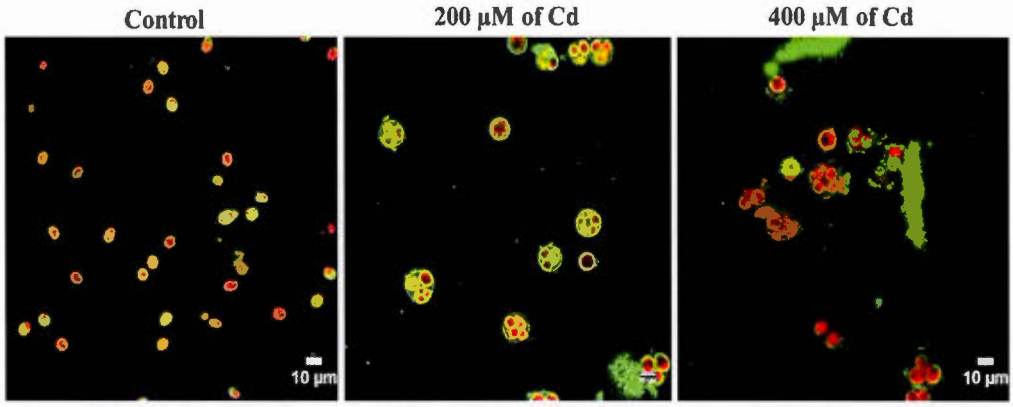

Figure 5.7 Confocal microscopic images of CC-125 cells (scale bar of 10 µm) treated during 48 h to 0, 200 and 400 µM of Cd. For Cd-treated cells, microscopic images show clearly the formation of palmelloid colonies within a common cell wall. The green and red fluorescence indicate respectively the extracytoplasmic polyP-DAPI and chlorophylls.

Moreover, we determined the Cd accumulation in algal biomass of both strains CC-125 and CC-503 (Figure 5.8, Table 5.2), and the results showed a significant increase for all Cd-treated conditions compared to control ($p < 0.05$). Particularly, the accumulation of Cd was more dependent on the concentration of Cd (200-600 µM) than the time of exposure (24-72 h). At 24 h, the maximum accumulation of Cd in CC-125 was reached (2.96 µg Cd / mg dry mass) under 600 µM of Cd. Under this condition, CC-503 presented a higher accumulation level (3.44 µg Cd / mg dry mass), probably because of its cell wall deficiency. Furthermore, the strain CC-125 accumulated a similar amount of Cd at 48 h compared to 24 h. Concerning CC-503, the quantity of accumulated Cd decreased slightly by 10-13 % at 48 h under 400-600 µM of Cd, which might be caused by the toxicity impact. However, the methodology to determine the accumulation of Cd in algal biomass did not permit to discriminate the accumulation of Cd in living cells from debris. However, it was interesting to notice that at 24-48 h the inhibition of cell density was not significantly different between CC-125 and CC-503. At 72 h of exposure to 600 µM of Cd, the

accumulation of Cd in CC-125 was only higher by 10 % compared to CC-503. These results might explain the inhibition of the growth rate for both strains.

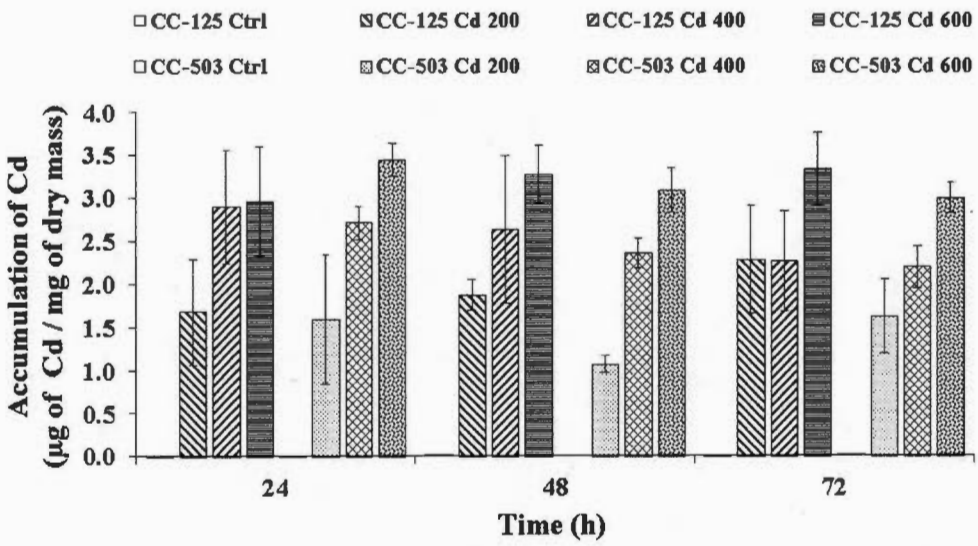

Figure 5.8 Accumulation of Cd in algal biomass of both *Chlamydomonas* strains exposed during 24-72 h to 200-600 µM of Cd. All treated-conditions showed significant differences to the control for $p < 0.05$.

Moreover, the change in polyP level was plotted in relation to the accumulation of Cd (Figure 5.9). For both strains, these results clearly showed that the decrease of the polyP level was correlated with the increase of Cd accumulation, and this decrease was stronger at 48 h than at 24 h. At 72 h, the polyP level decreased drastically (100 %) in relation to the increasing accumulation of Cd, only for the strain

Table 5.2 Significant differences between treatments for accumulation of Cd in algal biomass of both *Chlamydomonas* strains for each strain at each time of exposure ($p < 0.05$).

Comparison conditions [Cd] µM	Significant differences ($p < 0.05$)					
	CC-125			CC-503		
	24 h	48 h	72 h	24 h	48 h	72 h
200-400	Yes	No	No	Yes	Yes	Yes
200-600	Yes	Yes	Yes	Yes	Yes	Yes
400-600	No	No	Yes	Yes	Yes	Yes

CC-503. Therefore, the accumulated Cd (or dose) was correlated with the decrease in synthesis and/or the degradation of extracytoplasmic polyP under these treatment conditions. However, the polyP level increased by 20 % in relation to the increasing Cd accumulation for the strain CC-125 at 72 h, indicating the recovery of the polyP level. In fact, our results might suggest that the cell wall of CC-125 participated in this recovery. In addition, the restoration of the polyP level at 72 h was correlated with the formation of palmelloid colonies (Figure 5.4).

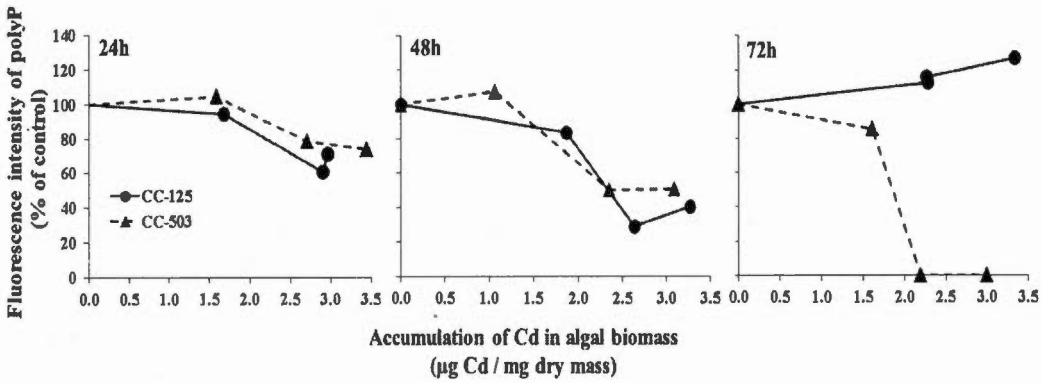

Figure 5.9 The level of extracytoplasmic polyP (% of control) in relation to the accumulation of Cd for CC-125 and CC-503 exposed during 24-72 h to Cd concentrations (200-600 µM).

The effect of Cd was also evaluated on the photochemical reactions of PSII, since this primary process of photosynthesis represents a sensitive indicator of metal toxicity in algal cells (Popovic *et al.*, 2003). Previously, Perreault *et al.* (2011) showed that Cd toxicity induced the inhibition of the PSII primary photochemistry and electron transport activity in *C. reinhardtii*. Already at 24 h, the authors demonstrated a strong correlation between the decrease in the maximal PSII quantum yield (F_V/F_M value) and the concentration of Cd (0.15, 0.96, 2.33, and 4.62 µM) (Perreault *et al.*, 2011). In our study, we determined the F_V/F_M value when algal cells were exposed to Cd stress effect, and the change of F_V/F_M was plotted in relation to the change of the polyP level (Figure 5.10). Under these conditions, the level of polyP decreased in relation to the decrease of F_V/F_M value, which was stronger at 48 h than at 24 h. At 72 h, both the polyP level and the F_V/F_M value decreased drastically only for CC-503, indicating a strong toxicity impact on the photosynthetic activity and the synthesis and/or degradation of polyP. However, the polyP level of CC-125 remained high while the F_V/F_M value indicated a strong deterioration of the photosynthetic processes. In this strain, the deterioration of PSII activity might explain the inhibition of growth rate even though the polyP level increased. Therefore, these results suggest that the extracytoplasmic polyP did not participate here in the sequestration of Cd.

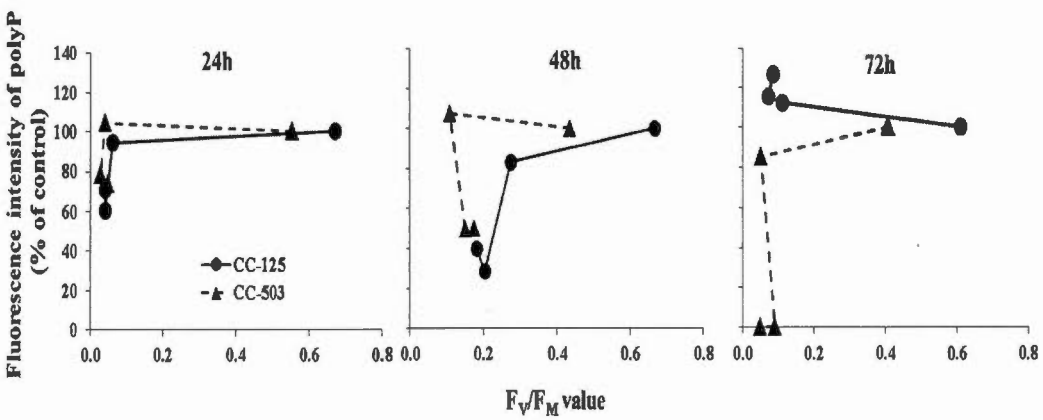

Figure 5.10 The level of extracytoplasmic polyP (% of control) in relation to the maximal PSII quantum yield (F_V/F_M) for CC-125 and CC-503 exposed during 24-72 h to Cd concentrations (200-600 µM).

5.2 Conclusion: physiological relevance of extracytoplasmic polyP

In this study, our results showed the accumulation and toxicity effect of Cd on the level of extracytoplasmic polyP under neutral pH using two strains of *Chlamydomonas reinhardtii*. Previously, Nishikawa *et al.* (2003, 2009) demonstrated the degradation of vacuolar polyP into Pi and Cd, when *Chlamydomonas acidophila* KT-1 was treated under acidic condition (pH 4) to 20 µM of Cd during 3 d. These authors suggested a Cd tolerance mechanism in this alga, involving the sequestration of Cd as a Cd-phosphate complex, and its excretion out of algal cell. Based on our experiments at pH 7, we showed that Cd toxicity did affect the synthesis and/or the degradation of polyP in *Chlamydomonas reinhardtii*. However, under the treatment conditions of our study (200-600 µM of Cd), the results did not suggest that polyP participated in the sequestration of Cd. In fact, we demonstrated a decrease in the synthesis and/or the degradation of polyP following the accumulation of Cd, even in the strain CC-503 having a lower level of polyP. Because of its cell wall-deficiency, the strong toxicity of Cd induced a high level of cell necrosis, and the initial level of polyP could not be recovered at 72 h in this strain. For CC-125, the level of polyP was restored at 72 h, which was correlated with the formation of palmelloid colonies having a common cell wall. Nevertheless, both strains were able to accumulate significant amount of Cd in their biomass. In addition, these results demonstrated that the impact of Cd on the polyP level was dependent on the Cd concentration, whereas the growth rate was inhibited regardless of the concentration of Cd. Therefore, a distinct impact of Cd on the metabolism of polyP (synthesis and/or degradation) can be used as a biomarker of metal toxicity such as Cd under tested conditions (24 and 48 h), even in the cell wall-deficient strain CC-503.

CHAPTER VI

EFFECT OF MERCURY ON THE POLYPHOSPHATE LEVEL OF ALGA *CHLAMYDOMONAS REINHARDTII*

6.1 Results

6.1.1 Inhibition of growth rate

As a toxicity indicator, the change in the cell density of CC-125 and CC-503 exposed to Hg effect was monitored during 72 h (Figure 6.1). The results showed a significant ($p < 0.05$) inhibitory effect of Hg on the cell density, which was dependent on the concentration of Hg and the time of exposure. Under 1 μM of Hg during 24 and 48 h, the cell density of CC-503 decreased respectively by 20 and 15 % compared to control, while for CC-125 it decreased respectively by 60 and 20 % (Figure 6.1). Under this condition, it appeared that the strain CC-503 was more tolerant than CC-125 to the exposure of Hg. Nevertheless, 1 μM of Hg triggered similar effect at 72 h for both strains. Furthermore, 3 μM of Hg inhibited completely the growth of cell density at 24 h for both strains (Figure 6.1), but the growth partly recovered from 48 to 72 h. Under 5 and 7 μM of Hg, the growth of cell density was totally inhibited during 24-72 h. Moreover, the growth rate of CC-125 and CC-503 was determined during 72 h (Table 6.1), and the results showed a decrease which was correlated with the concentration of Hg.

Table 6.1 Change in the growth rate (cell d^{-1}) for both strains CC-125 and CC-503 exposed during 72 h to different concentrations of Hg.

Growth rate (cell d^{-1})		
[Hg] µM	CC-125	CC-503
0	0.74 ± 0.01	0.80 ± 0.03
1	0.70 ± 0.02	0.77 ± 0.01
3	0.52 ± 0.04	0.63 ± 0.02
5	0.16 ± 0.04	0.15 ± 0.09
7	-	-

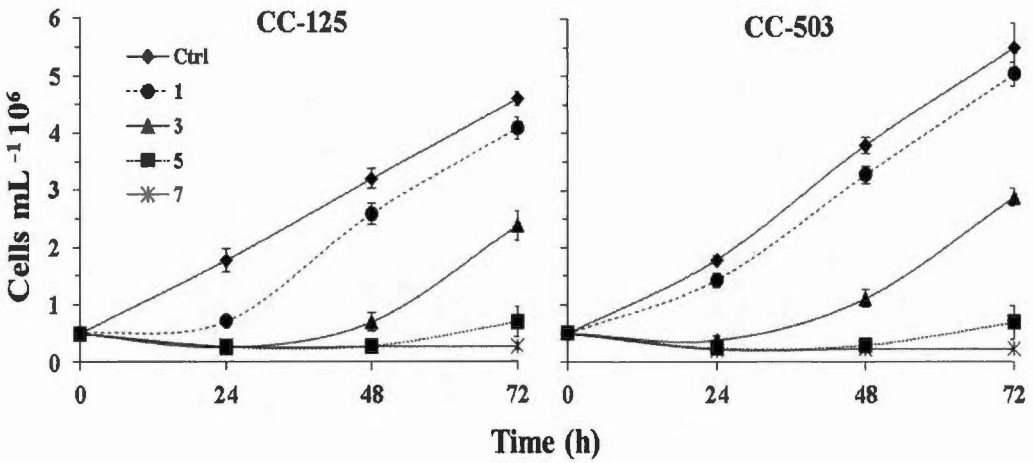

Figure 6.1 Change in the cell density for both strains CC-125 and CC-503 exposed during 24-72 h to different concentrations of Hg (1-7 µM). Differences between treated-samples and control were all significant ($p < 0.05$), except for CC-503 exposed to 1 µM of Hg during 48-72 h.

6.1.2 Change of polyP level under Hg stress

For the first time, we determined the fluorescence emission of PolyP-DAPI of viable cells by using confocal microscopy. Our methodological approach permitted to

acquire the fluorescence imaging of extracytoplasmic polyP (related to the cell wall) in algal samples, since DAPI compounds were not able to pass through the cell membrane of viable cells. As a negative control, fluorescence emission from extracytoplasmic polyP (measured at 525 nm) was not detected without the addition of DAPI staining. Therefore, polyP-DAPI fluorescence from confocal microscopy images showed that non treated-cells (control sample) had specific peaks, which was directly related to cell wall (for CC-125, Figure 6.2A, a_1 and a_2; and for CC-503, Figure 6.3A, a_1 and a_2). In particular, the fluorescence intensity of polyP from CC-503 was half compared to CC-125, which is explained by the cell wall deficiency in this mutant strain.

The change of the polyP level associated to the cell wall was investigated under Hg effect to understand the polyP role on the cell physiology. Therefore, the change of polyP-DAPI fluorescence intensity was investigated for both strains during 24-72 h of exposure to different concentrations of Hg (Figure 6.4). When algal cells were exposed to high concentrations of Hg (5 and 7 μM), it was not possible to evaluate the polyP level of the cell wall, even at 24 h. In fact, confocal microscopy images showed for both strains that the toxicity impact induced by these concentrations of Hg caused cellular necrosis, which was correlated with the loss of fluorescence peaks from extracytoplasmic PolyP-DAPI. Under this condition, DAPI compounds penetrated inside dead cells, as indicated by the fluorescence emission of PolyP-DAPI in unshaped dead cells (for CC-125 see Figure 6.2B, b_1 and b_2; for CC503 see Figure 6.3B, b_1 and b_2).

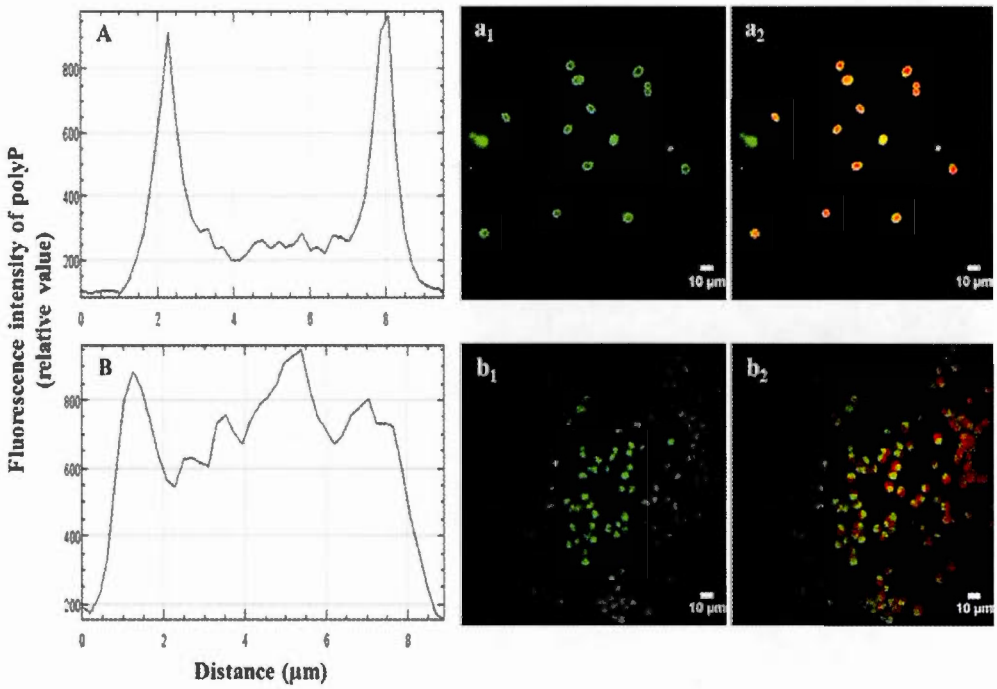

Figure 6.2 Fluorescence emission of polyP-DAPI in cells of CC-125 determined by confocal microscopy imaging. A, a_1 and a_2, non-treated cells; B, b_1 and b_2, 24 h treated-cells to 5 µM of Hg. In confocal microscopic images, green and red fluorescence represent respectively polyP and chlorophylls (scale bar of 10 µm).

Moreover, our results showed that the exposure to 1 and 3 µM of Hg during 24-72 h affected the polyP level of the cell wall (Figure 6.4). When both strains were exposed during 24-48 h to 3 µM of Hg, the fluorescence intensity of polyP-DAPI decreased significantly compared to control ($p < 0.05$), but at 72 h, the intensity level returned to the same level of the control. At 24 and 48 h, the fluorescence intensity decreased respectively by 69 and 56 % for CC-125, and by 73 and 77 % for CC-503.

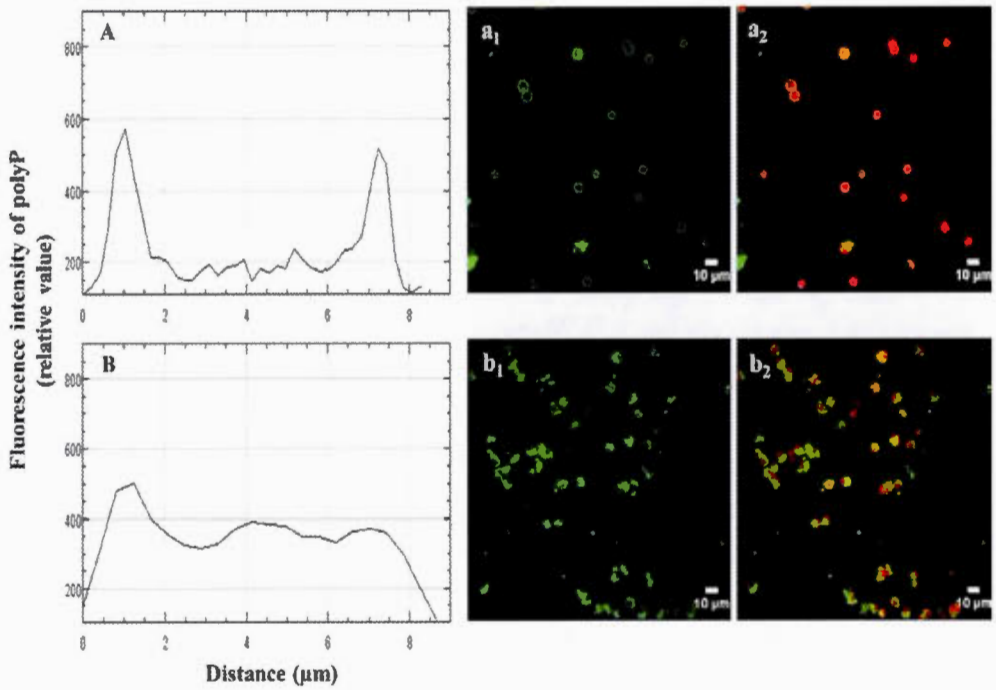

Figure 6.3 Fluorescence emission of polyP-DAPI in cells of CC-503 determined by confocal microscopy imaging. A, a_1 and a_2, non-treated cells; B, b_1 and b_2, 24 h treated-cells to 5 µM of Hg. In confocal microscopic images, green and red fluorescence represent respectively polyP and chlorophylls (scale bar of 10 µm).

When the strain CC-125 was exposed to 1 µM of Hg, the fluorescence intensity of polyP decreased significantly by 28 % (compared to control, $p < 0.05$), only at 24 h. Under the same treatment, the fluorescence intensity decreased significantly by 70 % (compared to the control, $p < 0.05$) for CC-503, only at 48 h (Figure 6.4). Therefore, these results indicated that the toxicity effect of Hg was correlated with the decrease of the polyP level during 24-48 h.

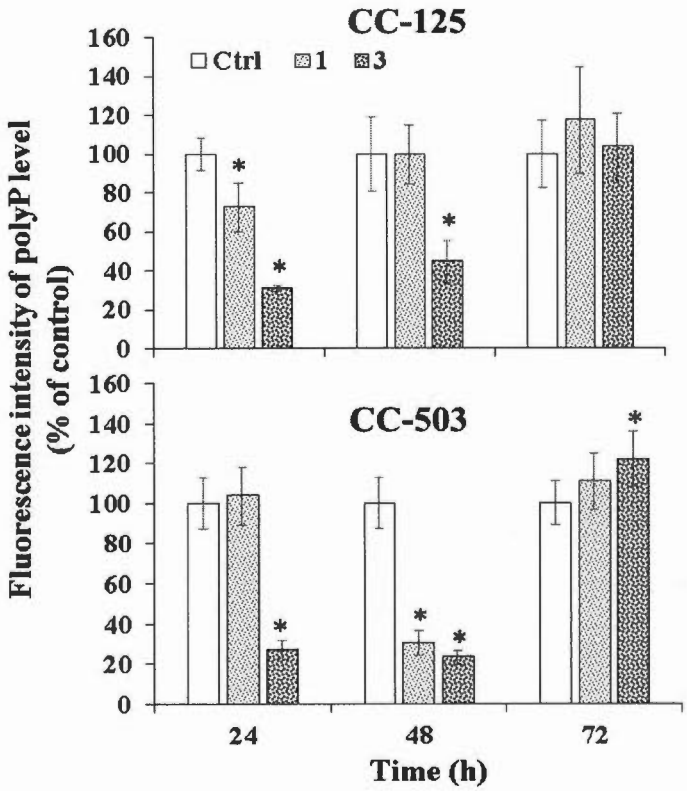

Figure 6.4 Change in the polyP level of the cell wall (% of control) for CC-125 and CC-503 exposed during 24-72 h to 1 and 3 μM of Hg. It was not possible to detect the fluorescence intensity of extracytoplasmic polyP-DAPI for treated-cells under 5 and 7 μM of Hg. *significant differences relative to the control for $p < 0.05$.

6.1.3 Level of polyP related to growth rate

The change of polyP level was plotted in relation to the cell density at 24, 48 and 72 h (Figure 6.5). Independently to the time of exposure, the results showed for both strains that the level of polyP decreased in correlation to the decline of the cell density. When the polyP level decreased completely to zero, it was correlated with the highest growth inhibition of the cell density. In comparison to CC-503, the decrease in the polyP level of CC-125 was correlated with a stronger decline of the cell density, which was more distinct at 48 h compared to 24 h or 72 h. Especially at

48 h, the polyP level of CC-503 was lower than CC-125, although the effect Hg was less strong on the cell density. However, at 72 h, when the cell density diminished by half, the level of polyP did not decrease for both strains.

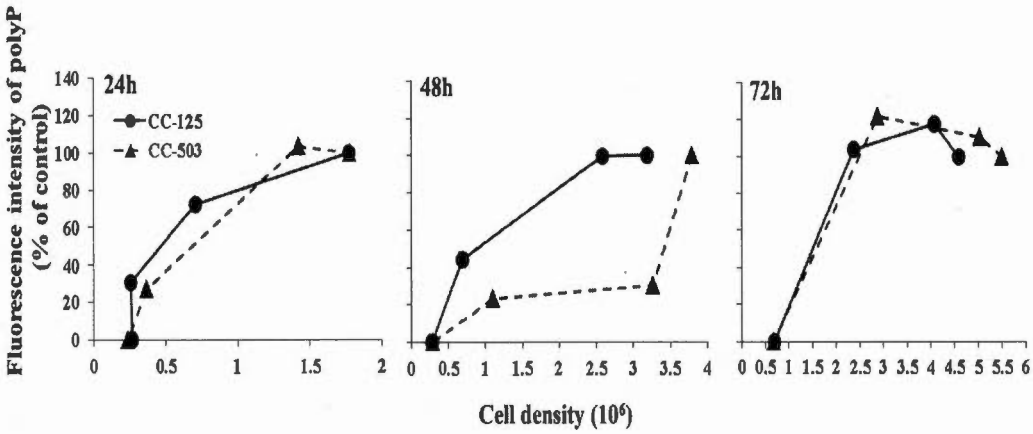

Figure 6.5 Change in the fluorescence intensity of the polyP level in relation to the change of the cell density, for CC-125 and CC-503 exposed during 24-72 h to different concentrations of Hg (1-5 μM).

6.1.4 Accumulation of Hg in algal biomass

When CC-125 and CC-503 were exposed during 24-72 h to different concentrations of Hg, the accumulation of Hg in algal biomass was determined to better understand the toxicity effect of Hg. Under 1 μM of Hg, the accumulation of Hg was not significantly different compared to control for both strains during 24-72 h ($p < 0.05$). At 24 h of exposure to 3 μM of Hg, the accumulation of Hg was only of 0.18 (± 0.02) and 0.21 (± 0.07) μg of Hg / mg of dry mass for CC-125 and CC-503, respectively. Under the same condition at 48 h, the accumulation of Hg for CC-125 and CC-503 was respectively of 0.04 (± 0.02) and 0.08 ± (0.02) μg of Hg / mg of dry mass, and at 72 h, it was respectively of 0.024 and 0.020 (± 0.01) μg of Hg / mg of dry mass. Under 3 μM of Hg, the accumulation of Hg was maximum at 24 h, but it

strongly decreased at 48 and 72 h. Moreover, there was no significant differences between CC-125 and CC-503 concerning the accumulation of Hg in algal biomass.

When both strains were exposed during 24-72 h to 5 and 7 µM of Hg, the accumulation of Hg in algal biomass are presented in Figure 6.6. When the strain CC-125 was exposed during 24 h to 5 and 7 µM of Hg, the accumulation of Hg in algal biomass was of 0.31 (± 0.13) and 0.69 µg of Hg / mg of dry mass, respectively. However, for CC-503, it was of 0.16 (± 0.05) and 0.25 (± 0.12) µg of Hg / mg of dry mass, respectively. Therefore, the accumulation of Hg was the highest at 24 h, especially for the strain CC-125 which had a higher accumulation than the cell wall-less strain CC-503. At 48 and 72 h, the accumulation of Hg decreased for both algal strains, probably due to the toxicity effect of Hg on algal cells.

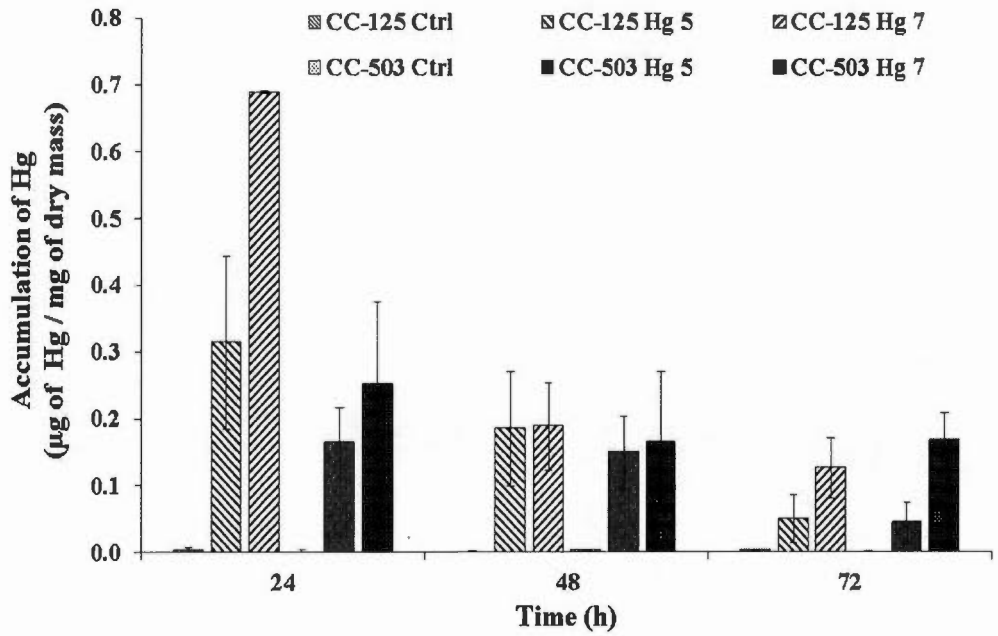

Figure 6.6 Accumulation of Hg in algal biomass (µg of Hg / mg of dry mass) for CC-125 and CC-503 exposed during 24-72 h to 5 and 7 µM of Hg. Data represents the average of 4 replicates, and the bars indicate the standard deviation. The accumulation of Hg in algal biomass for all treated conditions was significantly different to the control for $p < 0.05$. For

treatments of 1 and 3 µM of Hg, the accumulation of Hg in algal biomass was described in the results section.

6.1.5 Level of polyP related to the accumulation of Hg

The change of polyP level was plotted in relation to the accumulation of Hg in algal biomass under tested conditions (Figure 6.7). The results showed for both strains that the level of polyP decreased when the accumulation of Hg increased, but this correlation was dependent on the time of exposure. When it decreased to zero, the polyP level was correlated with the highest accumulation of Hg, already at 24 h. At 72 h, the slight increase of polyP level was related to a very low accumulation of Hg in algal biomass, which was similar for both algal strains (Figure 6.7).

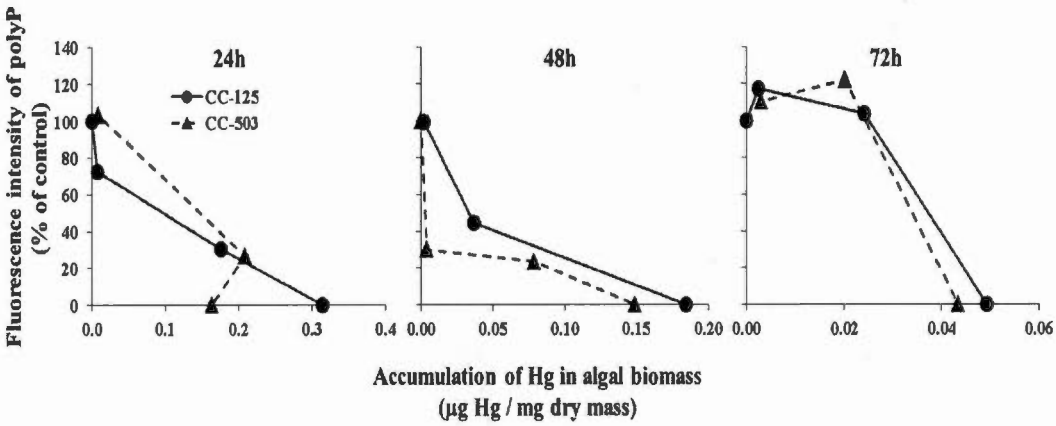

Figure 6.7 Change in the fluorescence intensity of the polyP level in relation to the accumulation of Hg in algal biomass, for CC-125 and CC-503 exposed during 24-72 h to different concentrations of Hg (1-5 µM). The results concerning the treatment condition of 7 µM of Hg were similar to the 5 µM of Hg.

6.1.6 Inhibition of Photosystem II photochemistry

The toxicity effect of Hg on the PSII photochemical reactions was investigated by monitoring the maximum PSII quantum yield, as the ratio F_V/F_M, and the polyP level was plotted under similar conditions for comparison (Table 6.2 and 6.3). Independently to the time of exposure, the F_V/F_M value did not decrease significantly

compared to control ($p < 0.05$) for both strains exposed to low concentrations of Hg (1 and 3 µM of Hg). Under the same condition, the level of polyP decreased significantly compared to control ($p < 0.05$) for both strains exposed during 24 and 48 h. This was with the exception of CC-125 exposed 48 h to 1 µM of Hg, and CC-503 exposed 24 h to 1 µM of Hg.

Table 6.2 Change in the ratio of F_V/F_M (% of control) and the fluorescence intensity of extracytoplasmic polyP (% of control), when CC-125 was exposed during 24-72 h to different concentrations of Hg. N.D., not determined due to high mortality. *significantly different to the control ($p < 0.05$).

[Hg] µM	24 h		48 h		72 h	
	F_V/F_M	polyP	F_V/F_M	polyP	F_V/F_M	polyP
Ctrl	100	100	100	100	100	100
1	100	72* ±12	99	100 ±15	100	117 ±28
3	94	31*	98	44* ±11	100	104 ±17
5	91*	0*	92*	0*	N. D.	0*
7	N.D.	0*	66* ±19	0*	N. D.	0*

Under 5 and 7 µM of Hg, the F_V/F_M value decreased significantly for both strains at 24 h and 48 h (Table 6.2 and 6.3). However, the maximum PSII quantum yield of CC-503 was more affected than CC-125 by high concentrations of Hg (5 and 7 µM). In addition, these inhibitory effects were correlated with a complete decrease of the polyP level. However, at 72 h, it was not possible to determine the F_V/F_M value for both strains, probably because of a high number of dead cells.

Table 6.3 Change in the ratio of F_V/F_M (% of control) and the fluorescence intensity of extracytoplasmic polyP (% of control), when CC-503 was exposed during 24-72 h to different concentrations of Hg. N.D., not determined due to high mortality. *significantly different to the control ($p < 0.05$).

[Hg] µM	24 h		48 h		72 h	
	F_V/F_M	polyP	F_V/F_M	polyP	F_V/F_M	polyP
Ctrl	100	100	100	100	100	100
1	110	103 ±15	106	30*	100	111 ±14
3	93	27*	117	23*	118	122* ±14
5	N.D.	0*	65* ±11	0*	N. D.	0*
7	N.D.	0*	47*	0*	N. D.	0*

6.2 Discussion

6.2.1 Effect of Hg on algal cells

In this study, we characterized the accumulation and toxicity effect of Hg on two strains of *Chlamydomonas reinhardtii*, CC-125 and CC-503 as a cell wall-deficient mutant. Although only a few studies had investigated the toxicity of Hg on algal cells, it was found that physiological alterations induced by Hg were dependent on the algal species or the strain, and the experimental conditions. By using the pulse-amplitude-modulation fluorometric method, the inhibitory effect of Hg (3.7 to 370 nM) on PSII photochemical reactions was previously investigated on different algal species for 96 h (Juneau *et al.*, 2001). The authors found that the most sensitive algal species to the effect of Hg were *Microcystis aeruginosa* and *Ankistrodesmus falcatus*. More

recently, it was showed that the exposure during 96 h to a low concentration of Hg (1.1 µM) was able to inhibit the growth rate by 90 % of the marine diatom *Thalassiosira weissflogii* (Wu *et al.*, 2012). It was also demonstrated that the toxicity effect induced by Hg could not be recovered, when treated diatom cells were maintained in a fresh medium without Hg (Wu et Wang, 2012). Furthermore, Elbaz *et al.* (2010) showed that the growth rate of *C. reinhardtii* was inhibited when exposed during 96 h to 2, 4, 6 and 8 µM of Hg. However, the growth rate slightly increased under 1 µM of Hg, and a stimulation of the metabolism was suggested to be related to this increase (Elbaz *et al.*, 2010). However, based on our study, the growth rate of both strains did not increase (compared to control) when algal cells were exposed to 1 µM of Hg.

When algal cells were exposed to 3 µM of Hg during 24-72 h, the accumulation of Hg was low and the PSII photochemical reactions were not affected. The growth of the cell density was strongly inhibited at 24 h, but partially recovered from 48 to 72 h. This recovery of growth was correlated with the decrease of the accumulation of Hg in algal biomass. Therefore, these results may explain that both *Chlamydomonas* strains were able to tolerate the exposure to 3 µM of Hg during 24-72 h. In addition, both strains had similar tolerance for Hg, even if CC-503 (cw 92 mt^+) was a cell wall-deficient mutant. In a previous study, Macfie and Welbourn (2000) showed that the cell wall-less strain of *C. reinhardtii* had lower growth rates, when exposed during 24 h to 10 µM of Cd, 15 µM of Co, 2 µM of Cu, and 7.5 µM of Ni. They also demonstrated that walled-strain accumulated more Cd per unit weight than the wall-less one, but both strains showed a comparable uptake of Cu. The authors of this work suggested that others defensive mechanisms might be involved in addition to the protective role of the cell wall barrier (Macfie et Welbourn, 2000).

Moreover, our results clearly showed for both strains that high concentrations of Hg (5 and 7 µM of Hg) induced a strong toxicity impact during 24-72 h, indicated

by the inhibition of the growth rate and the deterioration of the PSII photochemical reactions. The accumulation of Hg in algal biomass was the highest at 24 h, but then it decreased at 48 and 72 h. Therefore, we suggest that this reduction was related to the strong toxicity effect of Hg on algal cells. In fact, the confocal microscopy analysis clearly presented that the exposure to these concentrations of Hg caused cellular necrosis.

6.2.2 Physiological role of polyP

In this study, we investigated the level of extracytoplasmic polyP under Hg stress effect to understand the participation of polyP on algal cell. Indeed, few studies had previously investigated the physiological role of polyP in microorganisms. Working with the bacteria *E. coli*, Keasling (1997) proposed that the degradation of polyP was involved in the detoxification of intracellular metals (Keasling, 1997). He showed that the activity of polyphosphatase (PPX) was increased upon the exposure to metals, leading to the irreversible depolymerization of polyP into orthophosphate (Pi). Then, generated complexes of inorganic phosphate with metals and hydrogen ions were transported out of the cell via the Pit system. More recently, when *A. ferrooxidans* was exposed to 20 mM of Cu^{2+} during 4 h, Alvarez and Jerez (2004) observed a decrease of 20 % in the level of polyP, which was correlated with the increase in PPX activity (Alvarez et Jerez, 2004). Under the exposure to 20 and 50 mM of Cu^{2+} during 48 h, the authors demonstrated by ^{32}Pi labeling that the Pi produced from the hydrolysis of polyP was transported out of the cells.

In fact, our results clearly showed for both strains that the accumulation of Hg in algal biomass was correlated with the degradation of polyP (the decrease in the polyP level). Additionally, there was a correlation between the change of the polyP level and the inhibition of growth rate under Hg stress effect. Therefore, we suggest that the degradation of polyP might participate in the sequestration of Hg, especially when algal cells were exposed to low concentrations of Hg (1 and 3 μM of Hg) (Figure

6.8). This mechanism can explain from 48 to 72 h the recovery of the polyP level, the performance of PSII photochemical reactions, and the low accumulated Hg in algal biomass. Surprisingly, the strain CC-503 (cw 92 mt^+) was able to employ such mechanism to protect against the effect of low Hg concentration. Therefore, the initial level of polyP present in the cell wall-deficient CC-503 was sufficient for the activation of polyP metabolism (degradation/recovery). Indeed, it was demonstrated that the metabolism of polyP was similar for two strains of *Chlamydomonas* (*C. acidophila* KT-1 and *C. reinhardtii* C-9) having different initial level of polyP, when exposed under phosphate stress condition (Nishikawa *et al.*, 2006).

Under the toxicity effect of high concentrations of Hg (5 and 7 μM), the degradation of polyP for both strains was total and the initial quantity of polyP could not be recovered. This effect was correlated with a high accumulation of Hg already at 24 h and a strong toxicity impact on algal cells. Under this condition, unshaped dead cells were observed by confocal microscopy analysis.

Previously, the metabolism of polyP was investigated on *Chlamydomonas acidophila* (KT-1) exposed to Cd stress effect (20 μM of Cd during 3 days). The authors observed a complete degradation of polyP which was related to the accumulation of Cd and phosphate in vacuoles (Nishikawa *et al.*, 2003). When these Cd-treated algal cells were put into a Cd-free medium during 24 h, they showed a decrease of 43 % in the accumulation of Cd and a recovery of 77 % in the level of intracellular phosphate (Nishikawa *et al.*, 2009). Therefore, they suggested that the metabolism of polyP in alga *C. acidophila* KT-1 was involved in the cellular detoxification of Cd, by using the inorganic phosphate to sequester the Cd and to release it out of the cell as a Cd-phosphate complex. In agreement to this hypothesis, we also propose that the release of Pi from the degradation of polyP led to the sequestration of Hg^{2+}, which was then transported out of the cell wall *via* the Pit system. When comparing our results with previous works, we can affirm that this

detoxification process in *Chlamydomonas* is dependent on the metal toxicity mechanism and the tested algal species or strain.

6.3 Conclusion

This study demonstrated in *Chlamydomonas reinhardtii* that the level of extracytoplasmic polyP was correlated with the accumulation and the effect of Hg on algal cells. Based on our results, we suggest that the metabolism of polyP was involved in the cellular tolerance for Hg, probably by the sequestration of Hg^{2+} and its transport out of the cell as a Hg-phosphate complex. In addition, measurement of PolyP-DAPI fluorescence by confocal microscopy was used here for the first time to quantify the level of extracytoplasmic polyP, and to analyse its participation in the cellular tolerance for Hg. Indeed, the role of extracytoplasmic polyP was poorly investigated under metal stress effects, and more works need to be done concerning the involvement of polyP on the cellular physiology of algae.

The World Health Organization estimated that levels of mercury in groundwater and surface water are naturally less than 0.5 ppb (WHO, 2005). However, total mercury concentration may vary depending on the area, due to the presence of industrial effluents. In cellular toxicology, the level of polyP in viable algal cells can be analyzed as a biomarker of Hg toxicity effects without fixation or extraction procedures. In laboratory bioassays, the change of this biomarker may have two phases dependent on the concentration of Hg and the time of exposure. During 24 and 48 h, the decrease of polyP shows the degradation of polyP induced by the effect of Hg, and at 72 h, the recovery or the collapse of the polyP level indicates the capacity of algal cells to tolerate the Hg stress effect (Figure 6.8). To continue in this perspective, more studies need to be performed on how environmental factors (such as the pH, temperature and light irradiance) may affect the mercury speciation and toxicity on the level of polyP.

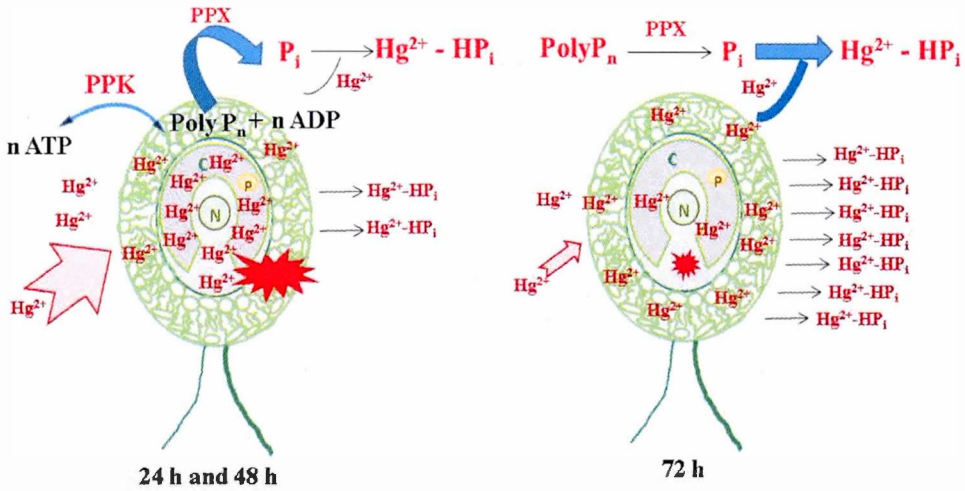

Figure 6.8 Scheme representing the degradation of extracytoplasmic polyP, its participation to sequester Hg, and the release of the Hg-phosphate complex out of the cell for *C. reinhardtii* exposed to 1 and 3 µM of Hg.

CONCLUSION

The research presented in this thesis focuses on the ability of different algal strains to accumulate and tolerate different toxic metals under controlled laboratory conditions. In particular, the main objective of this research project was to investigate the accumulation and the sequestration of two metals, cadmium and mercury, in different algal strains of *Chlamydomonas* (*C. reinhardtii* CC-125 and CC-503, and CPCC 121). Moreover, the accumulated effects of these metals and the involvement of cellular defensive mechanisms were investigated in-depth at molecular level in these algal strains of *Chlamydomonas*.

In the perspective of the first study (Chapter IV), results demonstrated the potential use of green algal strains *C. reinhardtii* and CPCC 121 to accumulate Cd under two pH conditions (pH 4 and 7), permitting the removal of Cd in aqueous solution. At neutral pH, *C. reinhardtii* showed higher ability to accumulate Cd compared to CPCC 121, although its efficiency to accumulate Cd^{2+} was limited by the concentration of Cd and the time of exposure. However, CPCC 121 showed more tolerant for Cd^{2+} as indicated by analyzing the performance of PSII activity, the cellular growth rate, and also the changes in cellular morphology. Indeed, the higher tolerance of CPCC 121 was correlated with the decrease of intracellular Cd accumulation, even though a higher distribution of Cd was observed within its cell wall at pH 7 compared to pH 4. Indeed, the high protonation at the cell surface at pH 4 reduced possibly the accumulation of Cd in algal biomass of CPCC 121 compared to pH 7 condition. These results confirmed that this algal strain, CPCC 121, was not enough efficient to be considered for any phycoremediation of Cd. Therefore, the obtained results of this study suggested that the use of both strains of

Chlamydomonas for bioremediation applications under acidic condition was not recommended. Consequently, this study demonstrated strongly that the capacity of algal cells to accumulate and tolerate cadmium was different depending on the concentration of Cd, the time of exposure, and the environmental condition. All of these factors should be considered in the future development of the phycoremediation of toxic metals.

In the second part of this thesis (Chapter V), our results showed the accumulation and toxicity effect of Cd on the level of extracytoplasmic polyP under neutral pH using two strains of *C. reinhardtii*, CC-125 and CC-503 having an impaired cell wall. In particular, the results of this study demonstrated the decrease in synthesis and/or the degradation of extracytoplasmic polyP that was correlated with the accumulation of Cd, even in CC-503 having a lower level of polyP. However, our results indicated that polyP did not participate in the sequestration of Cd. Moreover, the initial level of polyP could not be recovered in CC-503, whereas CC-125 was able to restore its polyP level. In response to the toxic effects of Cd, the observed formation of colonies by CC-125 cells was correlated with the recovery of the polyP level. Otherwise, CC-503 was not able to make such cellular colonies probably due to its cell wall-deficiency and the toxicity impact of Cd. Nevertheless, both algal strains were able to accumulate significant amount of Cd in their biomass. In addition, these results demonstrated that the impact of Cd on the polyP level was dependent on the Cd concentration in both algal strains, whereas Cd inhibited the growth rate regardless of the concentration of Cd. Therefore, a distinct impact of Cd on the metabolism of polyP (synthesis and/or degradation of polyP) can be used as a biomarker of metal toxicity such as Cd under tested conditions (24 and 48 h), even in CC-503 which has an impaired cell wall.

Finally, in the third part of this research project (Chapter VI), the results showed the accumulation and toxicity effect of Hg on two algal strains of *C. reinhardtii*, CC-

125 and CC-503 (cell wall-deficient), by monitoring the cellular growth rate, the performance of PSII photochemistry, and the level of extracytoplasmic polyP. Our results demonstrated that the change of the polyP level in *C. reinhardtii* was correlated with the accumulation of Hg. In both algal strains, the degradation of polyP participated in the sequestration of Hg^{2+}, especially for low quantity of accumulated Hg. Moreover, the recovery of the level of polyP was noticed for both algal strains over time, which demonstrated its participation in the tolerance of Hg by using the phosphate and its transport as a Hg-phosphate complex out of the cell. This cellular protective mechanism permitted to explain the performance of PSII photochemistry and low inhibition of growth rate over time, even in algal strain CC-503 having a lower level of polyP. However, the polyP participation in the sequestration and tolerance of Hg was affected by the concentration of Hg, since the degradation of polyP was total under the high tested concentrations of Hg. Based on these results, the level of polyP can be used as a biomarker of Hg that may have two phases dependent on the concentration of Hg and the time of exposure: During 24 and 48 h of exposure, the decrease of polyP can indicate the degradation of polyP induced by the effect of Hg, and at 72 h of exposure, the recovery or the collapse of the polyP level can indicate the capacity of algal cells to tolerate the Hg stress effect.

In conclusion, this research project presented original results concerning the accumulation and the sequestration of two heavy metals, Cd and Hg in three different algal strains of *Chlamydomonas* (CC-125, CPCC 121, and CC-503). Particularly, the results of this project demonstrated that algal cells use different protective mechanisms against the toxic effects of Cd and Hg: First, the low accumulation of Cd in the algal biomass of CPCC 121 indicated that this strain has a strong tolerance property for Cd^{2+} under both neutral and acidic conditions; Second, the degradation of extracytoplasmic polyP permitting the chelation of Hg in cells of *C. reinhardtii*; Third, the importance of the cell wall in the formation of colonies (with a common cell wall) which was seen for cells of *C. reinhardtii*, CC-125, under high Cd stress

effect. Moreover, environmental conditions were able to affect the tolerance of algal cells against metal stress. For instance, a higher level of exclusion of Cd^{2+} by the high protonation at the cell surface of CPCC 121 was seen under acidic condition reducing the electrostatic interactions between the cell wall and Cd^{2+}. In addition, when compared to Cd, Hg showed different toxic effects on two algal strains of *Chlamydomonas*, CC-125 and CC-503, indicating that the accumulation and the toxicity of a metal is strongly dependent on their chemical characteristics. This must be considered in toxicological evaluations using microalgae. Therefore, the research presented in this thesis contributed to a better understanding of metals accumulation, sequestration, and tolerance mechanisms in cells of *Chlamydomonas* under metal stress effect. Finally, in the perspective to develop the phycoremediation of metals, it would be interesting to investigate in laboratory conditions the accumulation, the sequestration, and the effect of others metals (such as Zn^{2+}, Cu^{2+}, and Ag^{2+}) on different algal strains or species.

REFERENCES

Adan, A., Alizada, G., Kiraz, Y., Baran, Y. et Nalbant, A. (2017). Flow cytometry: basic principles and applications. *Critical Reviews in Biotechnology*, 37(2), 163-176.

Adriano, D.C., Bolan, N.S., Vangronsveld, J. et Wenzel, W.W. (2005). Heavy metals. Dans D, H. (dir.), *Encyclopedia of Soils in the Environment* (p. 175-182). Amsterdam : Elsevier.

Aguilera, A. et Amils, R. (2005). Tolerance to cadmium in *Chlamydomonas* sp. (Chlorophyta) strains isolated from an extreme acidic environment, the Tinto River (SW, Spain). *Aquatic Toxicology*, 75(4), 316-329.

Ahn, K. et Kornberg, A. (1990). Polyphosphate kinase from *Escherichia coli*. Purification and demonstration of a phosphoenzyme intermediate. *Journal of Biological Chemistry*, 265, 11734-11739.

Akiyam, M., Crooke, E. et Kornberg, A. (1993). An Exopolyphosphatase of *Escherichia coli*. *Journal of Biological Chemistry*, 268(1), 633-639.

Allan, R.A. et Miller, J.J. (1980). Influence of S-adenosylmethionine on DAPI-induced fluorescence of polyphosphate in the yeast vacuole. *Canadian Journal of Microbiology*, 26, 912-920.

Alvarez, S. et Jerez, C.A. (2004). Copper ions stimulate polyphosphate degradation and phosphate efflux in *Acidithiobacillus ferrooxidans*. *Applied and Environmental Microbiology*, 70(9), 5177-5182.

Ault-Riché, D., Fraley, C.D., Tzeng, C.-M. et Kornberg, A. (1998). Novel assay reveals multiple pathways regulating stress-induced accumulations of inorganic polyphosphate in *Escherichia coli*. *Journal of Bacteriology*, 180, 1841–1847.

Baker, N.R. (2008). Chlorophyll Fluorescence: A Probe of Photosynthesis In Vivo. *Annual Review of Plant Biology*, 59(1), 89-113.

Balkos, K.D. et Colman, B. (2007). Mechanism of CO_2 acquisition in an acid-tolerant *Chlamydomonas*. *Plant, Cell Environment*, 30, 745-752.

Bate, S.S., Tessier, A., Campbell, P.G.C. et Létourneau, M. (1985). Zinc-Phosphorus interactions and variation in zinc accumulation during growth of *Chlamydomonas variabilis* (Chorophyceae) in Batch Culture. *Canadian Journal of Fisheries and Aquatic Sciences*, 42, 86-94.

Bernard, A. (2011). Renal and neurological effects heavy metals in the environment. Dans O, N. J. (dir.), *Encyclopedia of Environmental Health* (Vol. 4, p. 801 - 805). Burlington : Elsevier.

Bonting, C.F.C., Kortstee, G.J.J. et Zehender, A.J.B. (1991). Properties of polyphosphate: AMP phosphotransferase of *Acinetobacter* strain 210A. *Journal of Bacteriology*, 173(20), 6484- 6488.

Boss, C.B. et Fredeen, K.J. (1997). *Concepts, Instrumentation and Techniques in Inductively Coupled Plasma Optical Emission Spectrometry.* (Second Edition éd.). USA : Perkin-Elmer.

Boudou, A. et Ribeyre, F. (1997). Aquatic Ecotoxicology: From the Ecosystem to the Cellular and Molecular Levels. *Environmental Health Perspectives*, 105, 21-35.

Breuwer, P., Drocourt, J.-L., Bunschoten, N., Zwietering, M.H., Rombouts, F.M. et Abee, T. (1995). Characterisation of uptake and hydrolysis of fluorescein diacetate and carboxyfluorescein diacetate by intracellular esterases in *Saccharomyces cerevisiae*, which result in accumulation of fluorescent product. *Applied and Environmental Microbiology*, 61, 1614-1619.

Campbell, P.G.C. et Couillard, Y. (2004). Prise en charge et détoxication des métaux chez les organismes aquatiques. Dans Pelletier, E., Campbell, P. G. C. et Denizeau, F. (dir.), *Écotoxicologie Moléculaire* (p. 10-61). Canada : Presses de l'Université du Québec.

Clarkson, T.W. (1998). Human toxicology of mercury. *Journal of Trace Elements in Experimental Medicine*, 11, 303-317.

Clarkson, T.W. (2002). The Three Modern Faces of Mercury. *Environmental Health Perspectives*, 110, 11-23.

Clemens, S. (2001). Molecular mechanisms of plant metal tolerance and homeostasis. *Planta*, 212, 475–486.

Cobbett, C.S. (2000). Phytochelatins and Their Roles in Heavy Metal Detoxification *Plant Physiology*, 123, 825–832.

Compeau, G.C. et Bartha, R. (1985). Sulfate-reducing bacteria: principal methylators of mercury in anoxic estuarine sediment. *Applied and Environmental Microbiology*, 50(2), 498-502.

Dent, R.M., Han, M. et Niyogi, k.k. (2001). Functional genomics of plant photosynthesis in the fast lane using *Chlamydomonas reinhardtii*. *TRENDS in Plant Science*, 6(8), 364-371.

Docampo, R. et Moreno, S.N. (2001). The acidocalcisome. *Molecular and Biochemical Parasitology*, 114, 151–159.

Elbaz, A., Wei, Y.Y., Meng, Q., Zheng, Q. et Yang, Z.M. (2010). Mercury-induced oxidative stress and impact on antioxidant enzymes in *Chlamydomonas reinhardtii*. *Ecotoxicology*, 19(7), 1285-1293.

Faller, P., Kienzler, K. et Krieger-Liszkay, A. (2005). Mechanism of Cd^{2+} toxicity: Cd^{2+} inhibits photoactivation of Photosystem II by competitive binding to the essential Ca^{2+} site. *Biochimica et Biophysica Acta*, 1706, 158-164.

Farineau, J. et Morot-Gaudry, J.-F. (2006). *La photosynthèse, processus physiques, moleculaires et physiologiques*. Paris : INRA.

Fortin, C., Denison, F.H. et Garnier-Laplace, J. (2007). Metal-phytoplankton interactions: Modeling the effect of competing ions (H^+, Ca^{2+}, and Mg^{2+}) on uranium uptake. *Environmental Toxicology and Chemistry*, 26, 242-248.

Franklin, N.M., Stauber, J.L. et Lim, R.P. (2001). Development of flow cytometry-based algal bioassays for assessing toxicity of copper in natural waters. *Environmental Toxicology and Chemistry*, 20, 160-170.

Franqueira, D., Orosa, M., Torres, E., Herrero, C. et Cid, A. (2000). Potential use of flow cytometry in toxicity studies with microalgae. *Science of the Total Environment*, 247, 119-126.

Fu, F. et Wang, Q. (2011). Removal of heavy metal ions from wastewaters: a review. *Journal of Environmental Management*, 92(3), 407-418.

Gimmler, H., Jesus, D.J. et Greiser, A. (2001). Heavy metal resistance of the extreme acidotolerant filamentous fungus *Bispora* sp. *Microbial Ecology*, 42, 87-98.

Gimmler, H., Treffny, B., Kowalski, M. et Zimmermann, U. (1991). The resistance of *Dunaliella acidophila* against heavy metals: The importance of the zeta potential. *Journal of Plant Physiology*, 138, 708-716.

Gomez-Garcia, M.R. et Kornberg, A. (2004). Formation of an actin-like filament concurrent with the enzymatic synthesis of inorganic polyphosphate. *Proceedings of the National Academy of Sciences U S A*, 101(45), 15876-15880.

Goodenough, U.W. et Heuser, J.E. (1985). The *Chlamydomonas* cell wall and its constituent glycoproteins analyzed by the quick-freeze, deep-etch technique. *Journal of Cell Biology*, 101, 1550 – 1568.

Govindjee, Kern, J.F., Messinger, J. et Whitmarsh, J. (2010). Photosystem II. Dans Whitmarsh, J. et Govindjee (dir.), *Encyclopedia of Life Sciences*. Chichester : John Wiley & Sons, Ltd.

Grill, E., Loffler, S., Winnacker, E.L. et Zenk, M.H. (1989). Phytochelatins, the heavy-metal-binding peptides of plants, are synthesized from glutathione by a specific γ-glutamylcysteine dipeptidyl transpeptidase (phytochelatin synthase). *Proceedings of the National Academy of Sciences U S A*, 86, 6838–6842.

Hanikenne, M. (2003). *Chlamydomonas reinhardtii* as a eukaryotic photosynthetic model for studies of heavy metal homeostasis and tolerance. *New Phytologist*, 159(2), 331-340.

Harris, E.H. (1989). *The Chlamydomonas Sourcebook: a comprehensive guide to biology and laboratory use*. San Diego : Academic Press.

Harris, E.H. (2009). *The Chlamydomonas Sourcebook: Introduction to Chlamydomonas and its laboratory use*. (Second edition éd. Vol. 1). San Diego, USA : Academic Press.

Howe, G. et Merchant, S. (1992). Heavy metal-activated synthesis of peptides in *Chlamydomonas reinhardtii*. *Plant Physiology*, 98, 127–136.

Hsieh, P.C., Shenoy, B.C., Jentoft, J.E. et Phillips, N.F.B. (1993). Purification of polyphosphate and ATP glucose phosphotrnsferase from Mycobacterium tuberculosis H37Ra: evidence that poly(P) and ATP glucokinase activities are catalyzed by the same enzyme,. *Protein Expression and purification*, 4, 76-84.

Jamers, A., Lenjou, M., Deraedt, P., Bockstaele, D.V., Blust, R. et Coen, W.d. (2009). Flow cytometric analysis of the cadmium-exposed green alga *Chlamydomonas reinhardtii* (Chlorophyceae). *European Journal of Phycology*, 44(4), 541-550.

Jarup, L. et Akesson, A. (2009). Current status of cadmium as an environmental health problem. *Toxicology and Applied Pharmacology*, 238(3), 201-208.

Jensen, T.E., Baxter, M., Rachlin, J.W. et Jani, V. (1982a). Uptake of heavy metals by *Plectonema boryanum* (Cyanophyceae) into cellular components especially polyphosphate bodies: an X-ray energy dispersive study. *Environmental Pollution Series A, Ecological and Biological*, 27, 119-127.

Jensen, T.E., Rachlin, J.W., Jani, V. et Warkentine, B. (1982b). An X-ray energy dispersive study of cellular compartmentalization of lead and zinc in *Chlorella saccharophila* (Chloropyhta), *Navicula insertia* and *Nitzschia closterium* (Bacillariophyta). *Environmental and Experimental Botany*, 22, 319–328.

Juneau, P., Dewez, D., Matsui, S., Kim, S.-G. et Popovic, R. (2001). Evaluation of different algal species sensitivity to mercury and metolachlor by PAM-fluorometry. *Chemosphere*, 45, 589-598.

Keasling, J.D. (1997). regulation of intracellular toxic metals and other cations by hydrolysis of polyphosphate. *Annals of the New York Academy of Sciences*, 829, 242-249.

Keasling, J.D., Bertsch, L. et Kornberg, A. (1993). Guanosine pentaphosphate phosphohydrolase from *Escherichia coli* is a long-chain polyphosphatase. *Proceedings of the National Academy of Sciences U S A*, 90, 7029-7033.

Komine, Y., Eggink, L.L., Park, H. et Hoober, J.K. (2000). Vacuolar granules in *Chlamydomonas reinhardtii*: Polyphosphate and a 70-kDa polypeptide as major components. *Planta*, 210, 897–905.

Kornberg, A. (1995). Inorganic polyphosphate: toward making a forgotten polymer unforgettable. *Journal of Bacteriology*, 177, 491-496.

Kornberg, A., Rao, N.N. et Ault-Riché, D. (1999). Inorganic polyphosphate: a molecule of many functions. *Annual Review of Biochemistry*, 68, 89–125.

Kukarskikh, G.L., Graevskaia, E.E., Krendeleva, T.E., Timofeedv, K.N. et Rubin, A.B. (2003). Effect of methylmercury on primary photosynthesis processes in green microalgae *Chlamydomonas reinhardtii. Biofizika*, 48(5), 853-859.

Kulaev, I., V., V. et Kulakovskaya, T. (1999). New Aspects of Inorganic Polyphosphate Metabolism and Function. *Journal of Bioscience and Bioengineering*, 88, 111-129.

Kulaev, I.S., Vagabov, V.M. et Kulakovskaya, T.V. (2004). *The biochemistry of inorganic polyphosphates*. (2nd ed éd.). Chichester, England : John Wiley.

Kumar, K.S., Dahms, H.-U., Won, E.-J., Lee, J.-S. et Shin, K.-H. (2015). Microalgae – A promising tool for heavy metal remediation. *Ecotoxicology and Environmental Safety*, 113, 329–352.

Lavoie, M., Faucheur, S.L., Fortin, C. et Campbell, P.G.C. (2009). Cadmium detoxification strategies in two phytoplankton species: Metal binding by newly synthesized thiolated peptides and metal sequestration in granules. *Aquatic Toxicology*, 92, 65–75.

Lavoie, M., Fortin, C. et Campbell, P.G.C. (2012). Influence of essential elements on cadmium uptake and toxicity in a unicellular green alga: The protective effect of trace zinc and cobalt concentrations. *Environmental Toxicology and Chemistry*, 31(7), 1445-1452.

Macey, M.G. (2007). Principles of Flow Cytometry. Dans Macey, M. G. (dir.), *Flow Cytometry: Principles and Applications*. Totowa, New Jersey : Human Press.

Macfie, S.M., Tarmohamed, Y. et Welbourn, P.M. (1994). Effects of cadmium, cobalt, copper, and nickel on growth of the green alga *Chlamydomonas reinhardtii*: the influences of the cell wall and pH. *Archives of Environmental Contamination and Toxicology*, 27, 454-458.

Macfie, S.M. et Welbourn, P.M. (2000). The Cell Wall as a Barrier to Uptake of Metal Ions in the Unicellular Green Alga *Chlamydomonas reinhardtii* (Chlorophyceae). *Archives of Environmental Contamination and Toxicology*, 39(4), 413-419.

Malkin, R. et Niyogi, M. (2000). Photosynthesis. Dans Buchanan, B. B., Gruissem, W. et Jones, R. L. (dir.), *Biochemistry and molecular biology of plants* (p. 568-628). Rockville, Maryland, USA : the American Society of Plant Physiologists

Mallick, N. et Mohn, F.H. (2003). Use of chlorophyll fluorescence in metal-stress research: a case study with the green microalga *Scenedesmus*. *Ecotoxicology and Environmental Safety*, 55, 64-69.

Mendez-Alvarez, S., Leisinger, U. et Eggen, R.I.L. (1999). Adaptive responses in *Chlamydomonas reinhardtii*. *International Microbiology*, 2, 15–22.

Monteiro, C.M., Castro, P.M. et Malcata, F.X. (2012). Metal uptake by microalgae: underlying mechanisms and practical applications. *Biotechnol Prog*, 28(2), 299-311.

Morel, F.M.M., Kraepiel, A.M.L. et Amyot, M. (1998). The chemical cycle and bioaccumulation of mercury. *Annual Review of Ecology and Systematics*, 29, 543-566.

Munoz, R., Jacinto, M., Guieysse, B. et Mattiasson, B. (2005). Combined carbon and nitrogen removal from acetonitrile using algal-bacterial bioreactors. *Applied Microbiology and Biotechnology*, 67(5), 699-707.

Nassiri, Y., Mansot, J.L., Wéry, J., Ginsburger-Vogel, T. et Amiard, J.C. (1997). Ultrastructural and electron energy loss spectroscopy studies of sequestration mechanisms of Cd and Cu in the marine diatom *Skeletonema costatum*. *Archives of Environmental Contamination and Toxicology*, 33, 147-155.

Newman, M.C. et Unger, M.A. (2002). *Fundamentals of ecotoxicology*. (Second Edition éd.). USA : Lewis.

Nishikawa, K., Machida, H., Yamakoshi, Y., Ohtomo, R., Saito, K., Saito, M. et Tominaga, N. (2006). Polyphosphate metabolism in an acidophilic alga *Chlamydomonas acidophila* KT-1 (Chlorophyta) under phosphate stress. *Plant Science*, 170(2), 307-313.

Nishikawa, K. et Tominaga, N. (2001). Isolation, growth, ultrastructure, and metal tolerance of the green alga *Chlamydomonas acidophila* (Chlorophyta). *Bioscience, Biotechnology, and Biochemistry.*, 65, 2650-2656.

Nishikawa, K., Tominaga, N., Uchino, T., Oikawa, A. et Tokunaga, H. (2009). Polyphosphate contributes to Cd tolerance in *Chlamydomonas acidophila* KT-1. Dans Hagen, K. N. (dir.), *Algae: Nutrition, Pollution Control and Energy Sources* (p. 13-21). New York USA : Nova Science.

Nishikawa, K., Yamakoshi, Y., Uemura, I. et Tominaga, N. (2003). Ultrastructural changes in *Chlamydomonas acidophila* (Chlorophyta) induced by heavy metals and polyphosphate metabolism. *FEMS Microbiology Ecology*, 44(2), 253-259.

Olaveson, M.M. et Stokes, P.M. (1989). Responses of the acidophilic alga *Euglena mutabilis* (Euglenophyceae) to carbon enrichment at pH 3. *Journal of Phycology*, 25, 529-539.

Paddock, S.W. (2000). Principles and Practices of Laser Scanning Confocal Microscopy. *Molecular Biotechnology*, 16, 127-149.

Pal, R. et Rai, J.P. (2010). Phytochelatins: peptides involved in heavy metal detoxification. *Applied Biochemistry and Biotechnology*, 160(3), 945-963.

Pan-Hou, H., Kiyono, M., Omura, H., Omura, T. et Endo, G. (2002). Polyphosphate produced in recombinant *Escherichia coli* confers mercury resistance. *FEMS Microbiology Letters*, 10325, 159–164.

Paquet, N., Lavoie, M., Maloney, F., Duval, J.F.L., Campbell, P.G.C. et Fortin, C. (2015). Cadmium accumulation and toxicity in the unicellular alga *Pseudokirchneriella subcapitata*: Influence of metal-binding exudates and exposure time. *Environmental Toxicology and Chemistry*, 34, 1524-1532.

Parent, L. et Campbell, P.G.C. (1994). Aluminum bioavailability to the green alga *Chlorella pyrenoidosa* in acidified synthetic soft water. *Environmental Toxicology and Chemistry*, 13, 587-598.

Pepin, C.A. et Wood, H.G. (1986). Polyphosphate glucokinase from *Propionibacterium sherrnanii*. Kinetics and demonstration that the mechanism involves both processive and nonprocessive type reactions. *Journal of Biological Chemistry*, 261, 4476-4480.

Perales-Vela, H.V., Pena-Castro, J.M. et Canizares-Villanueva, R.O. (2006). Heavy metal detoxification in eukaryotic microalgae. *Chemosphere*, 64(1), 1-10.

Perreault, F., Dewez, D., Fortin, C., Juneau, P., Diallo, A. et Popovic, R. (2010). Effect of aluminum on cellular division and photosynthetic electron transport in *Euglena gracilis* and *Chlamydomonas acidophila*. *Environmental Toxicology and Chemistry*, 29(4), 887-892.

Perreault, F., Dionne, J., Didur, O., Juneau, P. et Popovic, R. (2011). Effect of cadmium on photosystem II activity in *Chlamydomonas reinhardtii*: alteration of O–J–I–P fluorescence transients indicating the change of apparent activation energies within photosystem II. *Photosynthesis Research,* 107, 151–157.

Pettersson, A., Kunst, L., Bergman , B. et Roomans, G.M. (1985). Accumulation of aluminum by *Anabaena cylindrica* into polyphosphate granules and cell walls: an x-ray energy-dispersive microanalysis study. *Journal of General Microbiology*, 131, 2545-2548.

Pick, U., Bental, M., Chitlaru, E. et Weiss, M. (1990). Polyphosphate hydrolysis-a protective mechanism against alkaline stress. *FEBS Letters*, 274, 15-18.

Pick, U. et Weiss, M. (1991). Polyphosphate hydrolysis within acidic vacuoles in responce to amine-induced alkaline stress in the halotolerant alga *Dunaliella salina*. *Plant Physiology*, 97, 1234–1240.

Pinto, E., Sigaud-Kutner, T.C.S., Leitao, M.A.S., Okamoto, O.K., Morse, D. et Colepicolo, P. (2003). Heavy metal-induced oxidative stress in algae. *Journal of Phycology*, 39, 1008-1018.

Popovic, R., Dewez, D. et Juneau, P. (2003). Applications of chlorophyll fluorescence in ecotoxicology: Heavy metals, herbicides, and air pollutants. Dans DeEll, J. R. et

Toivonen, P. M. A. (dir.), *Practical Applications of Chlorophyll Fluorescence in Plant Biology* (p. 151–184). London, UK : Kluwer Academic Publishers.

Prasad, M.N.V., Drej, K., Skawinska, A. et Stratka, K. (1998). Toxicity of cadmium and copper in *Chlamydomonas reinhardtii* wild-type (WT 2137) and cell wall deficient mutant strain (CW 15). *Bulletin of Environmental Contamination and Toxicology*, 60, 306-311.

Rai, L.C., Jensen, T.E. et Rachlin, J.W. (1990). A morphometric and X-ray energy dispersive approach to monitoring pH-altered cadmium toxicity in *Anabena flos-aquae*. *Archives of Environmental Contamination and Toxicology*, 19(4), 479–487.

Rao, N.N. et Kornberg, A. (1996). Inorganic polyphosphates support resistance and survival of stationary-phase *Escherichia coli*. *Journal of Bacteriology*, 178, 1394–1400.

Roberts, K., Gurney-Smith, M. et Hills, G.J. (1972). Structure, composition and morphogenesis of the cell wall of *Chlamydomonas reinhardii*. I. Ultrastructure and preliminary chemical analysis. *Journal of Ultrastructure Research*, 40, 599 – 613

Ruiz, F.A., Marchesini, N., Seufferheld, M., Govindjee et Docampo, R. (2001). The polyphosphate bodies of *Chlamydomonas reinhardtii* possess a proton-pumping pyrophosphatase and are similar to acidocalcisomes. *Journal of Biological Chemistry*, 276(49), 46196-46203.

Sacan, M.T., Oztay, F. et Bolkent, S. (2007). Exposure of *Dunaliella tertiolecta* to lead and aluminum: toxicity and effects on ultrastructure. *Biological Trace Element Research*, 120(1-3), 264-272.

Samadani, M., Perreault, F., Oukarroum, A. et Dewez, D. (2018). Effect of cadmium accumulation on green algae *Chlamydomonas reinhardtii* and acid-tolerant *Chlamydomonas* CPCC 121. *Chemosphere*, 191, 174-182.

Satarug, S., Garrett, S.H., Sens, M.A. et Sens, D.A. (2010). Cadmium, environmental exposure, and health outcomes. *Environmental Health Perspectives*, 118, 182-190.

Schwarzenbach, R.P., Egli, T., Hofstetter, T.B., von Gunten, U. et Wehrli, B. (2010). Global Water Pollution and Human Health. *Annual Review of Environment and Resources*, 35(1), 109-136.

Sianoudis, J., C., K.A., Mayer, A., Grimme, L.H. et Leibfritz, D. (1986). Distribution of polyphosphates in cell-compartments of *Chlorella fusca* as measured by ^{31}P NMR-spectroscopy. *Archives of Microbiology*, 144, 48– 54.

Siderius, M., Musgrave, A., Ende, H.V.D., Koerten, H., Cambier, P. et Meer, P.V.D. (1996). *Chlamydomonas eugametos* (Chlorophyta) stores phosphate in polyphosphate bodies together with calcium. *Journal of Phycology*, 32, 402–409.

Sivakumar, G., Xu, J., Thompson, R.W., Yang, Y., Randol-Smith, P. et Weathers, P.J. (2012). Integrated green algal technology for bioremediation and biofuel. *Bioresource Technology*, 107, 1-9.

Skoog, D.A., Holler, F.J. et Crouch, S.R. (2007). *Principles of instrumental analysis.* (Sixth Edition éd.). USA : Thomson Brooks/Cole.

Spijkerman, E., Barua, D., Gerloff-Elias, A., Kern, J., Gaedke, U. et Heckathorn, S.A. (2007). Stress responses and metal tolerance of *Chlamydomonas acidophila* in metal-enriched lake water and artificial medium. *Extremophiles*, 11(4), 551-562.

Stauber, J.L., Franklin, N.M. et Adams, M.S. (2002). Applications of flow cytometry to ecotoxicity testing using microalgae. *TRENDS in Biotechnology*, 20, 141-143.

Stirbet, A. et Govindjee. (2011). On the relation between the Kautsky effect (chlorophyll a fluorescence induction) and Photosystem II: Basics and applications of the OJIP fluorescence transient. *Journal of Photochemistry and Photobiology B: Biology*, 104(1-2), 236-257.

Stoiber, T.L., Shafer, M.M. et Armstrong, D.E. (2010). Differential effects of copper and cadmium exposure on toxicity endpoints and gene expression in *Chlamydomonas reinhardtii*. *Environmental Toxicology and Chemistry*, 29, 191–200.

Strasser, R.J., Srivastava, A. et Govindjee. (1995). Polyphasic chlorophyll a fluorescence transient in plants and cyanobacteria. *Photobiochemistry and Photobiology*, 61, 32-42.

Strasser, R.J., Tsimilli-Michael, M. et Srivastava, A. (2004). Analysis of the chlorophyll a fluorescence transient. Dans Papageorgiou, G. C. et Govindjee (dir.), *Chlorophyll Fluorescence: A signature of photosynthesis* (Vol. 19, p. 321-362). Dordrecht : Springer.

Streichan, M., Golecki, J.R. et Schön, G. (1990). Polyphosphate-accumulating bacteria from sewage plants with different processes of biological phosphorus removal. *FEMS Microbiology Ecology*, 73, 113-124.

Sueoka, N., Chiang, K.S. et Kates, J.R. (1967). Deoxyribonucleic acid replication in meiosis of *Chlamydomonas reinhardtii*. Isotopic transfer experiments with a strain producing eight zoospores. *Journal of Molecular Biology*, 25, 44–67.

Szivak, I., Behra, R. et Sigg, L. (2009). Metal-Induced Reactive Oxygen Species Production in *Chlamydomonas reinhardtii* (Chlorophyceae). *Journal of Phycology*, 45(2), 427-435.

Tchounwou, P.B., Ayensu, W.K., Ninashvili, N. et Sutton, D. (2003). Environmental exposure to mercury and its toxicopathologic implications for public health. *Environmental Toxicology*, 18(3), 149-175.

Tripathi, B.N., Mehta, S.K., Amar, A. et Gaur, J.P. (2006). Oxidative stress in *Scenedesmus* sp. during short- and long-term exposure to Cu^{2+} and Zn^{2+}. *Chemosphere*, 62(4), 538-544.

Twiss, M.R. et Nalewajko, C. (1992). Influence of phosphorus nutrition on copper toxicity to three strains of *Scenedesmus acutus* (Chlorophyceae). *Journal of Phycology*, 28, 291-298.

Ullrich, S.M., Tanton, T.W. et Abdrashitova, S.A. (2001). Mercury in the Aquatic Environment: A Review of Factors Affecting Methylation. *Critical Reviews in Environmental Science and Technology*, 31(3), 241-293.

UNEP. (2010). *Final review of scientific information on cadmium.* : United Nations Environment Programme, Chemicals Branch, DTIE Récupéré de http://www.unep.org/chemicalsandwaste/Portals/9/Lead_Cadmium/docs/Interim_reviews/UNEP_GC26_INF_11_Add_1_Final_UNEP_Lead_review_and_apppendix_Dec_2010.pdf.

Vega, J.M., Garbayo, I., Domínguez, M.J. et Vigara, J. (2006). Effect of abiotic stress on photosynthesis and respiration in *Chlamydomonas reinhardtii*, induction of oxidative stress. *Enzyme and Microbial Technology*, 40, 163-167.

Visviki, I. et Rachlin, J.W. (1994). Acute and chronic exposure of *Dunaliella salina* and *Chlamydomonas bullosa* to copper and cadmium: Effects on ultrastructure. *Archives of Environmental Contamination and Toxicology*, 26, 154-162.

Walsh, R.S. et Hunter, K.A. (1992). Influence of phosphorus storage on the uptake of cadmium by the marine alga *Macrocystis pyrifera*. *Limnology and Oceanography*, 37, 1361-1369.

Weber, J.H. (1993). Review of possible paths for abiotic methylation of mercury (II) in the aquatic environment. *Chemosphere*, 26, 2063-2077.

Werner, T.P., Amrhein, N. et Freimoser, F.M. (2007). Inorganic polyphosphate occurs in the cell wall of *Chlamydomonas reinhardtii* and accumulates during cytokinesis. *BMC Plant Biology*, 7(1), 1-11.

Whitmarsh, J. et Govindjee. (1999). The photosynthetic process. Dans Singhal, G. S., Renger, G., Sopory, S. K., lrrgang, K. D. et Govindjee. (dir.), *Concepts in Photobiology: Photosynthes is and Photomorphogenesis* (p. 11-51). New Delhi, India : Narosa.

WHO. (2005). *Mercury in Drinking-water*. : Background document for development of WHO Guidelines for Drinking-water Quality.

Williams, D.B. et Carter, C.B. (2009). *Transmission Electron Microscopy A Textbook for Materials Science*. (Second Edition éd.). USA : Springer.

Wong, S.L., Nakamoto, L. et Wainwright, J.F. (1994). Identification of toxic metals in affected algal cells in assays of wastewaters. *Journal of Applied Phycology*, 6, 405-414.

Worms, I., Simon, D.F., Hassler, C.S. et Wilkinson, K.J. (2006). Bioavailability of trace metals to aquatic microorganisms: importance of chemical, biological and physical processes on biouptake. *Biochimie*, 88(11), 1721-1731.

Wu, Y. et Wang, W.-X. (2012). Thiol compounds induction kinetics in marine phytoplankton during and after mercury exposure. *Journal of Hazardous Materials*, 217–218, 271–278.

Wu, Y., Zeng, Y., Qu, J.N.Y. et Wang, W.-X. (2012). Mercury effects on *Thalassiosira weissflogii*: applications of two-photon excitation chlorophyll fluorescence lifetime imaging and flow cytometry. *Aquatic Toxicology*, 110–111, 133–140.

Zhang, M. et Majidi, V. (1994). Monitoring the cellular response of *Stichococcus bacillaris* to exposure of several different metals using in vivo ^{31}P NMR and other spectroscopic techniques. *Environmental Science and Technology*, 28, 1577-1581.

ANNEXE A

PUBLICATIONS FROM THIS THESIS

1. Samadani, M., Perreault, F., Oukarroum, A. et Dewez, D. (2018). Effect of cadmium accumulation on green algae *Chlamydomonas reinhardtii* and acid-tolerant *Chlamydomonas* CPCC 121. *Chemosphere*, 191, 174-182.

2. Samadani, M. et Dewez, D. (2018). Cadmium accumulation and toxicity affect the extracytoplasmic polyphosphate level in *Chlamydomonas reinhardtii*. *Ecotoxicology and Environmental Safety*. Manuscript number: EES-18-1197.

3. Samadani, M. et Dewez, D. (2018). Effect of mercury on the polyphosphate level of alga *Chlamydomonas reinhardtii*. *Environmental Pollution*. 240: 506-513.